1967

Some physical properties of silicon nitride thin films prepared by audio frequency sputtering in a nitrogen plasma

Hugh M. McKnight
Lehigh University

SOME PHYSICAL PROPERTIES OF SILICON NITRIDE THIN FILMS PREPARED BY AUDIO FREQUENCY SPUTTERING IN A NITROGEN PLASMA

by

Hugh M. McKnight

A Thesis

Presented to the Graduate Faculty

of Lehigh University

in Candidacy for the Degree of

Master of Science

Lehigh University

1967

CERTIFICATE OF APPROVAL

This thesis is accepted and approved in partial fulfillment of the requirements for the degree of Master of Science.

May 11, 1967
Date

Richard N. Tauber
Professor in Charge

T. Tiedsch
Chairman, Department of
Metallurgy and Materials Science

ACKNOWLEDGEMENTS

The author expresses appreciation to Dr. Richard N. Tauber for his guidance and suggestions in this work. Sincere thanks are also due to Dr. Joe R. Ligenza of the Bell Telephone Laboratories for suggesting this line of work. The help of Dr. E. J. Shaw and Dr. M. W. Sagal is also sincerely appreciated. The author also acknowledges the help of many people of the Western Electric Company's Princeton Research Center.

Gratitude is also expressed to my wife, Naydean, for her forebearance during the period of thesis preparation.

TABLE OF CONTENTS

LIST OF FIGURES

LIST OF TABLES

ABSTRACT

Thin silicon nitride films have been deposited on silicon substrates by audio frequency reactive sputtering in a hollow cathode supported nitrogen plasma. This technique is unique to this investigation. Some physical properties were determined for Si_3N_4 films deposited at substrate temperatures between 200° and 600°C and plasma currents up to 5.0 amperes. All films were amorphous and had properties comparable to or better than that of films produced by other techniques. Substrate temperature and plasma current had little effect on the film index of refraction, dielectric strength, and density. The energy gap and dielectric strength of the silicon nitride films was determined to be 5.72 eV and 6×10^6 V/cm respectively. The IR absorption peak occurs between 10.1 and 11.9μ for films prepared at 400°C and 1.0 ampere plasma current and between 10.8 and 11.3μ for films prepared at 600°C and 5.0 amperes plasma current. The absorption peak of crystalline Si_3N_4 occurs at a wavelength of 10.7μ. The shift to longer wavelengths is attributed to the weaker bonding of the amorphous films as opposed to that of crystalline Si_3N_4. The broadening of the absorption peak is attributed to the larger distribution of interatomic distances of the amorphous films.

The large plasma currents make it possible to obtain high deposition rates at low sputtering voltages. Deposition rates up to 1600 Å/min. were obtained at a 5.0 amperes plasma current and a sputtering peak to peak voltage of 3200 V. However, at deposition rates greater than 300 Å/min., the film density was

found to decrease with increasing sputtering rates. This decreasing film density was accompanied by a decreasing index of refraction which was approximately linearly related to film density. As the film density approached the theoretical value of 3.18 g/cm^3, the index of refraction approached the crystalline value of 2.1. IR spectra of films prepared at high deposition rates also show a broad absorption peak between 10.5 and 11.8μ.

INTRODUCTION

Attractive Features of Silicon Nitride

Silicon nitride is a dielectric material whose chemical and physical properties make it a potentially important material for use in the manufacture of semiconductor devices. Among its attractive features are its chemical inertness to many molten metals such as aluminum at 1000°C, lead at 400°C, tin at 300°C, and zinc at 550°C. It is resistant to oxidation up to about 1200°C when a layer of silica begins to form at its surface, and is resistant to many corrodents[16]. The coefficient of thermal expansion, $2.5 \times 10^{-6}/^{\circ}C$, is a close match to that of silicon - $4.0 \times 10^{-6}/^{\circ}C$.

Silicon nitride has a demonstrated high resistance to the diffusion of sodium[49], phosphorus[41], and boron[41], and a believed high resistance to the diffusion of aluminum, potassium, and gallium. The dielectric strength is from 10^6 to 10^7 V/cm and the dielectric constant is from 5 to 11 depending of the forming technique and the measuring frequency. The above physical properties of silicon nitride make it potentially important for use as an insulator, diffusion mask, or passivator in the manufacture of semiconductor devices. Figure 1a shows a typical application of silicon nitride as a diffusion mask in the manufacture of diffused junction transistors, and Figure 1b shows a typical application as an insulator in a MIS transistor. A layer of silicon nitride over a completed integrated circuit is an example of a useful application of silicon nitride as a passivator.

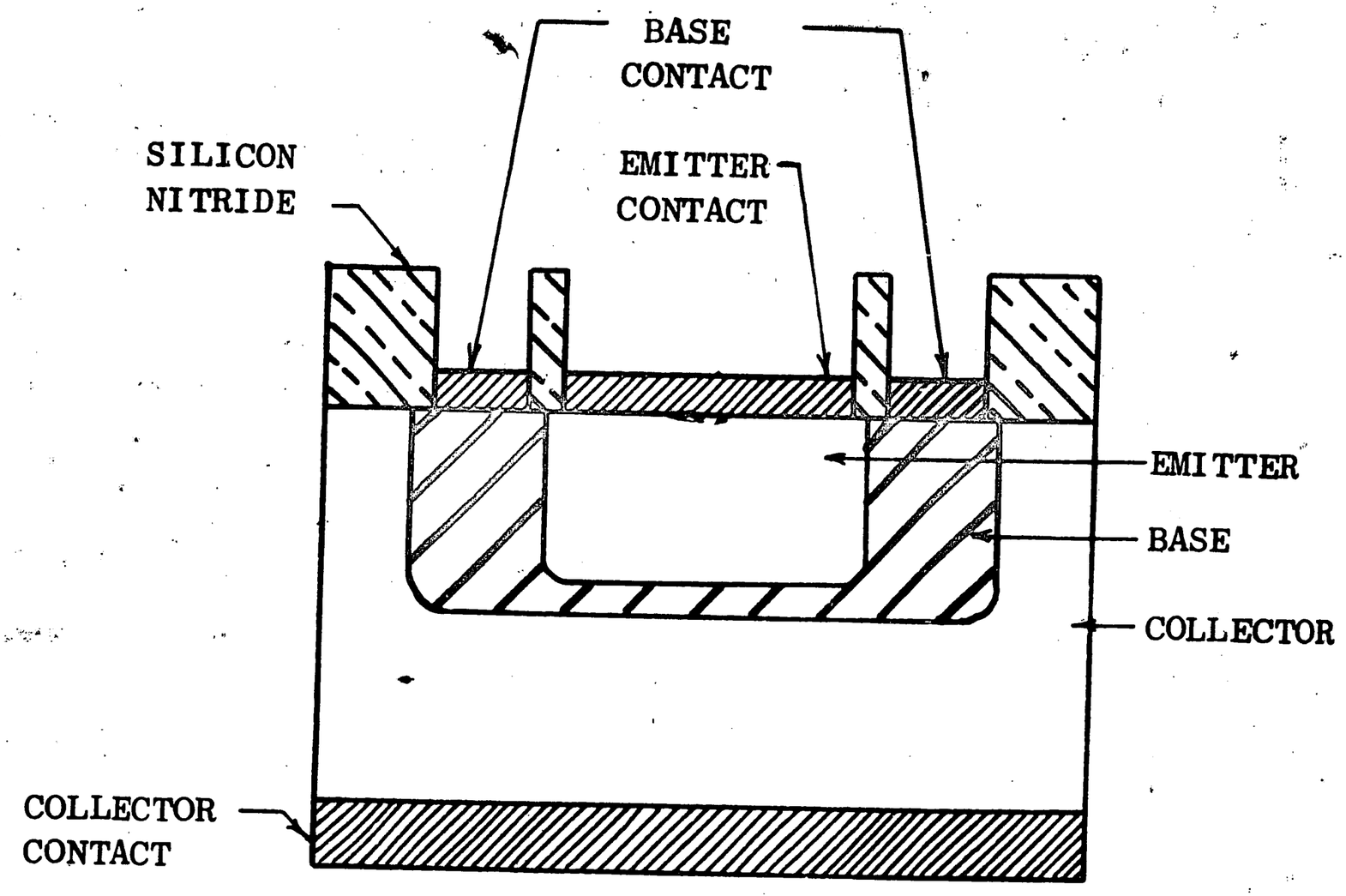

a.

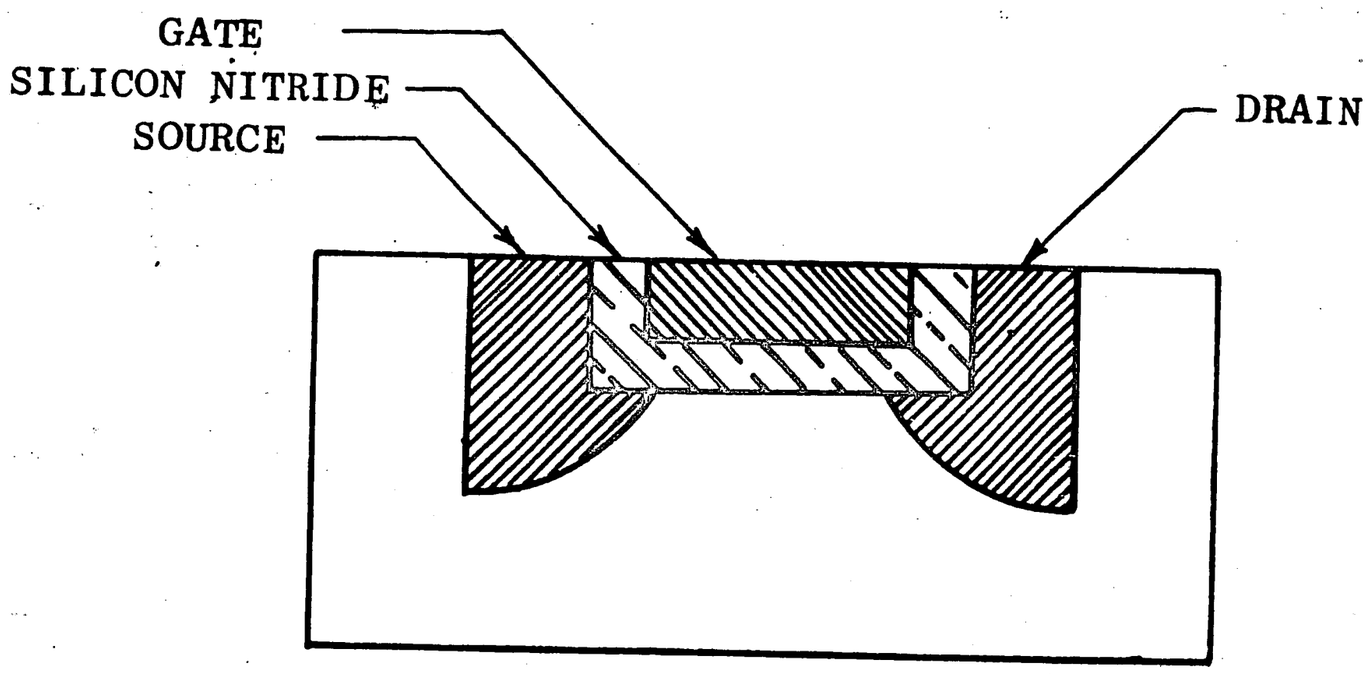

b.

FIGURE 1

(a.) Diffused Junction Transistor Showing an Application of Silicon Nitride as a Diffusion Mask. (b.) MIS Field Effect Transistor Showing an Application of Silicon Nitride as an Insulator.

To prevent further diffusion of the junctions in some passivation and diffusion masking applications, it is desirable to have a process for depositing silicon nitride on wafers held at low temperatures. A technique unique to this investigation is used to prepare amorphous silicon nitride films at low substrate temperatures. This technique involves reactive audio frequency sputtering from a silicon cathode in a hollow cathode supported nitrogen plasma.

Preparation and Properties of Silicon Nitride

A review of the preparation and properties of silicon nitride is given in Appendix I. Only a brief description of the methods of preparing bulk and thin film silicon nitride will be presented here.

Bulk Silicon Nitride

Bulk silicon nitride is prepared by heating silicon, usually in the form of powders, in a nitrogen atmosphere at temperatures of 1200^{o} to 1600^{o}C. Two crystalline phases are formed over this range. α-Si_3N_4 is formed at temperatures of 1200^{o} to 1400^{o}C and β- Si_3N_4 is formed at temperatures greater than 1450^{o}C[15]. α - Si_3N_4 has been transformed to β - Si_3N_4 by heating to 1550^{o}C, but attempts to transform β - Si_3N_4 to α - Si_3N_4 by heating at temperatures below 1500^{o}C have failed[15]. Both forms are thought to have a hexagonal crystal structure[11,14,15,29].

The refractive index of β - Si_3N_4 is about 2.1. The measured density is 3.15 g/cm^3 for β - Si_3N_4 and 3.16 g/cm^3 for α - Si_3N_4 which compares well to the theoretical density of 3.187 and 3.184 respectively. These density values are probably derived from measurements on single crystals and are not valid for densities measured on Si_3N_4 formed by nitriding silicon powders to form bulk silicon nitride. The bulk density varies from 2.0 to 2.6 g/cm^3 [20].

Silicon Nitride Films

Recently, much effort has been directed toward developing methods for preparing continuous films of silicon nitride having bulk properties which make it suitable for use as an insulator,

passivator, and diffusion mask in the production of semiconductor devices, integrated circuits, and capacitors.

Amorphous films are preferred because their greater flexibility enables continuous films, which are highly resistant to the diffusion of impurities, to be formed. The methods used for preparing silicon nitride films can be divided into three categories: (1) pyrolytic decomposition; (2) DC and RF plasma activated chemical vapor deposition; (3) sputtering.

(1) Pyrolytic Decomposition

Films of silicon nitride are prepared pyrolytically by reacting a compound of silicon, such as $SiCl_4$, $SiBr_4$, or SiH_4, with NH_3 at temperatures from 550° to 1200°C. The films prepared at temperatures below 900°C are amorphous with some crystallites appearing in films prepared at temperatures greater than 900°C[43]. A typical reaction is

$$3SiH_4 + 4NH_3 \longrightarrow Si_3N_4 + 12H_2 \qquad (1)$$

(2) DC and RF Plasma Activated Chemical Vapor Deposition

Silicon nitride films are prepared at low substrate temperatures by reacting a chemical vapor of SiH_4, $SiBr_4$, or $SiH_4 + NH_3$ in a direct current (DC) or radio frequency (RF) supported nitrogen discharge or plasma. The reaction of silane with ammonia as given in equation (1) is utilized to prepare films at substrate temperatures less than 500°C by using RF energy instead of high temperatures to force the reaction to completion[42]. Similarly, the reduction of silane or silicontetrabromide in a DC nitrogen plasma is utilized to

form silicon nitride films at substrate temperatures of 300° to 400°C[48]. The two reactions can be summarized as follows:

$$3SiH_4 + 4NH_3 \xrightarrow{\text{RF Plasma}} Si_3N_4 + 12H_2 \quad (2)$$

$$3SiH_4 + 2N_2 \xrightarrow{\text{DC Plasma}} Si_3N_4 + 6H_2 \quad (3)$$

The films prepared by these methods are amorphous.

(3) Sputtering

Four techniques of sputtering have been used to form amorphous films of silicon nitride on various substrates at temperatures less than 500°C. These four methods can be summarized as follows: (1) RF sputtering from a silicon nitride cathode in an argon atmosphere; (2) DC sputtering reactively from a silicon cathode in a nitrogen atmosphere; (3) RF sputtering reactively from a silicon cathode in a nitrogen atmosphere; (4) DC sputtering reactively in a separately supported nitrogen discharge. Some properties of Si_3N_4 films prepared by the various methods are compared in Table I.

Deposition rates for the pyrolytic method increase exponentially with increasing temperature and are strongly dependent on the composition of the reactants. In the range below 900°C where amorphous films are prepared, the upper limit appears to be about 1500 Å/min.[44] Data is not available for the film properties at high deposition rates, but it has been reported[72] that film cracking occurs at deposition rates greater than 500 Å/min. and when films are thick. The normal growth rate is about 120 Å/min.[72] Deposition rates reported for the plasma activated vapor deposition methods are considerably below the maximum reported for pyrolytic deposition,

TABLE I

THE PHYSICAL PROPERTIES OF SILICON NITRIDE FILMS

	T_s (°C)	R_d Å/min.	$\frac{SiH_4}{NH_3}$	Vac [KV (P-P)]	Vdc (KV)	P (μ)	IR (μ)	R (Ω·cm)	n	ρ g/cm³	E V/cm	Ko	Eg (eV)	Ref.
PYROLYTIC:	600						11.5		1.94		.8/2.3·10⁷	5.6-6.8	4.5-5.5	51,74
	900						12.0	10^{15}	1.98		~10⁷	6.2		71
	800-1000	5000	1/40-1/20						2.1/1.98					43
1.SiH_4+NH_3	700-1150	1500							2.0		10^6-10^7			
	750-1100	850	1/40-1/20				(10-12)12		2.0/2.06	3.02/3.21		8-4	4.3	44
	800-1200	400							1.975/2.02	2.78/2.92		6.34		72
2.$SiCl_4$+NH_3	550-1250	600							1.99/2.01					41
											~10⁷	7	5.6	45
PLASMA ACTIVATED CHEMICAL VAPOR DEPOSITION														
1.RF DISCHARGE (SiH_4+NH_3)	<500	200	.03-.50				12.1	$8·10^{16}$						
2.DC PLASMA a.(SiH_4)	<500	400	.1%SiH_4			1000			2.0		$6-1·10^6$	7-11		42
b.($SiBr_4$)		400	.1%$SiBr_4$			1000			1.93	3.1/3.2				48
														48
SPUTTERING														
1.RF, Si_3N_4 Cathode in Ar		100					12					8.6		46,50
2.DC, Si Cathode in N_2	200-400	3			2-5	10								47,71
50% N_2+50%Ar		60			1.5	150						10-12		50
3.RF(13.6MHz), Si Cathode in N_2	25-500	200		3	1.5	5-25	11.3	$>10^{15}$	2.05	2.8/3.0		6-8.3	4-6	47,71
4.DC, Si Cathode in N_2 Supported Discharge	50-230	110			.8	1.5	12.0	$3.4·10^{13}$	2.1	2.82/3.02	1.2-6.0 x10⁵	6.2-6.8		46,50

T_s = Substrate temperature
R_d = Deposition rate
Vac= AC Sputtering potential
P = Gas pressure
IR = Infrared absorption peak
ρ = Film density
E = Dielectric strength
K = Dielectric constant
Eg = Energy gap
R = Film resistivity
Ref = Reference

but are in the normal growth rate range. These rates may not represent the maximum obtainable. Sputtering deposition rates vary considerably, depending on the technique used. The deposition rate for DC reactive sputtering from a silicon cathode in a nitrogen atmosphere (2-3 Å/min.) is extremely low due to a silicon nitride insulation layer building up on the cathode surface. This insulation layer prevents the neutralization of on-coming positive ions resulting in a positive charge accumulation at the cathode surface which repels the bombarding nitrogen ions. Consequently, the sputtering rate is reduced significantly. The films are generally of lower quality and display evidence of electron and negative ion bombardment damage. The Si-O band is present in infrared absorption spectra showing that oxygen is present in the films[47].

If argon is added to the nitrogen atmosphere, the sputtering rate is increased considerably. However, arcing at the cathode due to diffusion of silicon nitride to the cathode surface is still present and impairs reproducibility[50].

Deposition rates for sputtering from a pressed silicon nitride target in an argon atmosphere and DC reactive sputtering from a silicon target in a supported nitrogen discharge are about 100 Å/min. Film damage due to arcing at the substrate surface is observed using the latter technique, but can be eliminated by insulating the substrate holder from ground[50]. The RF reactive sputtering rate of 200 Å/min. is greater than that for the other sputtering methods. This rate decreases with increasing nitrogen pressure over the range

of 5 to 25 microns. The film properties deteriorate at higher nitrogen pressures[47].

The etch rate of the silicon nitride films has been observed to decrease with increasing sputtering voltage[46,50] and with increasing temperature when producing pyrolytic films[43,51]; the latter indicates an increase in the film density. The IR absorption spectrum of amorphous Si_3N_4 films shows an absorption peak for the Si-N stretching band at a wavelength between 11.3 and 12.1 microns. This represents a shift to higher wavelengths from the absorption peak of β- Si_3N_4 which occurs at a wavelength of 10.7 microns.

Amorphous films of silicon nitride show a considerable shift of the Si-N stretching band to longer wavelengths. The maximum occurs at wavelengths between 11.3 and 12.1μ, depending on the method of preparation, and have a band width of 9 to 14μ. Absorption peaks for β - Si_3N_4 occur at 10.7μ with a band width of 9 to 13μ. This has been attributed to weaker bonded structure of the films and to the distribution of interatomic distances[71].

A resistivity of 10^{15} ohm-cm at 400^{o}C has been measured for both pyrolytically prepared films and RF sputtered films[71]. This is similar to that measured at room temperature for films prepared by the low temperature reaction of silane and ammonia in a RF discharge ($8 \cdot 10^{16}$ ohm-cm). This value decreases to $5 : 10^{12}$ ohm-cm for films prepared at a silane/ammonia ratio of 0.5[42]. Films prepared by DC sputtering in a supported discharge have a resistivity of 3.4×10^{13} ohm-cm which is low compared to that of other films[50].

The index of refraction of pyrotytically prepared films varies from 1.94 to 2.1 and is related to reactant composition and preparation temperature. For high silane/ammonia ratios, n is greater than 2.1 indicating an excess of silicon in the films prepared at 800°C and 900°C, but n remains less than 2.1 for films prepared at the same reactant compositions at 1000°C[43]. Films prepared pyrolytically at 600°C and subsequently heat treated show a decrease in index of refraction with increasing temperature. At a wavelength of 5000 Å, n decreases from 1.96 at 600°C to 1.58 at 1300°C. Above 1200°C the films become visibly dull indicating a decrease in index of refraction[51]. The index of refraction of films prepared by the plasma and sputtering techniques are in the same range as that of the pyrolytically prepared films.

The density of RF sputtered films increases with increasing sputtering power or voltage[47,71]. This density range of 2.8 to 3.0 g/cm^3 is about the same as that for films prepared by DC sputtering in a supported discharge and for some pyrolytically grown films[41]. However, films grown pyrolytically by another investigator[72] have densities varying from 3.02 to 3.21 g/cm^3 and films prepared by reducing $SiBr_4$ in a nitrogen plasma have densities from 2.1 to 2.2 g/cm^3. These values approach the theoretical density of 3.18 g/cm^3.

Dielectric strength measurements are dependent on the type of contact made to the film. A value of 8×10^6 V/cm was determined for pyrolytically grown films using a 1mm^2 contact area and a value of

2.3×10^7 V/cm using a point contact[51]. The dielectric strength of films prepared by reacting silane and ammonia in a RF discharge depended on the silane/ammonia ratio. The variation was from 6×10^6 V/cm at a 0.03 ratio to 1×10^6 at a 0.50 ratio[42]. Dielectric strengths at an order of magnitude less were obtained for films prepared by DC sputtering in a supported discharge[46,50].

The dielectric constant is influenced by deposition conditions and heat treatment. Pyrolytic films deposited at 600°C have a dielectric constant from 5.6 to 6.8 which increases to 9 after heat treatment at 1100°C[51]. Films prepared by reacting silane and ammonia in a RF discharge show a strong dependence of dielectric constant on the silane/ammonia ratio. The dielectric constant increases from 7 at a ratio of 0.03 to 11 at a ratio of 0.50[42]. The dielectric constant of films prepared by DC sputtering in a 50% argon - nitrogen atmosphere varied from 10 to 12, which is high compared to that of 5 to 9 reported for the other deposition methods. A microprobe analysis showed these films to be contaminated with silicon and 5 to 15% SiO_2[50]. RF sputtered films show a dependence of dielectric constant with sputtering power, increasing from 6 to 8.3 for power densities from about 1 to 5 watts/cm^2 [47].

The energy gap of the films prepared by the pyrolytic methods varies from 4.3 to 5.6. Pyrolytic films prepared at 600°C show a variation in energy gap from 4.5 to 5.5 eV. The energy gap of these films increases by about 0.35 eV as the heat treating temperature increases from 600° to 1300°C[51].

Audio Frequency Reactive Sputtering in a Supported Nitrogen Plasma

Sputtering of metals is usually carried out by applying a high negative DC potential to the cathode which is made of the metal to be sputtered. This potential ionizes the gas atmosphere in the sputtering chamber and attracts the positive gas ions to the cathode target material. The bombardment by the positive ions cause atoms of the cathode to be ejected. These atoms condense on a substrate placed near the cathode, forming a thin film of the cathode metal on the substrate. However, when reactively sputtering a metal in a reactive gas atmosphere, e.g., silicon in a nitrogen atmosphere, to form an insulating film on a substrate, back diffusion of the dielectric forms an insulating film on the cathode surface. This insulating film prevents the neutralization of the positive charge which accumulates at the cathode surface during positive ion bombardment. The accumulated positive charge repels the oncoming positive ions and reduces their kinetic energy to such an extent that the sputtering rate is greatly reduced. The positive charge buildup can be reduced by applying an RF potential to the metal cathode which will cause the cathode to be alternately ion and electron bombarded. The positive charge buildup during the negative half cycle will be neutralized by electrons attracted to the cathode during the positive half cycle. At RF frequencies, more electrons will accumulate at the cathode during the positive half cycle than ions during the negative half cycle, since the electron mobility is greater than the ion mobility. This negative charge buildup causes the cathode to be

self biased negatively with respect to the plasma and sputtering of the cathode will occur. If the frequency of the applied RF potential is too low, enough positive ions can flow to the cathode during the negative half cycle to neutralize the negative charge, and no sputtering can take place. Frequencies in the low megacycle range are needed for good results[52]. The use of RF energy is generally not desirable. RF energy is a safety hazard, power radiated causes interference with other equipment in the vicinity, and the frequencies available for use are limited by communication regulations making close frequency control mandatory.

This investigation shows that large deposition rates can be obtained when audio frequency potentials are applied to the cathode. This is accomplished by superimposing the audio potential on a DC potential such that the cathode is driven slightly positive with respect to the plasma during the positive half cycle. Electrons drawn from the plasma to the cathode neutralize the positive charge buildup caused by the insulating film which has formed on the cathode. A frequency of 10KHz was used in this experiment as a matter of convenience. Frequencies in the low audio range can be used if the polarity reversal rate is large compared to the rate at which insulation builds up at the cathode surface.

Hollow Cathode Supported Discharge

To further increase deposition rates and improve the quality of the resulting films, a separate discharge or source of nitrogen ions is used rather than depending on a high cathode potential to maintain a glow discharge. In this method the sputtering voltage

serves only to extract ions from the plasma and accelerate them toward the cathode. This results in much higher deposition rates at lower sputtering voltages.

When an elemental cathode is bombarded by high energy ions, atoms of the material having peak energies at about 20% of that of the incident ion energy are ejected. This energy is mostly in the form of kinetic energy. The atoms condensing on the substrate retain a large part of this energy in the form of surface mobility. Hence films having a high degree of structural perfection are expected. However, it is likely that some radiation - like damage to the film is done due to the high kinetic energy of the arriving atoms and electron bombardment. An alternative is to decrease the sputtering voltage, but the decrease in atom energy must be compensated for by increasing the substrate temperature to maintain surface mobility of the sputtered atoms. Hence the feature of low substrate temperature is lost at lower voltages.

By sputtering through a dense plasma the elemental atoms sputtered from the cathode at relatively low potential will have many inelastic collisions with the plasma atoms and ions in diffusing to the substrate. These collisions will transform the large kinetic energy of the sputtered atoms to the potential energy or excited states of the plasma. Hence the surface mobility of the atoms is maintained at low sputtering voltages and low substrate temperatures[73].

A thermionic emitter may be used as the auxiliary plasma cathode with a DC potential applied between the thermionic emitter cathode and the plasma anode. However, to obtain higher plasma densities, a hollow cathode is used to generate the auxiliary plasma. The hollow cathode has been known for some time as a means of generating relatively high - density steady state plasmas[53,58]. Compared with normal glow discharges, the hollow cathode discharges have current densities several orders of magnitude larger at lower sustaining voltages, the visible and ultraviolet radiation is more intense, the plasma density is much higher, the V-I curves of sustaining voltage versus discharge current may have a negative slope (negative resistance), and the vapor density of the cathode metal in the cathode cavity is extremely high[54]. Musha[53,54] developed a theory of the negative resistance of hollow cathode discharges based on considerations of energy balance composed of radiation and heating components. He concluded that the slope of the V-I curve is greatly affected by the rate of increase of radiation power compared to the discharge current. The two necessary conditions for a negative resistance to appear are as follows: (1) The radiation power must increase with an increase in discharge current, (2) V_β must be larger and V_α smaller than the sustaining voltage, where

$$V_\beta \approx \frac{1 + \gamma_i}{\gamma_p} - V_i - V_a \qquad (4)$$

and

$$V_\alpha \approx \frac{1}{\gamma_i}\left\{V_i - V_a + 2\ (1 + \gamma_i)V_e\right\} \qquad (5)$$

Here γ_i is the coefficient of secondary electron emission at the cathode by ion bombardment, γ_p is the coefficient of photoelectric emission at the cathode, eV_e represents the mean kinetic energy of an electron, V_i is the ionization potential of the filling gas, and V_a is the anode fall potential[54]. In general, the V-I curve depends on the geometry of the cathode tube, the material of the cathode, and the filling gas. The effective ionization potential of the mixture of sputtered metal atoms and the filling gas decreases as the discharge tube becomes smaller. This in turn makes V_α small and negative slopes are easier realized. Thus, a small hollow cathode tube is desirable. The most effective process in the hollow cathode is sputtering of the cathode which emits radiation that increases with increasing current and reduces the effective ionization potential of the filling gas.

In this investigation, physical properties of silicon nitride thin films were experimentally determined. The films were deposited on polished silicon substrates by audio frequency sputtering through a hollow cathode supported nitrogen plasma. The index of refraction, dielectric strength, density, infrared absorption spectrum, and optical energy gap of the films was measured as functions of substrate temperature and plasma current.

EXPERIMENTAL DETAILS

Description of the Apparatus

Sputtering of silicon nitride films was carried in a quartz deposition chamber made in the form of a cross (see Figures 2, 3, and 4). The target silicon cathode and anode are contained in the vertical portion which is made of 55mm diameter quartz tubing. The nitrogen plasma is generated in the horizontal arms. A hollow tantalum cathode in one arm and associated anode in the opposite arm are separated by about 10 inches. The arms are made of 13mm diameter quartz tubing. The target cathode is high purity, 100 ohm-cm, polycrystalline silicon. This silicon cathode is bonded to a pyrex glass tube which in turn is joined to a pyrex ground joint providing a vacuum seal with the quartz chamber. This allows electrical connections to be made to the silicon target externally. Another cylinder of high purity silicon is used as the substrate holder and anode and rests in a water cooled copper support which is inserted into the quartz chamber via a vacuum seal. A screw adjustment is provided in the support for varying the distance from the substrate to the target. An opening in the copper support provides a means of measuring the pedestal temperature by means of a thermocouple. The pedestal is heated by a 400KHz induction heater.

The hollow cathode is made of tantalum tubing ($\frac{1}{4}$ inch diameter, .005 inch wall thickness, and 3 inches long). A roll of .003 inch thick tantalum foil is inserted into the end of the tubing to a distance of 1 inch[73]. During operation the inner turns of the

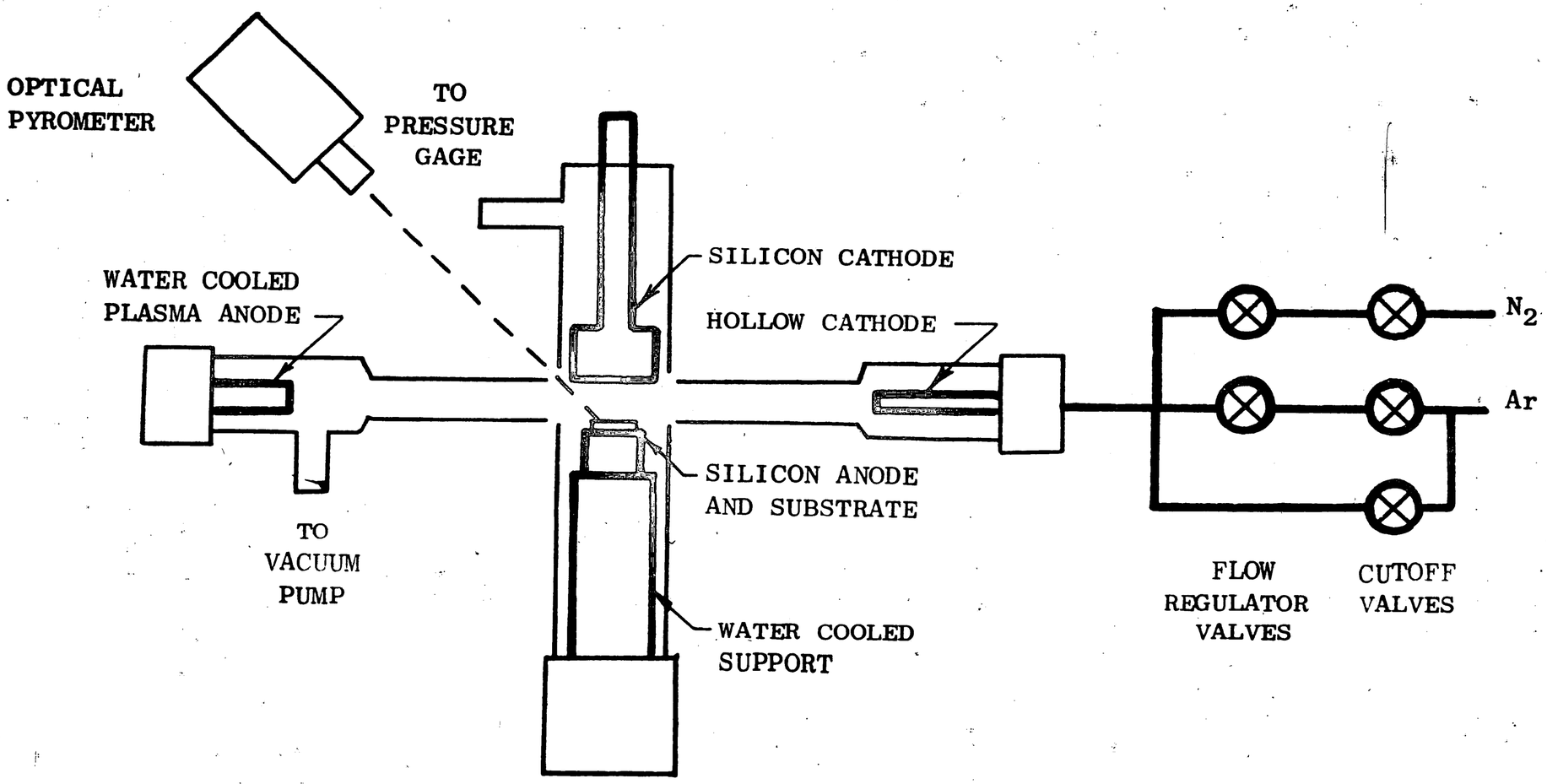

FIGURE 2

Experimental Apparatus Schematic

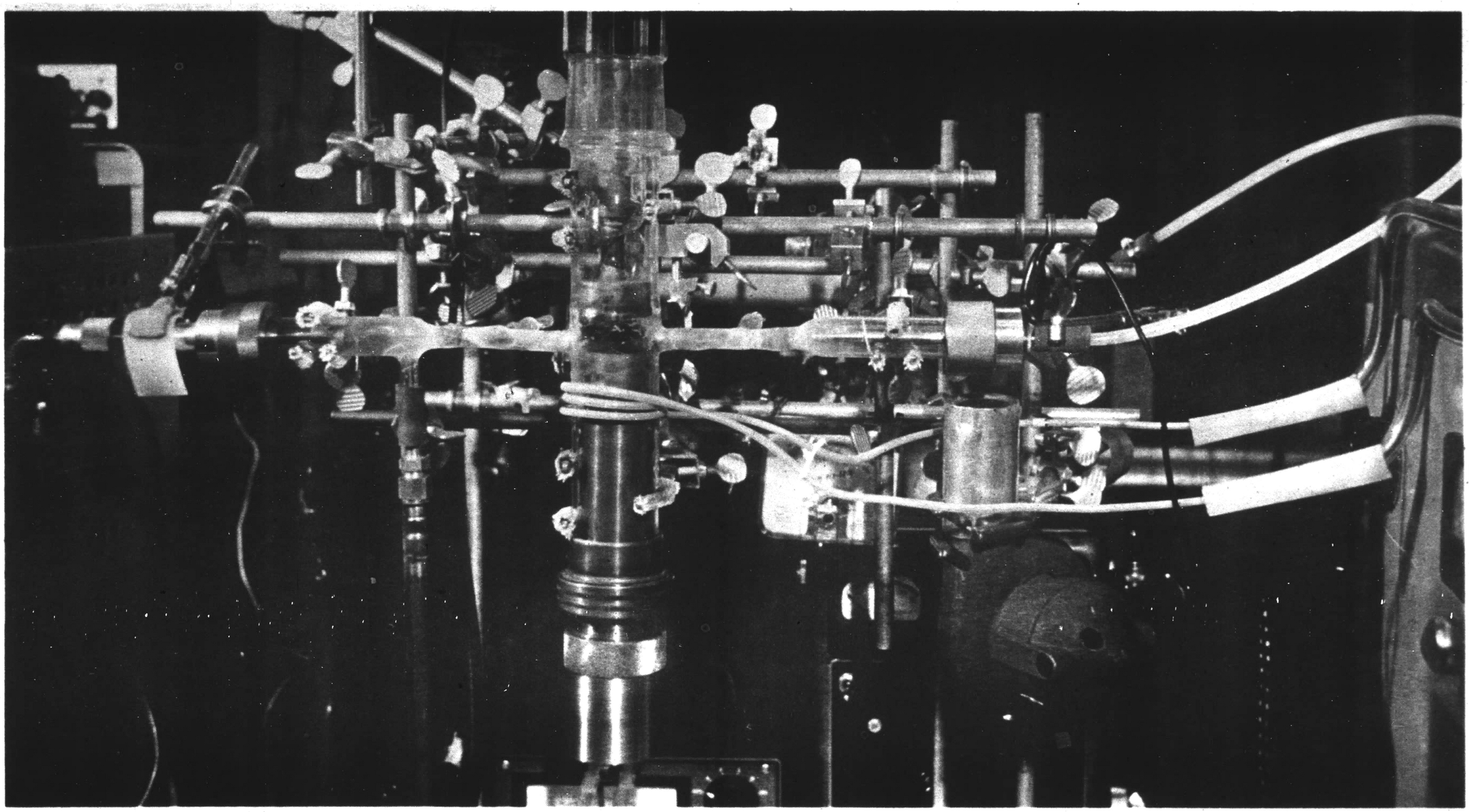

FIGURE 3

Photograph of Sputtering Chamber

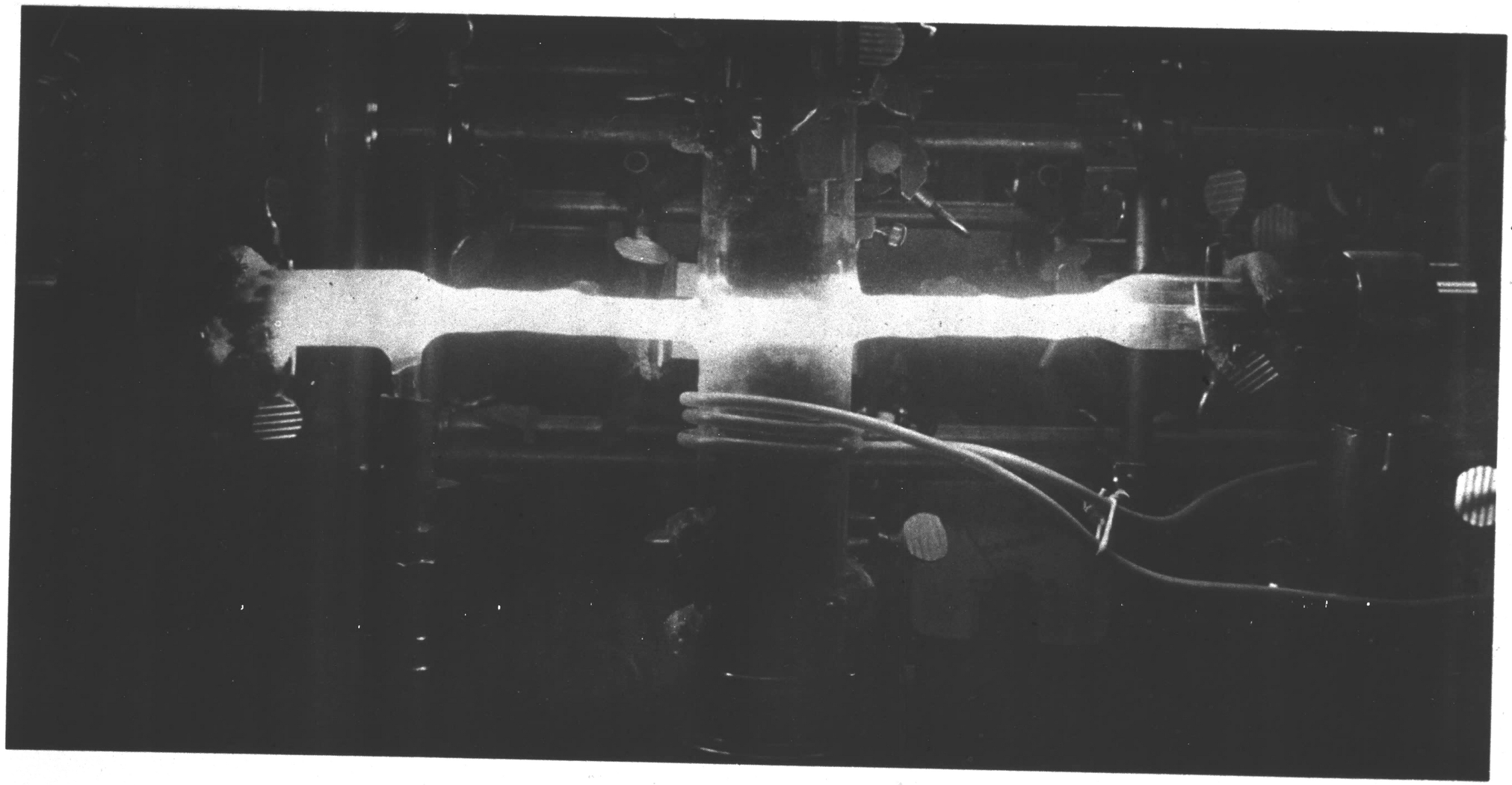

FIGURE 4

Photograph of Sputtering Chamber in Operation

inserted roll act as a hollow cathode itself and thereby limits the sputtering inside the hollow cathode to the outer end. This allows the main tube to operate at lower temperatures and results in less power loss in the cathode and hence a more efficient hollow cathode operation. The hollow cathode is connected to an aluminum vacuum couple to provide external electrical contact. Gas is fed into the system via an opening in the aluminum couple and travels through the hollow cathode tube into the quartz deposition chamber. A $\frac{1}{4}$ inch diameter teflon tube connected to the aluminum couple serves as a flexible connection and electrically insulates the gas source from the hollow cathode. The flow of the high purity (99.98%) nitrogen and argon gas into the chamber is regulated by flow and cut off valves connected in parallel between the hollow cathode and gas source.

Before the gases are introduced, a mechanical pump evacuates the quartz system to a vacuum of 1 micron. The pressure is measured with a thermocouple type vacuum gage.

The plasma anode located in the horizontal arm opposite the hollow cathode is a copper cylinder which is water cooled and gold plated and is 3/4 inch in diameter and 3 inches long.

The temperature of the substrate during sputtering is measured by a Latronics model BC711 optical pyrometer focused on the surface of the silicon wafer. The optical pyrometer was calibrated by heating the silicon pedestal that supports the silicon substrate to a temperature of 700^{o}C and making simultaneous temperature measurements

with the optical pyrometer and a thermocouple inserted through an opening in the pedestal. The emissivity of the silicon was determined to be 0.75. The distribution of the plasma in the sputtering chamber was varied by means of a magnetic field supplied by permanent magnets. The field strength at the center of the deposition chamber was approximately 64 gauss as determined by Hall probe measurements.

The sputtering and plasma voltages are applied as shown in Figure 6; both are floating with respect to ground potential. The horizontal plasma portion of the circuit contains a 100 ohm ballast resistor connected in series with the variable DC power supply and the hollow cathode and anode. The power supply is an Opad model SR-100 and is capable of supplying 10 amperes at 1000 volts. The vertical sputtering portion of the circuit consist of a variable Consolidated Electrodynamics Corporation LG031 DC power supply in series with an AC supply. The AC supply is a Hewlett Packard model 205AG 30KHz variable audio frequency oscillator which drives a Bogen model M0200A, 200 watt, audio frequency power amplifier. The output voltage of the power amplifier is increased to a peak to peak value of about 4KV maximum by the stepup transformer which also serves to isolate the circuit. The maximum AC voltage capability is determined by the impedance of the nitrogen plasma and is about 3200 volts peak to peak at a plasma current of 5.0 amperes. The output capability of the CVC power supply is 5KV at 750 milliamperes. An oscilloscope is used to determine the relative AC and DC voltage

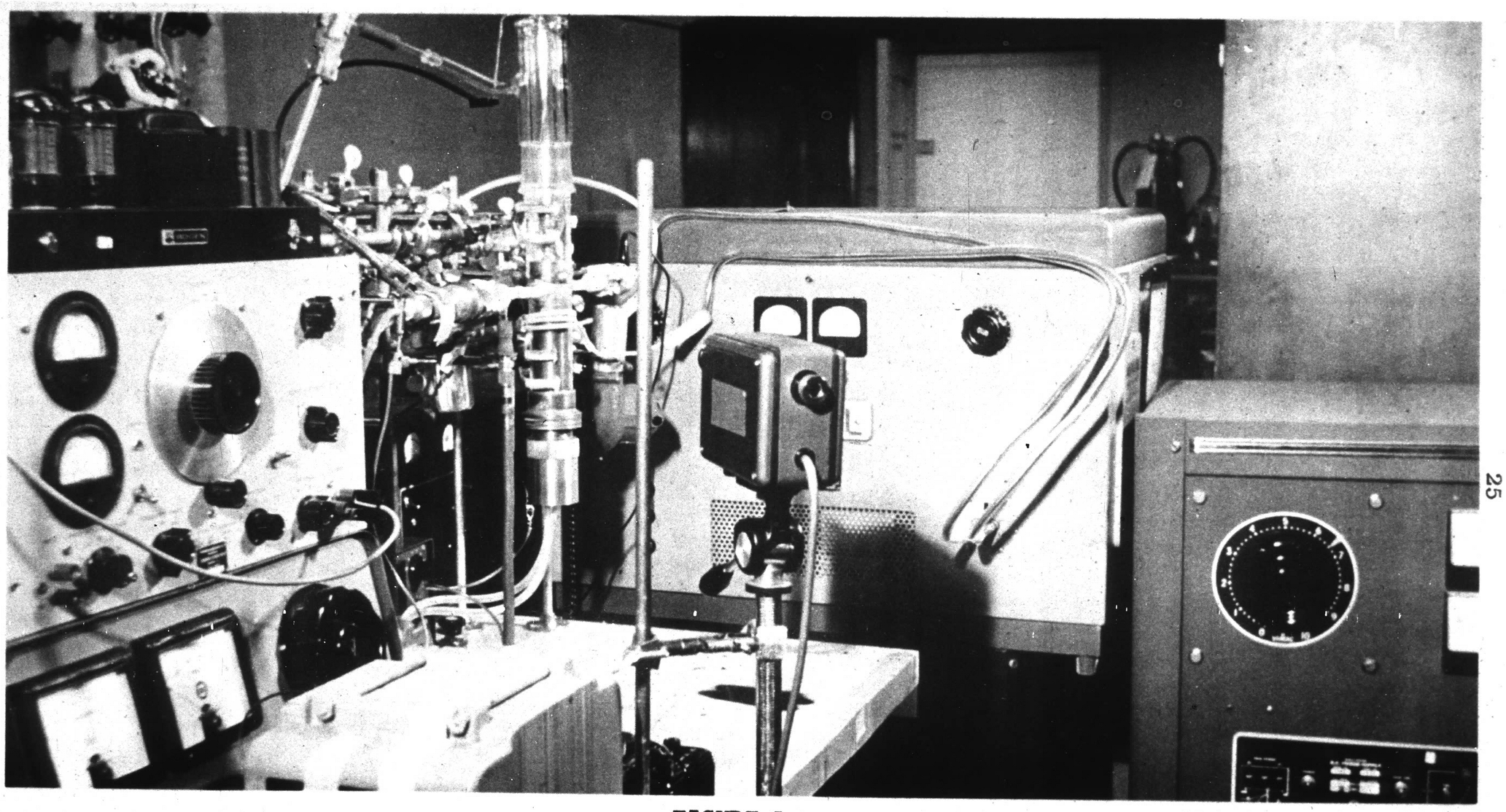

FIGURE 5

Photograph of Experimental Apparatus

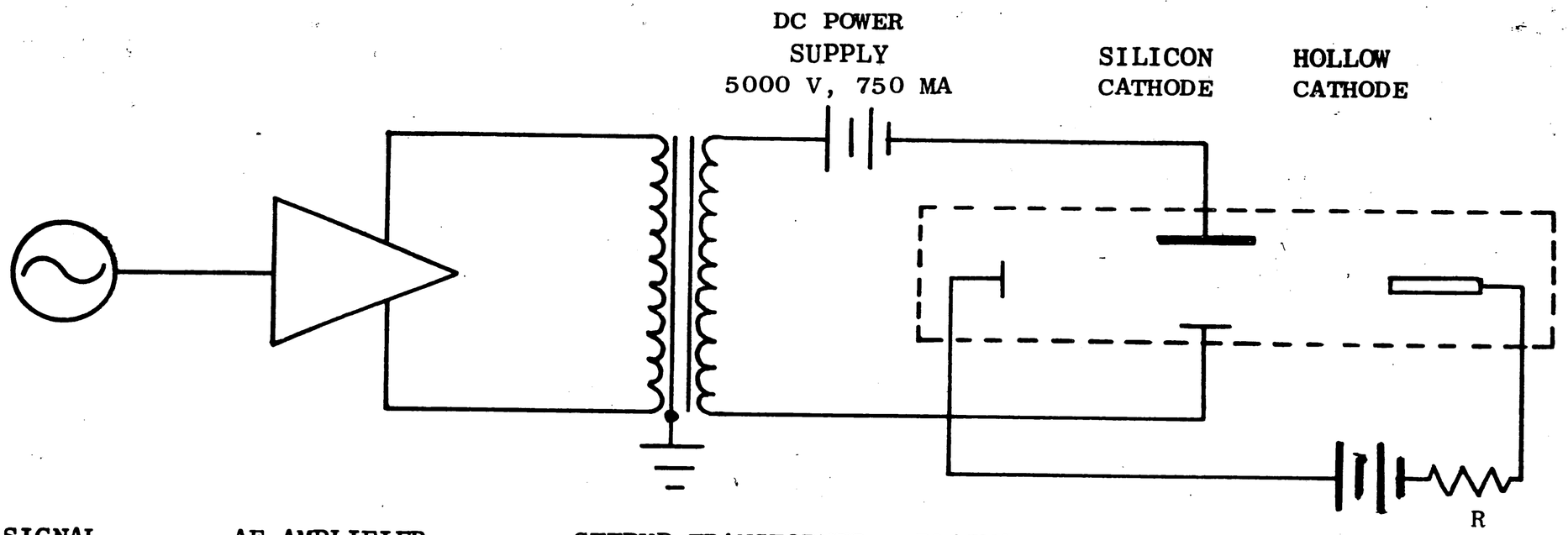

FIGURE 6

Electrical Schematic Diagram of the
Sputtering and Plasma Circuit

amplitudes applied to the sputtering electrodes. A photograph of the experimental apparatus is shown in Figure 5.

Deposition Conditions and Procedure

The silicon nitride films were deposited on single crystal silicon wafers which are .007 inch thick and 7/8 inch in diameter. The wafers have a (111) crystallographic orientation, a resistivity of 6.5 ohm-cm, and are phosphorus doped. Prior to the deposition of silicon nitride on the silicon wafers, they are cleaned by the following procedure:

1. Degrease wafer with trichloroethylene solvent for 2 minutes in ultrasonic cleaner.
2. Ultrasonically clean the wafer in wetting agent #9117 (Leconal, diluted to a 2% concentration by volume) for 15 minutes.
3. Rinse wafer in flowing deionized water for 1 minute.
4. Boil wafer in 15% aqueous H_2O_2 solution for 15 minutes.
5. Rinse wafer in flowing deionized water for 1 minute.
6. Etch in 10% aqueous HF solution for 30 seconds.
7. Rinse wafer in flowing deionized water for 5 minutes
8. Dry wafer in flowing nitrogen.

Nitrogen is relatively difficult to ignite compared to some of the other gases. With the experimental configuration used in this investigation, potentials of about 1000 volts at a pressure of 1000 microns are required. For this reason argon, which will ionize at about 700 volts at a pressure of 1000 microns, was used to start the plasma discharge. The nitrogen was then admitted into the chamber and the argon turned off.

A nitrogen pressure of 200 microns was used throughout this experiment. The nitrogen plasma could be maintained to a pressure as low as 50 microns. This could probably be extended into the low micron range by introducing a magnetic field around the hollow cathode by means of a solenoid. Plasma currents from one to five amperes were used in this experiment; the voltage drop across the plasma varied from 210 to 160 volts. This represents a variation in plasma power density from 7.2 to 16.3 watts/cm^3, and an electron energy from 1.5 to 3.1 electron volts as determined by Langmuir probe measurements using the double probe method of Johnson and Malter[59].

The substrate temperature was controlled during deposition by heating the substrate support with RF induction heating or by water cooling the substrate support. Due to the heating effect of the plasma and sputtering current, the substrate could not be cooled below 200°C. The maximum substrate temperature used in this experiment was 600°C.

Most of the films were deposited at a sputtering current of 100 ma with the applied voltage varying from 4KV peak to peak at a 1.0 ampere plasma current to 1.6KV peak to peak at a 5.0 amperes plasma current (see Figure 7). The frequency of the sputtering potential was held constant at 10KHz throughout the experiment.

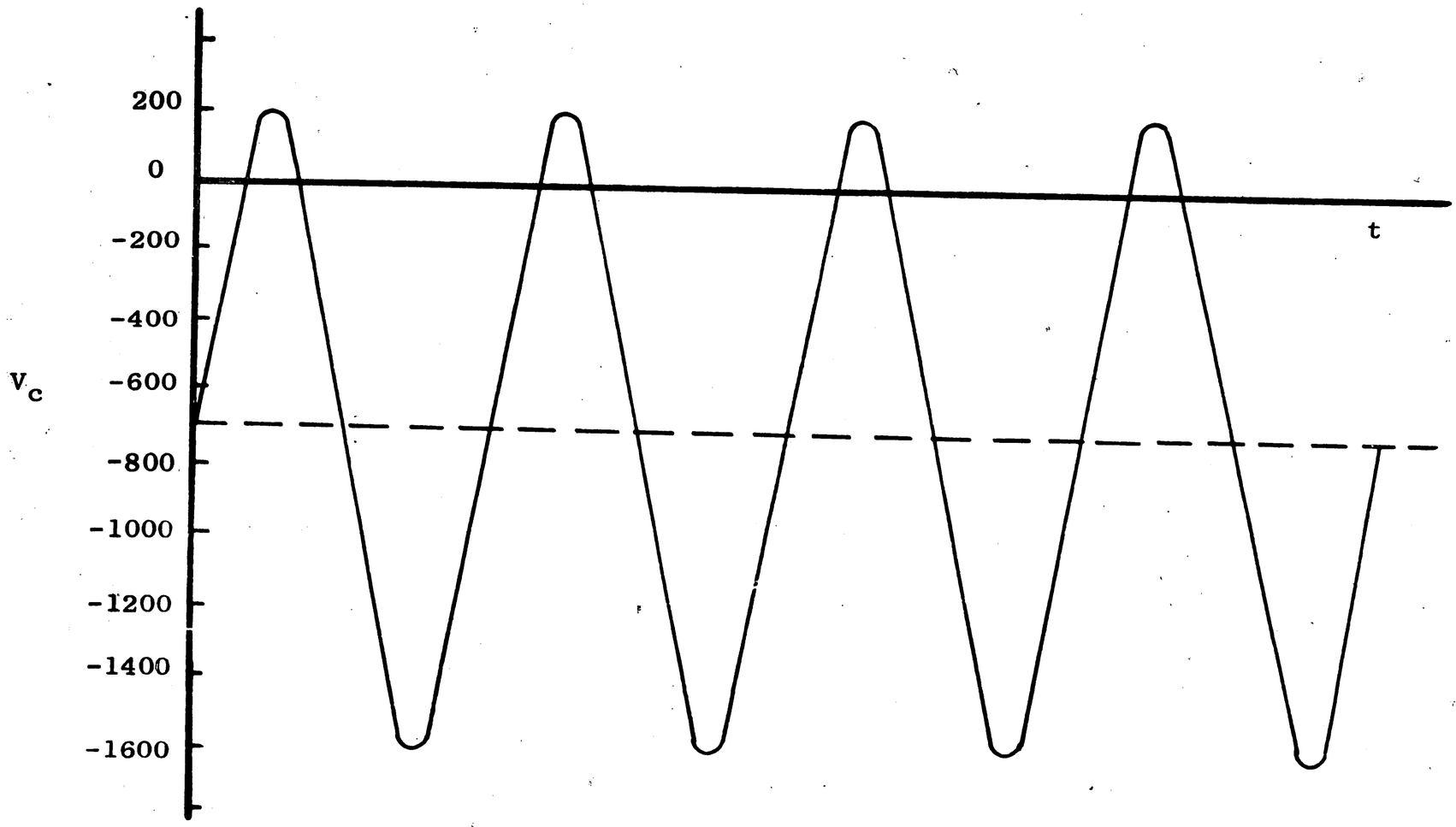

FIGURE 7

Waveform of Cathode Sputtering Potential Versus Time

MEASUREMENTS

Index of Refraction and Film Thickness

An ellipsometer was used to determine the film thickness and index of refraction of the silicon nitride films on silicon substrates. The ellipsometer is an optical instrument that measures the effect of reflection on the state of polarization of light. Suppose that plane polarized light is incident at an angle of 45^{o} to the plane of incidence. This vector can be resolved into two equal components. One is in the plane of incidence and is denoted E_p. The other is perpendicular to the plane of incidence and is denoted E_s.

If the reflecting object is non-metallic, both components after reflection have suffered a 180^{o} phase shift and the relative amplitudes have changed as indicated in Figure 8a. The relative phase shift, Δ, is given by

$$\Delta = \delta_p - \delta_s \tag{6}$$

where δ_p and δ_s is the phase change due to reflection in the p and s components respectively. For the case mentioned above, $\Delta = 0$, and the reflected wave remains plane polarized (see Figure 8a).

If the reflecting object is metallic, the relative phase shift will be other than zero and will be accompanied by a change in amplitude. The result is that the reflected wave is elliptically polarized as shown in Figure 8b. The ellipticity of the reflected wave will be changed by an additional amount if a thin insulating

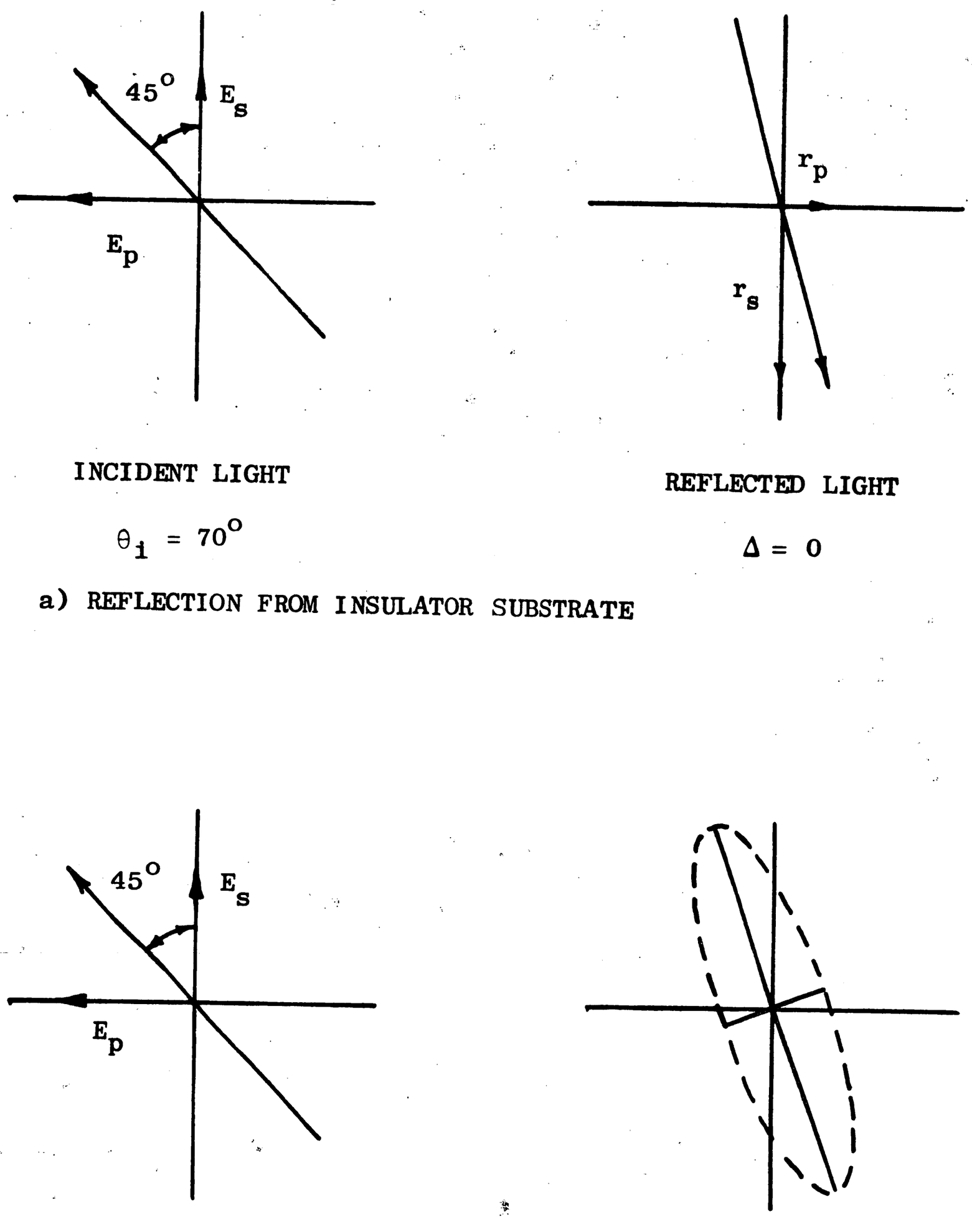

INCIDENT LIGHT

$\theta_i = 70^o$

REFLECTED LIGHT

$\Delta = 0$

a) REFLECTION FROM INSULATOR SUBSTRATE

INCIDENT LIGHT

$\theta_i = 70^o$

REFLECTED LIGHT

$\Delta \neq 0$

b) REFLECTION WITH METALLIC SUBSTRATE

FIGURE 8

Effect of Reflection on Linearly Polarized Light

film is present on the metallic surface.

Theoretical expressions can be derived using exact reflection theory which relate the changes in amplitude and phase to quantities measureable on the ellipsometer. A derivation of the reflection equations which relate index of refraction and film thickness to the phase change, Δ , and amplitude change, ψ , follows.

For reflection of plane polarized light at the plane interface between two isotropic media of index of refraction n_o and n_1, the ratio of reflected/incident amplitudes is given by:

$$r_{1p} = \frac{n_1 \cos \phi_o - n_o \cos \phi_1}{n_1 \cos \phi_o + n_o \cos \phi_1} \qquad (7)$$

$$r_{1s} = \frac{n_o \cos \phi_o - n_1 \cos \phi_1}{n_o \cos \phi_o + n_1 \cos \phi_1} \qquad (8)$$

These are the Fresnel (amplitude) reflection coefficients for plane polarized light in which the electric vector components lie parallel (p) and perpendicular (s) to the plane of incidence as shown in Figure 9. Equations (7) and (8) are obtained from the application of Maxwell's equations with appropriate boundary conditions.

The reflection of linearly polarized light from a metallic surface covered with an insulating film can be described in terms of the Fresnel equations[60]:

$$\frac{R_p}{E_p} e^{i\delta_p} = \frac{r_{1p} + r_{2p} e^{-ix}}{1 + r_{1p} r_{2p} e^{-ix}} \qquad (9)$$

$$\frac{R_s}{E_s} e^{i\delta_s} = \frac{r_{1s} + r_{2s} e^{-ix}}{1 + r_{1s} r_{2s} e^{-ix}} \qquad (10)$$

where:

$r_p = \frac{R_p}{E_p}$ = amplitude ratio of reflected wave component (R_s) and incident wave component (E_p).

$r_s = \frac{R_s}{E_s}$ = amplitude ratio of reflected wave component (R_s) and incident wave component (E_s).

δ_p = phase change of p wave component.

δ_s = phase change of s wave component.

r_{1p} = amplitude ratio, $\frac{R_{1p}}{E_{1p}}$, for single reflection of the p wave at the air - film interface.

r_{2p} = amplitude ratio, $\frac{R_{2p}}{E_{2p}}$, for single reflection of the p wave at the film - substrate interface.

r_{1s} = amplitude ratio, $\frac{R_{1s}}{E_{1s}}$, for single reflection of the s wave at the air - film interface.

r_{2s} = amplitude ratio, $\frac{R_{2s}}{E_{2s}}$, for single reflection of the s wave at the film - substrate interface.

x = optical path difference between the beams reflected at the air - film interface and those reflected at the film - substrate interface.

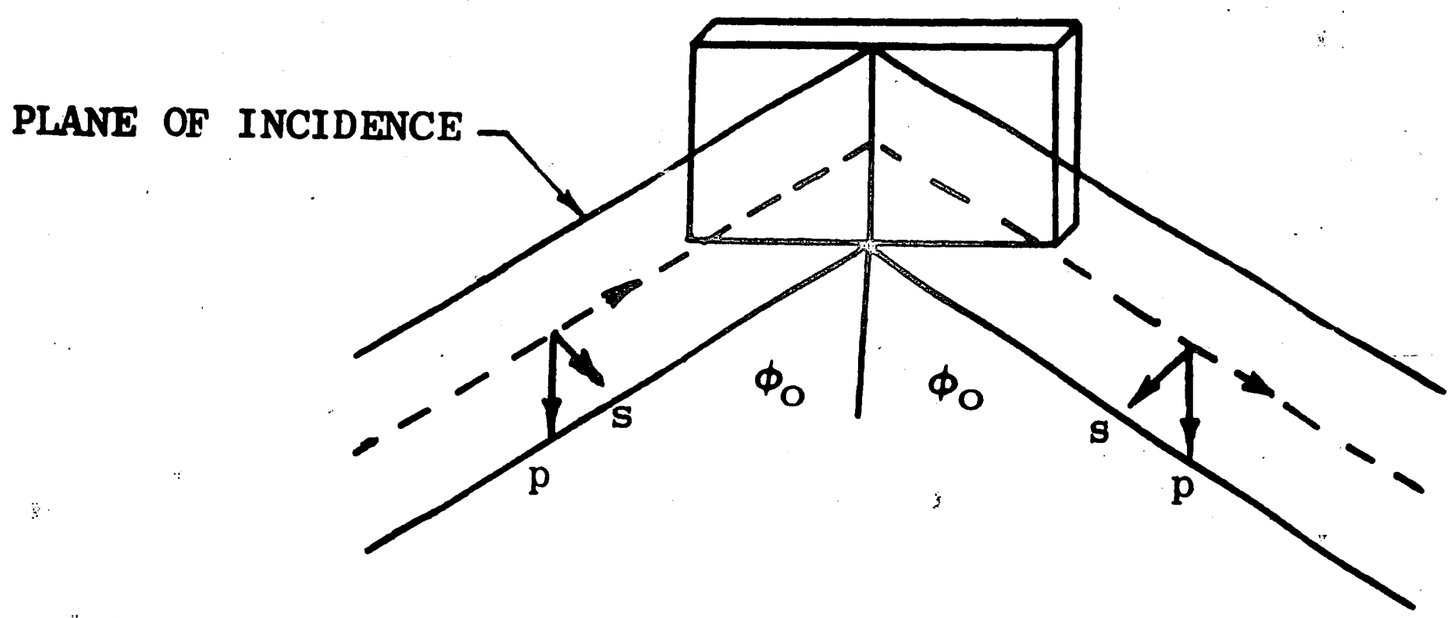

a.

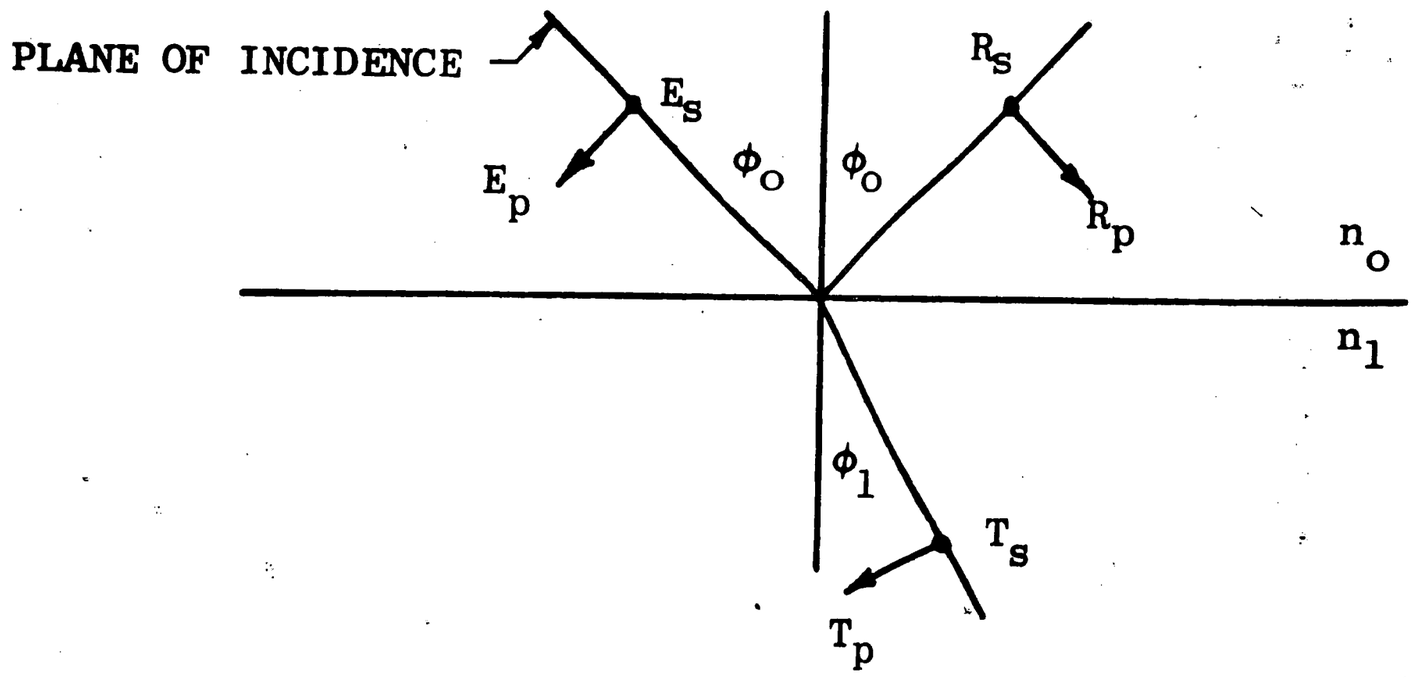

b.

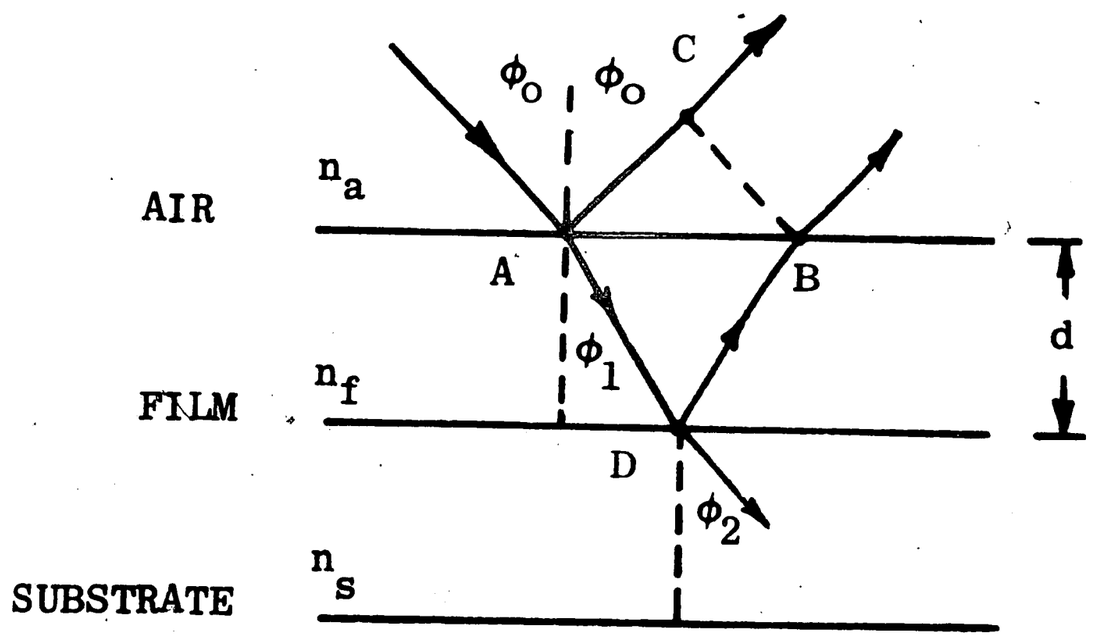

c.

FIGURE 9

(a) And (b) The Orientation of the S and P Wave Components for the Incident Plane Polarized Light at an Angle of 45^o to the Plane of Incidence. (c) The Reflection of Plane Polarized Light From a Film Coated Substrate.

Equations (9) and (10) are obtained by summing multiply reflected beams and represent the amplitude reflectance of the film - substrate combination.

The optical path difference can be written in terms of the thickness and index of refraction of the film. The path difference, x, between the ray reflected at the surface of the film and that traversing the film and reflected from the substrate is seen from Figure 9c to be

$$x = \left[(AD + DB)n_f - AC\right]\frac{2\pi}{\lambda} \tag{11}$$

The lengths AD, DB, and AC can be expressed in terms of the film thickness, d, and incidence and refraction angles, ϕ_o and ϕ_1, respectively. Thus,

$$x = \left[\frac{2dn_f}{\cos\phi_1} - \frac{2dn_f}{\cos\phi_1}\sin\phi_1 \sin\phi_o\right]\frac{2\pi}{\lambda} \tag{12}$$

This expression can be further simplified by substituting $\frac{\sin\phi_o}{n_f}$ for $\sin\phi_1$, which is permitted by Snell's law.

$$x = \left(\frac{2\pi}{\lambda}\right)2dn_f \cos\phi_1 \tag{13}$$

$n_f \cos\phi_1$ can be replaced by $n_f\sqrt{1 - \sin^2\phi_1}$, which in turn can be written as $\sqrt{n_f^2 - \sin^2\phi_o}$. This results in the final expression for the path difference in terms of n_f, ϕ_o, and d.

$$x = \left(\frac{2\pi}{\lambda}\right)2d\sqrt{n_f^2 - \sin^2\phi_o} \tag{14}$$

The azimuth of the restored plane of polarization is defined by

$$\tan\psi = r_p/r_s \tag{15}$$

and the phase change is defined by (6)

$$\Delta = \delta_p - \delta_s \tag{16}$$

The ratio of (9) and (10) gives the fundamental equation of ellipsometry.

$$\tan \psi \, e^{i\Delta} = \frac{r_{1p} + r_{2p} \, e^{-2i}}{1 + r_{1p} r_{2p} e^{-2i}} \cdot \frac{1 + r_{1s} r_{2s} e^{-2i}}{r_{1s} + r_{2s} e^{-2i}} \tag{17}$$

where

$$\delta = \frac{x}{2} = \frac{360}{\lambda} \, d \, (n_f^2 - \sin^2 \quad)^{\frac{1}{2}} \text{ degrees} \tag{18}$$

The ellipsometer measures Δ and ψ.

The Fresnel equations (7) and (8) written for the two boundaries, air - film and film - substrate, are as follows:

$$r_{1p} = \frac{n_f \cos \phi_o - n_a \cos \phi_1}{n_f \cos \phi_o + n_a \cos \phi_1}$$

$$r_{1s} = \frac{n_a \cos \phi_o - n_f \cos \phi_1}{n_a \cos \phi_o + n_f \cos \phi_1} \tag{19}$$

$$r_{2p} = \frac{n_s \cos \phi_1 - n_f \cos \phi_2}{n_s \cos \phi_1 + n_f \cos \phi_2}$$

$$r_{2s} = \frac{n_f \cos \phi_1 - n_s \cos \phi_2}{n_f \cos \phi_1 + n_s \cos \phi_2}$$

The indices of refraction and angles of incidence, reflectance, and refraction are defined in Figure 9c.

Substitution of (19) and (18) into (17) and replacing cos ϕ_1 and cos ϕ_2 by functions of (ϕ_o, n_f) and (ϕ_o, n_s) respectively by use of Snell's law give an expression for $\tan \psi \, e^{i\Delta}$ which is a function of n_a, n_f, n_s, d, ϕ_o, and λ . Since all these quantities except n_f and d are independently determined or are fixed constants, a solution for n_f and d can be obtained from the ψ and Δ quantities obtained from ellipsometer measurements by solving the equation using an iteration process or computer generated tables or graph.

Archer[61], with the aid of a computer, showed that the exact reflection theory can be used to determine the optical constants of surface films without the thickness limitations of approximate theory. He measured index of refraction and thickness for a variety of different films on silicon and concluded that the accuracy of thickness determinations is about $\pm$ 5Å, and about $\pm$ .004 for the index of refraction.

A plot of Δ versus ψ as a function of index of refraction and δ , or thickness, was constructed by Archer by programming the expressions for Δ and ψ on an IBM 7090 computer using the following fixed constants: angle of incidence 70.00°, wavelength 5461Å, and the complex index of refraction of the silicon substrate of 4.050 - 0.028i. A copy of this plot of approximate size one meter square was used in this experiment to obtain a graphical solution to equation 17.

Each curve in the graph is the locus of points of increasing thickness for a film of constant index of refraction. Δ and ψ are

cyclic functions of δ , or thickness, and repeat periodically every 180^{o} change in δ . For a film having an index of refraction of 1.95, this corresponds to a thickness period of 1600Å. Consequently, an approximate thickness within this range must be known.

A significant property of the dependence of Δ and ψ on the index of refraction of transparent films is that no two curves overlap or intersect except for very low and very high indices of refraction. Consequently, for all practical purposes, each point in the plane corresponds to a unique value of index of refraction and thickness of the film.

A schematic diagram of the ellipsometer used, a Gaertner Scientific Corporation model L118GT, is shown in Figure 10 along with the light source, monochromator, and detector portions of a Zeiss II spectrophotometer. A photograph of the ellipsometer is shown in Figure 11. Collimated light from the monochromator is linearly polarized by the Nicol prism polarizer and passes through the quarter - wave plate and is incident on the sample. The reflected light passes through the Nicol prism analyzer and into the detector. The quarter - wave plate compensates for any ellipticity in the reflected light, and thus restores it to linear polarization which can be extinguished by the analyzer. The analyzer, polarizer, and quarter wave plate are all mounted on divided circles which are free to rotate through 360^{o}; angles can be read to the nearest tenth of a degree.

A typical setting of the compensator and analyzer for extinction

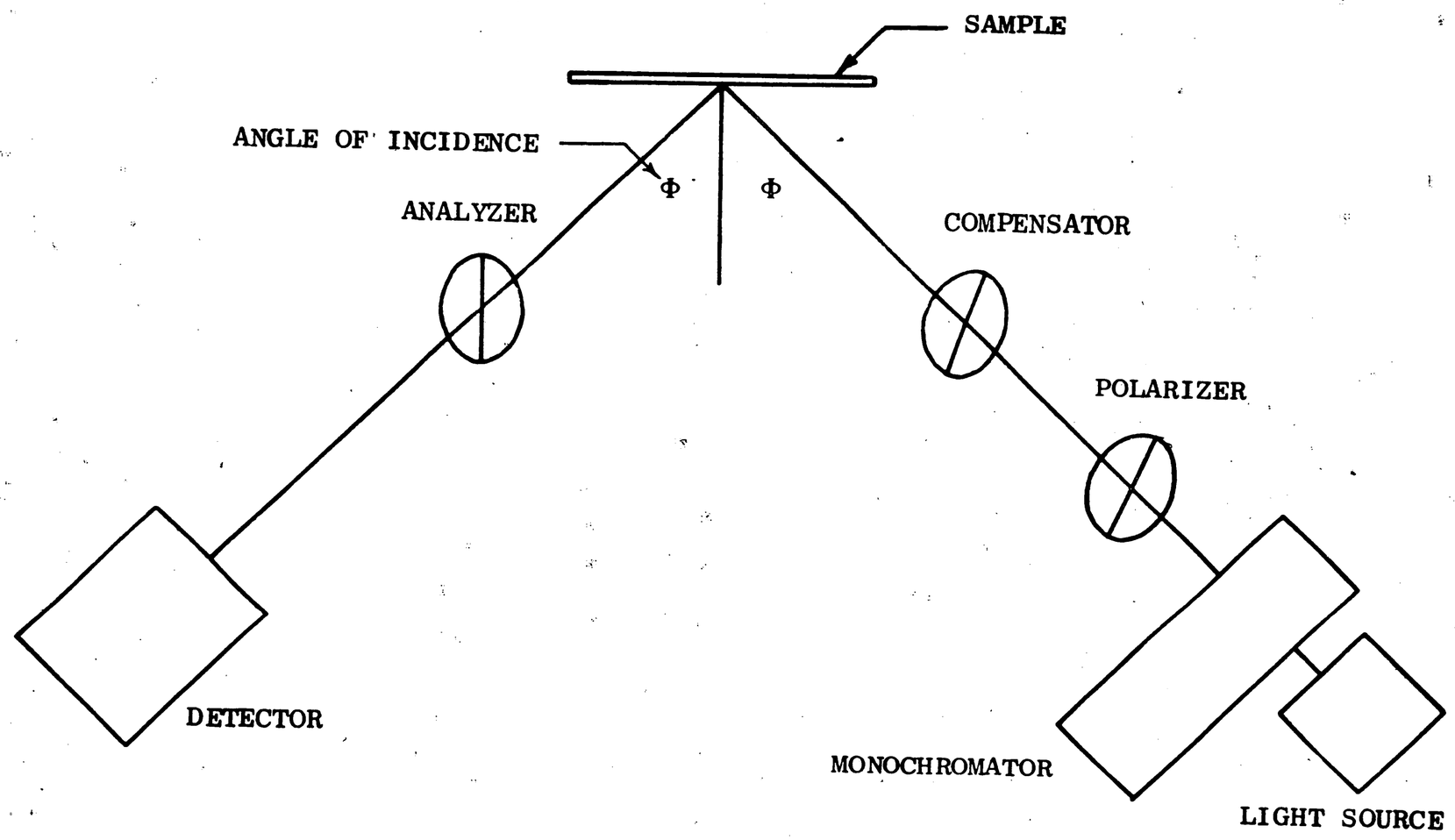

FIGURE 10

Schematic Diagram of Ellipsometer and Photodetector

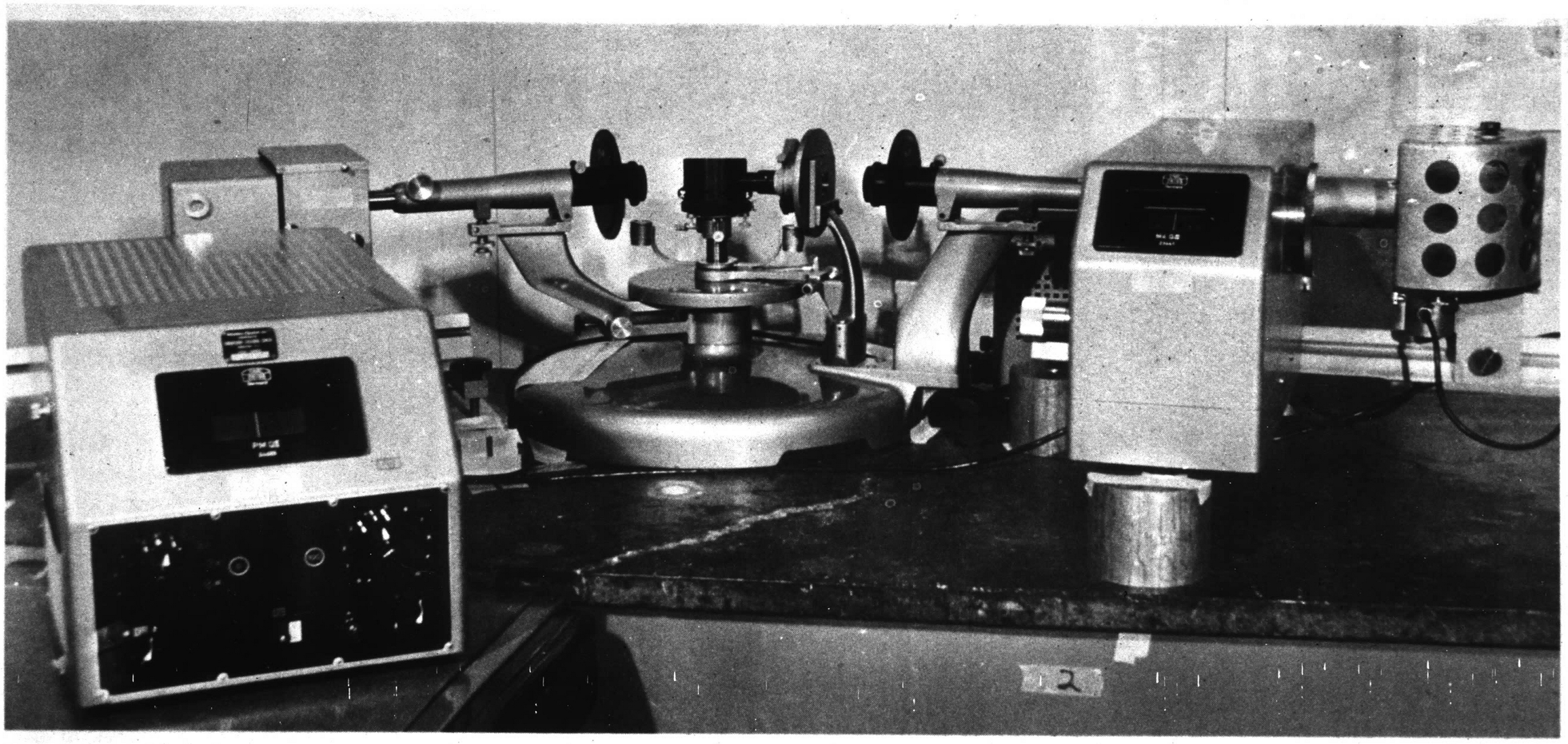

FIGURE 11

Photograph of the Ellipsometer and Spectrophotometer Used to Measure Film Thickness and Index of Refraction

of an elliptically polarized reflection for an incident polarization of 45^{o} is shown in Figure 12. The fast axis of the quarter wave plate is adjusted to coincide with the major axis of the ellipse. This restores the light to linear vibration in the direction shown which is dependent on the ratio of major to minor axis of the ellipse. Hence ψ is related to the analyzer setting required to extinguish the light. The rotation of the ellipse, determined by the quarter - wave plate setting, is related to the relative phase change between the p and s waves, or Δ .

If the fast axis of the quarter - wave plate is fixed at 45^{o}, the beam reflected from the sample can be extinguished by adjusting the analyzer and polarizer orientations. Normally, angles are measured relative to a coordinate system in which the positive z-axis is in the direction of propagation of the light beam and the xz plane is the plane of incidence. If the settings of the polarizer and analyzer at extinction are designated as P_o and A_o respectively, the relation of Δ and ψ to P_o and A_o is[61]

$$\tan \Delta = \sin \delta_q \tan (90^{o} - 2P_o) \qquad (20)$$

$$\tan \psi = \cot L \tan (-A_o) \qquad (21)$$

where

$$\cos 2L = -\cos \delta_q \cos 2P_o \qquad (22)$$

δ_q is the relative retardation of the quarter wave plate and is very close to 90^{o} for a wavelength of 5461Å. Hence (20) reduces to

$$\Delta = 90 - 2P_o \qquad (23)$$

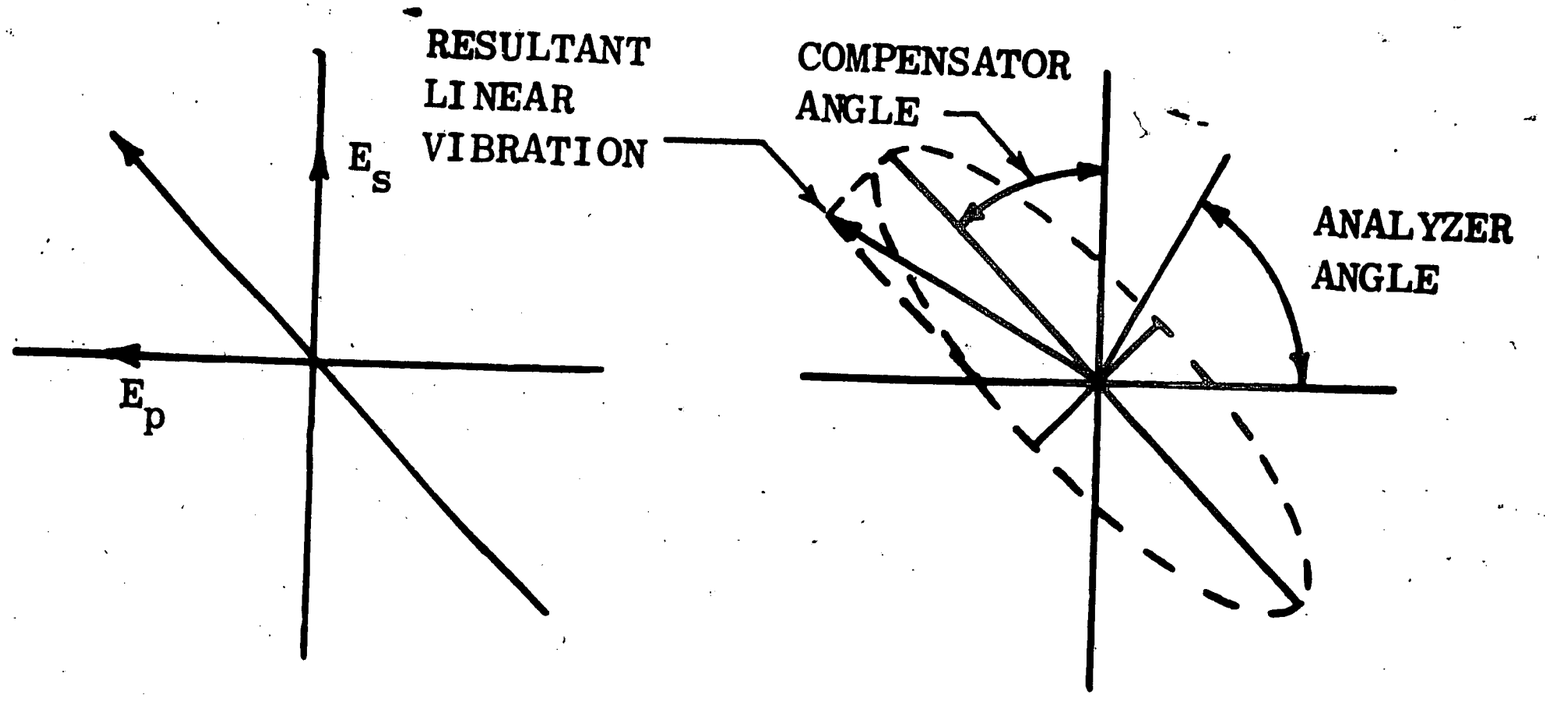

FIGURE 12

Effect of Reflection From a Transparent Film on a Metalic Substrate on Linearly Polarized Light.

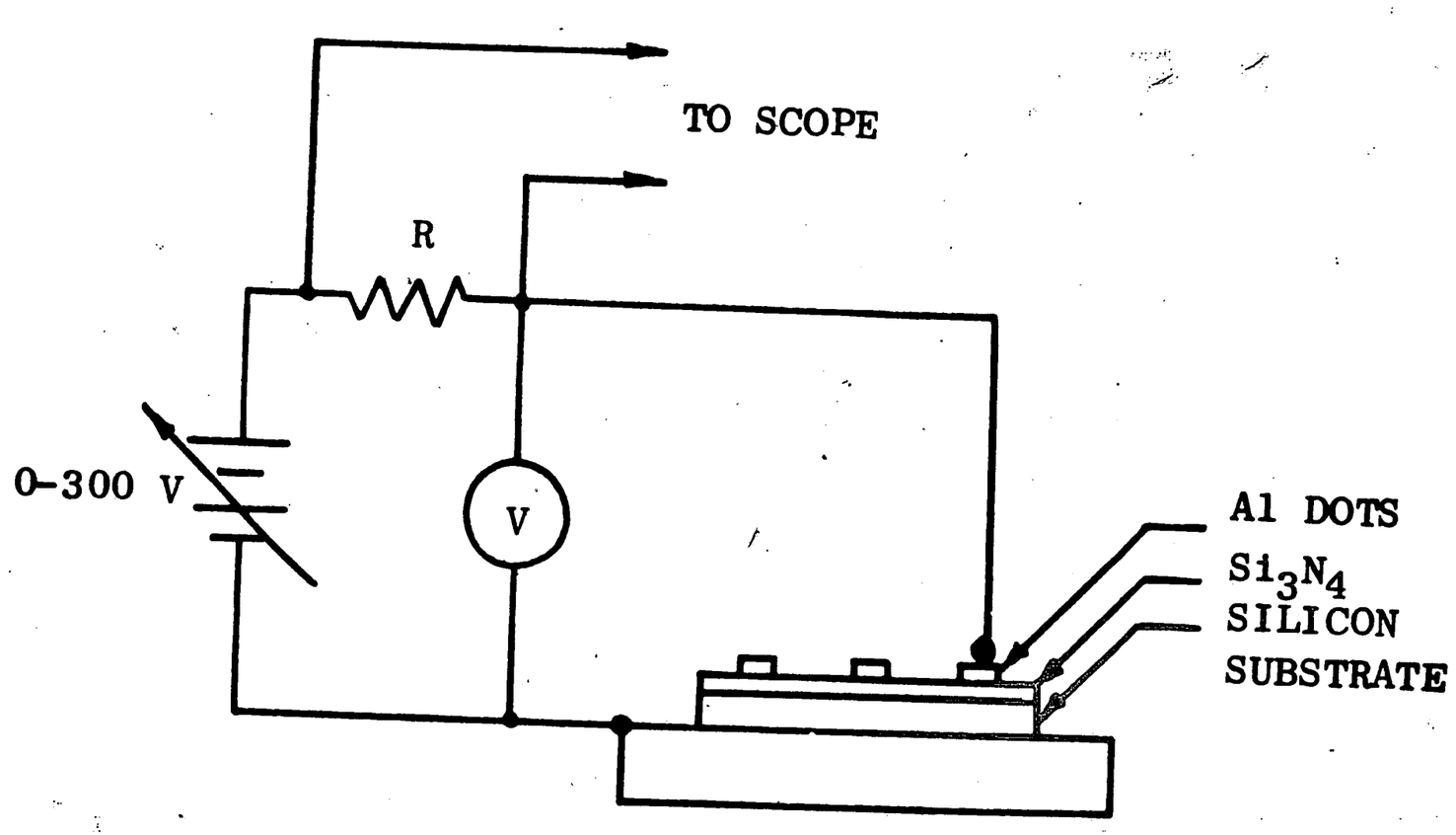

FIGURE 13

Schematic Diagram of Test Circuit For Dielectric Strength Measurements

and (21) becomes

$$\psi = -A_o \tag{24}$$

Density

The density of the silicon nitride films was determined using thickness and microbalance weight measurements to calculate the density. The weight of the silicon nitride film was determined by weighing the silicon substrate before and after depositing the silicon nitride film. For weight changes of 100 micrograms and thicknesses of about 1000Å, the accuracy of the density measurements is about $\pm$ 4%.

Dielectric Strength

When an insulator is placed between two metal plates and a large electric field is applied, a relative large current will flow between the plates when the electric field reaches a critical value. This critical field is called the dielectric strength of the insulator. The breakdown processes in insulators are not well understood, but it is possible to distinguish five distinct processes[62]:

1. Thermal breakdown is produced when ionic currents generate heat at a rate greater than it can be dissipated by the insulator. Since the heat conductivity of insulators is small, it is possible that temperatures greater than the melting point are attained in parts of the insulator. This melting enhances ionic mobilities and electrical breakdown occurs.

2. Electrolytic breakdown can occur when conducting paths form with the aid of dislocations, grain boundaries, or other imperfections in the insulator.

3. Dipole breakdown may be caused by polarizable atoms (molecules) or permanent dipoles already present in the insulator. When such dipoles surround a stressed region, they can produce local imperfection or impurity states lying in the forbidden - energy gap of the insulator, and the lower ionization potential of electrons attached to dipoles then facilitate breakdown.

4. Collision breakdown may occur when impurities in the insulator produce some electrons available for conduction. When the energy of these electrons become sufficiently great they collide, producing ever-increasing numbers of electrons and holes and avalanche breakdown occurs similar to that in semiconductors.

5. Gas - discharge breakdown can occur in insulators that contain occluded gas bubbles. The electric field required to ionize the gas ($\sim 10^4$ volts/cm) is much less than that required for breakdown in an insulator ($\sim 10^6$ volts/cm). The gas ionizes and then bombards the insulator's internal surfaces, causing them to deteriorate, until breakdown occurs.

One of the electrical contacts to the insulator film is the silicon substrate, and the other is .010 inch diameter aluminum dots

evaporated on the film surface. The dots, 9 per wafer, are spaced uniformly over the film surface. Contact to the dots is made using a micrometer probe. The breakdown potential of the films is measured using the test setup shown in Figure 13. The DC potential applied to the silicon nitride film is increased until breakdown occurs; this is evidenced by an instantaneous voltage appearing across the resistor, R, and displayed on the oscilloscope. The ratio of this open circuit potential to film thickness is the breakdown or dielectric strength of the film.

Energy Gap

Optical transmission measurements were used to determine the energy gap of the silicon nitride films. The optical absorption was obtained as a function of wavelength using a split beam Carey 14 recording spectrophotometer operating in the 0.20 to 0.40μ range. Films having thicknesses from 900 to 6400$\mathring{A}$ on fused quartz substrates were used for all measurements.

Optical absorption in solids may be divided into the following principal processes[63]:

1. Excitation of electrons across the gap from the valence band to the conduction band.
2. Formation of excitons.
3. Excitation of lattice vibrations.
4. Absorption due to the excitation of electrons and holes within allowed bands.
5. Absorption due to the presence of imperfections.
6. Excitation of electrons and holes from one band to another of the same type.

Of all the absorption processes listed, only the one involving excitation of electrons from the valence band to the conduction band is useful in determining the energy gap. The selection rule which determines whether or not the transition across the gap is allowed is that $\Delta k = 0$, i.e., a transition indicated by a vertical line on an E versus k plot, where k is the wave number and E is energy[66]. Such vertical or direct transitions are the only important transitions when the minima of the conduction band lie at the same part of k space as the maxima of the valence band. In Ge and Si and probably in many other materials, the conduction and valence band extrema are not located at the same value of k. In this case there is the possibility of indirect transitions, $\Delta k \neq 0$, as well as direct transitions, $\Delta k = 0$.

Theoretical expressions have been derived[64,67,68] which permit discrimination between direct and indirect transitions on the basis of both the magnitude of the absorption coefficient and the dependence of absorption coefficient on photon energy. The absorption coefficient usually reaches 10^4 to 10^5 cm^{-1} for direct transitions and 10 to 10^3 cm^{-1} for indirect transitions. The dependence of absorption coefficient, α, on photon energy, $h\nu$, and energy gap, Eg, for allowed transitions at $k = 0$ is[68]

$$\alpha^2 \propto h\nu - Eg \qquad (25)$$

for direct transitions, and

$$\alpha^{\frac{1}{2}} \propto h\nu - Eg \qquad (26)$$

for indirect transitions.

If the transition at k = 0 is not allowed, then

$$\alpha^{2/3} \propto h\nu - Eg \tag{27}$$

for direct transitions and

$$\alpha^{1/3} \propto h\nu - Eg \tag{28}$$

for indirect transitions.

In practice, for allowed transitions for example, α^2 is plotted against photon energy to give a straight line for direct transitions. The extrapolated intercept of this straight line with the energy axis gives the energy gap for direct transitions.

If sample imperfections or the spectral bandwidths used experimentally are such that interference effects are not resolved, the observed transmission is[69]

$$T = \frac{(1-R)^2(1+\frac{k^2}{n^2})}{e^{\alpha d} - R^2 e^{-\alpha d}} \tag{29}$$

where

α = absorption coefficient in cm^{-1}

d = film thickness in cm

R = reflectivity of sample

n = index of refraction

k = extinction coefficient

In any practical experiment on insulatons, $k^2 << n^2$ and $e^{2\alpha d} >> R^2$ so that (29) becomes

$$T = (1-R)^2 e^{-\alpha d} \tag{30}$$

If (30) is inverted and the log is taken of both sides, then

$$\log 1/T = \log \frac{1}{(1-R)^2} + \frac{\alpha d}{2.306} \qquad (31)$$

Thus, the log 1/T versus d curve is a straight line at a particular wavelength of radiation with the intercept on the log 1/T axis of $\log \frac{1}{(1-R)^2}$. Hence R can be solved for directly. This method was used to determine R for the silicon nitride films used in this investigation.

The transmission absorption measurements can now be used to determine the absorption coefficient as a function of photon energy. The absorption coefficient, from (31), is given by

$$\alpha = \left[\log 1/T - \log\left(\frac{1}{1-R}\right)^2\right] \frac{2.306}{d} \qquad (32)$$

Since log 1/T is given as a function of photon energy by the transmission absorption measurements, α can be determined as a function of photon energy and used to determine the energy gap as discussed previously.

Infrared Spectra

The infrared absorption spectra was determined at wavelengths of 1.5 to 15 microns with a Beckman IR-4 double beam spectrophotometer. Transmission spectra were determined for 1 micron thick films of silicon nitride on 0.007 inch thick silicon wafers relative to air. The scanning speed was 2 microns/min.

RESULTS

Index of Refraction

The index of refraction of the silicon nitride films prepared at substrate temperatures from 200° to 600°C and plasma currents from 1 to 5 amperes is in the range of 1.93 to 2.08. The average value is 1.97. The dependence of index of refraction, n, on substrate temperature and plasma current are shown in Figure 14 for deposition rates less than 300 Å/min. Each point on the graph represents the average value of n for the particular deposition conditions. The index of refraction has a slight variation with temperature and plasma current, but no definite relationship can be established.

Film density was found to be approximately linear with index of refraction as shown in Figure 16. The index of refraction approaches the crystalline value of 2.1 as the density approaches the theoretical value of 3.18 g/cm^3. If the curve is extrapolated to lower levels, it intersects the axes at the origin as expected.

Density

The density of the silicon nitride films prepared at deposition rates less than 300 Å/min. ranges from 2.90 to 3.14 g/cm^3. At deposition rates greater than 300 Å/min., the density decreases with increasing sputtering rate. This decrease in density is accompanied by a decrease in the index of refraction as illustrated by Figure 16. The dependence of density on deposition rate is shown in Figure 15.

Dielectric Strength

The dielectric strength of the silicon nitride films did not

vary significantly over the range of temperature and plasma current studied. The average dielectric strength of the films is about $6x10^6$ V/cm and does not vary appreciably with index of refraction as shown in Figure 17. The range of dielectric strength is from 0.2 to $2.2x10^7$ V/cm for n from 1.8 to 2.08.

Energy Gap

Before the energy gap of the silicon nitride films can be found, it is first necessary to determine the film reflectivity, R, in the region of the absorption edge. It was shown in equation (31)

$$\log 1/T = \log 1/(1-R)^2 + \alpha d/2.306 \qquad (31)$$

that a plot of log 1/T versus d should be a straight line at a fixed wavelength of light. If this straight line is extrapolated to zero film thickness, the value of log 1/T at the intercept point on the log 1/T axis will be equal to log $1/(1-R)^2$ which can be solved for R.

Figures 18, 19, and 20 are plots of log 1/T versus film thickness for films prepared at deposition rates of 200, 636, and 1600 Å/min. respectively. The dependence yields a series of straight lines with a different line for each value of wavelength. The extrapolation to zero thickness gives an intersection at a common point on the log 1/T axis. The wavelengths used in the plots are at the ultraviolet absorption edge of the films. The values of R thus determed are .06, .04, and .01 for films prepared at depositions rates of 200, 636, and 1600 Å/min. respectively. Since the index of refraction decreases with increasing deposition rate, it follows that the value of R should decrease with decreasing index of refraction.

With the values of R determined above, equation 32 can be solved for the absorption coefficient, α, as a function of photon energy. Equation (25) relates photon energy to the absorption coefficient for allowed direct transitions.

$$\alpha^2 \propto h\nu - Eg \qquad (25)$$

Thus a plot of α^2 versus $h\nu$ should be a straight line in the region of the absorption edge. If this straight line is extrapolated to the energy axis, the intercept is the value for the energy gap of the film. Figures 21, 22, and 23 are plots of α^2 versus $h\nu$ for films deposited at rates of 200, 636, and 1600 Å/min. respectively. The points in the region of the absorption edge fall on a straight line as predicted by equation 25. The values of energy gap determined from these curves are 5.72, 5.81, and 5.90 eV for films prepared at deposition rates of 200, 636, and 1600 Å/min. respectively. The peak absorption coefficients are 1.89×10^5, 1.22×10^5, and 1.6×10^4 cm^{-1} in the order of increasing deposition rate for the above films.

Figure 24 shows the dependence of index of refraction on energy gap of the silicon nitride films. The index of refraction decreases rapidly with increasing energy gap to a value of n of about 1.50 where the slope becomes more gradual.

Infrared Spectra

Infrared spectra plotting transmission versus wave number in cm^{-1} of six samples of silicon nitride prepared under varying conditions are shown in Figures 25, 26, and 27. Sample 25-1 of Figure 25 was prepared at a substrate temperature of 600°C and a

plasma current of 5.0 amperes. Sample 25-2 was prepared at a substrate temperature of 400°C and a plasma current 1.0 ampere. The deposition rate of both samples was 230 Å/min. An absorption peak occurs over a broad range from 10.1 to 11.9 μ and from 10.8 to 11.3 μ for samples 25-2 and 25-1 respectively.

The samples in Figures 26 and 27 were prepared at a substrate temperature of 400°C and a plasma current of 5.0 amperes. The deposition rate for samples 30-1 and 28-4 was 500 and 1000 Å/min. respectively, and that for samples 28-2 and 28-3 was 630 and 1600 Å/min. respectively. The absorption peak for all four samples occurs at about 11.1 μ. An expanded plot of transmittance versus wavelength in the region of the absorption peak is shown in Figure 28.

Etch Rate

The etch rate of the silicon nitride films in buffered HF as a function of index of refraction is shown in Figure 29. The buffered HF was prepared by dissolving 40 grams of NH_4F in 60 cc of deionized water and adding 15 cc of concentrated HF (49%). The etch rate was found to increase with decreasing film density.

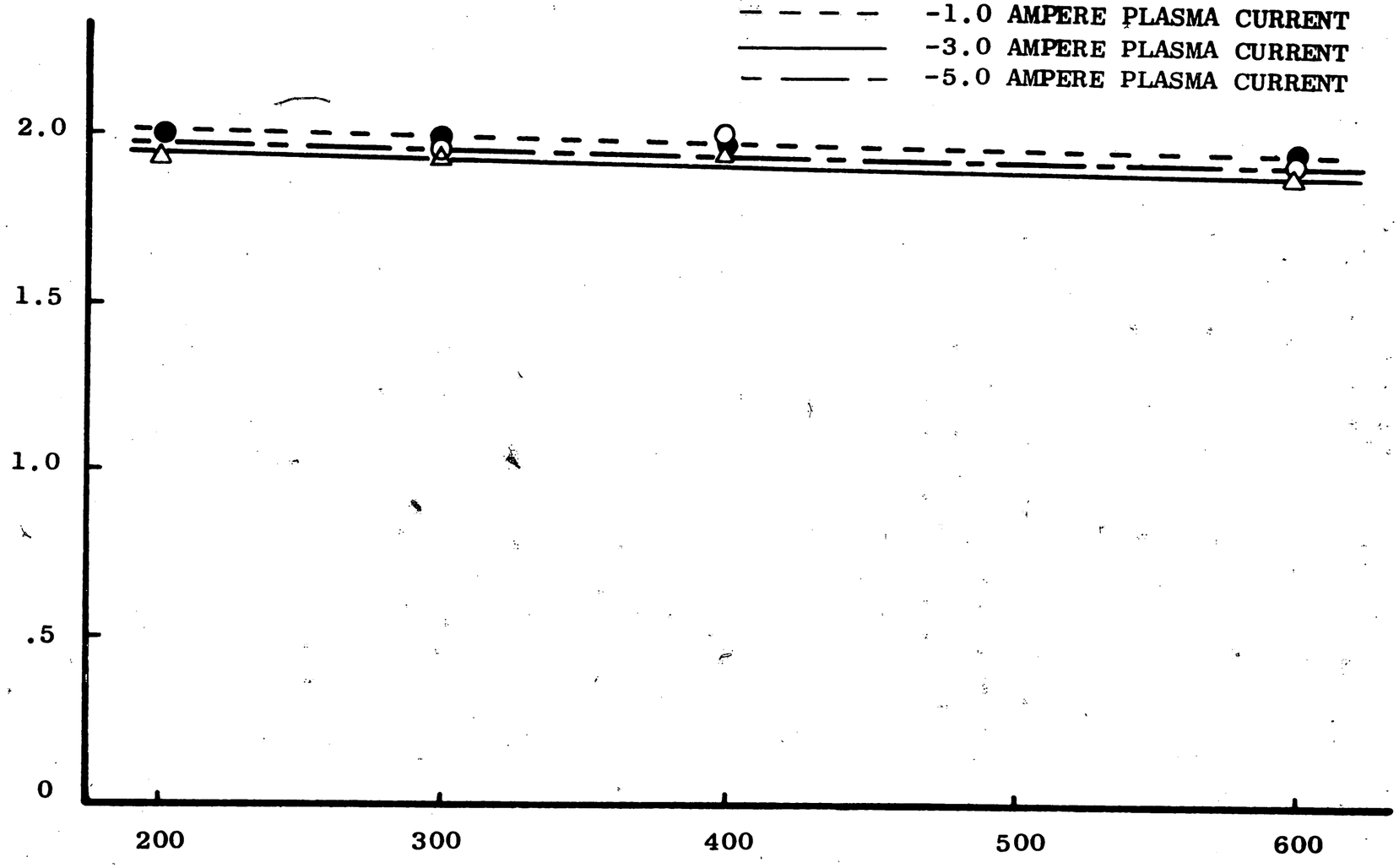

FIGURE 14

Index of Refraction Versus Substrate Temperature of Silicon Nitride Films

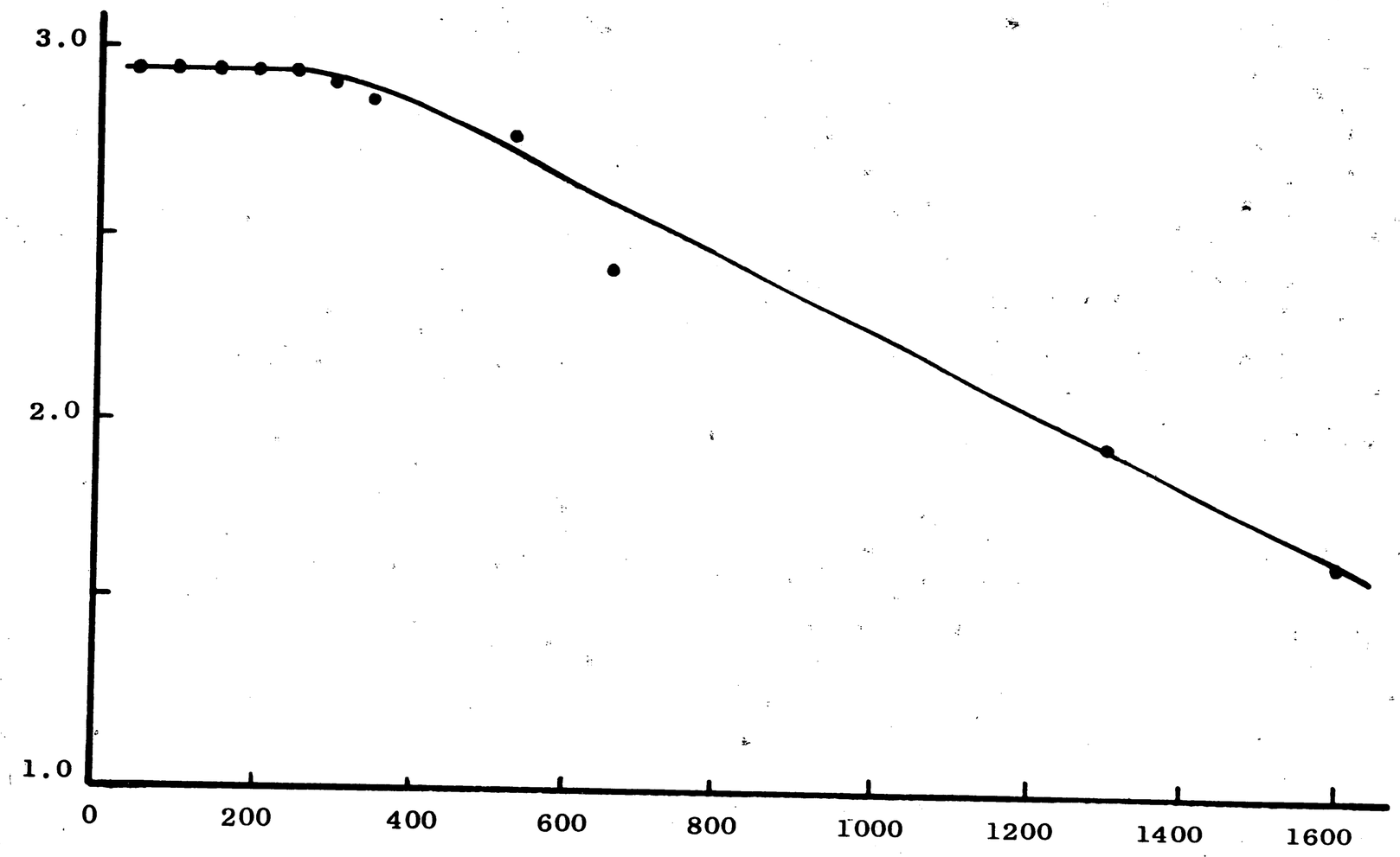

FIGURE 15

Density Versus Deposition Rate of Silicon Nitride Films

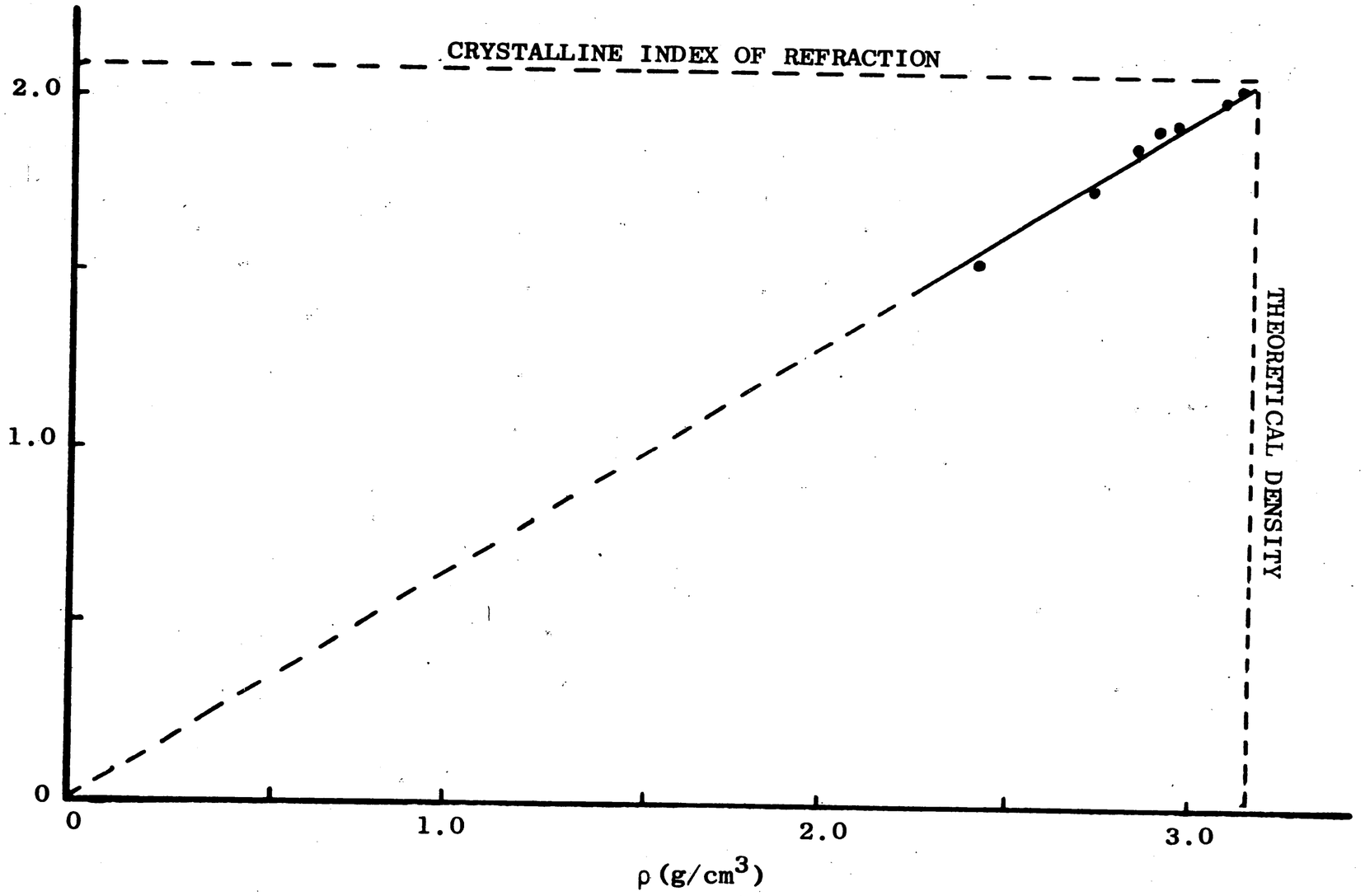

FIGURE 16

Index of Refraction Versus Density of Silicon Nitride Films

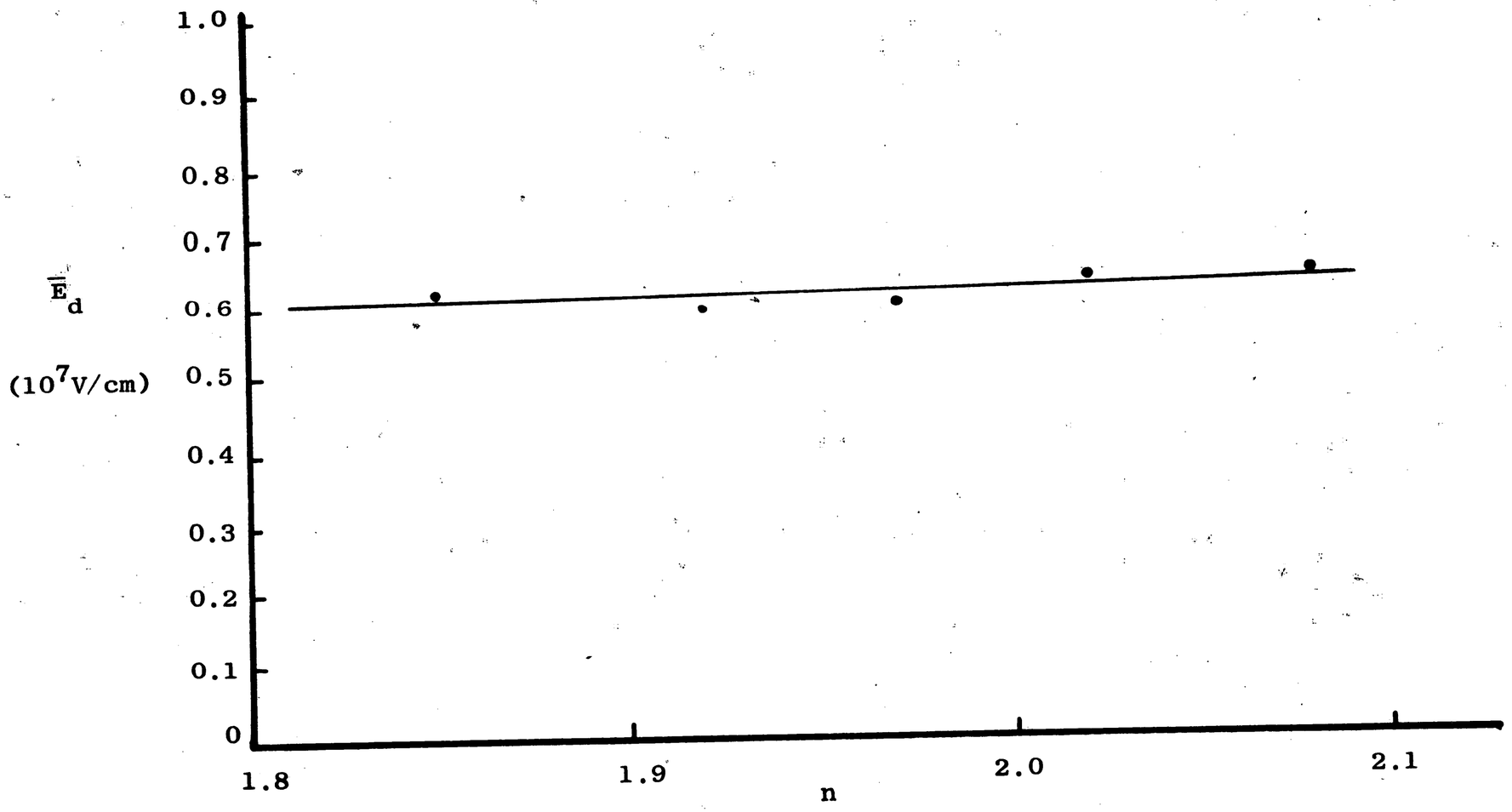

FIGURE 17

Dielectric Strength Versus Index of Refraction of Silicon Nitride Films

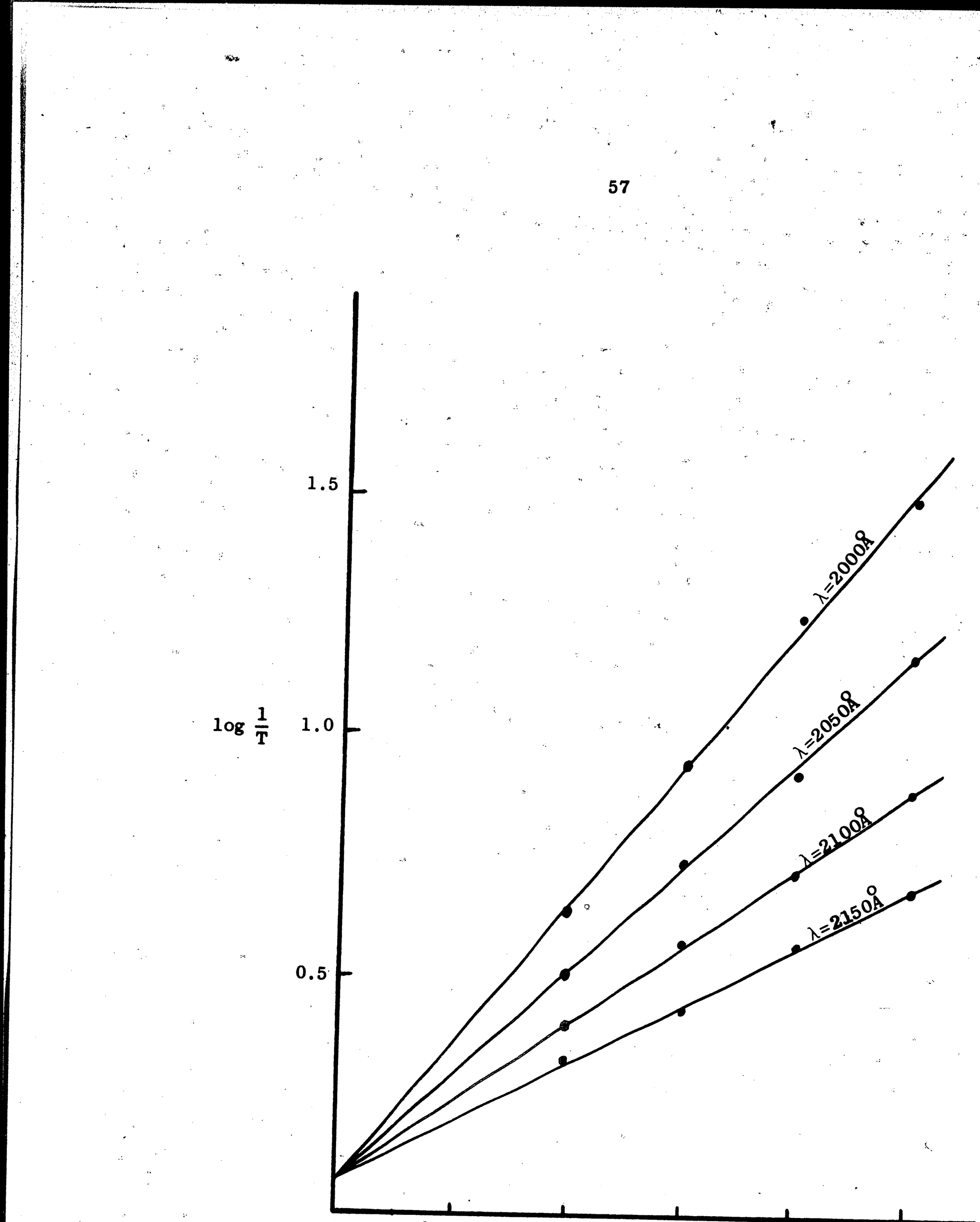

FIGURE 18

Optical Density ($\log \frac{1}{T}$) Versus Film Thickness for Films Deposited at a Rate of 200 A/min. The Reflectivity, R, was Determined to be 0.06.

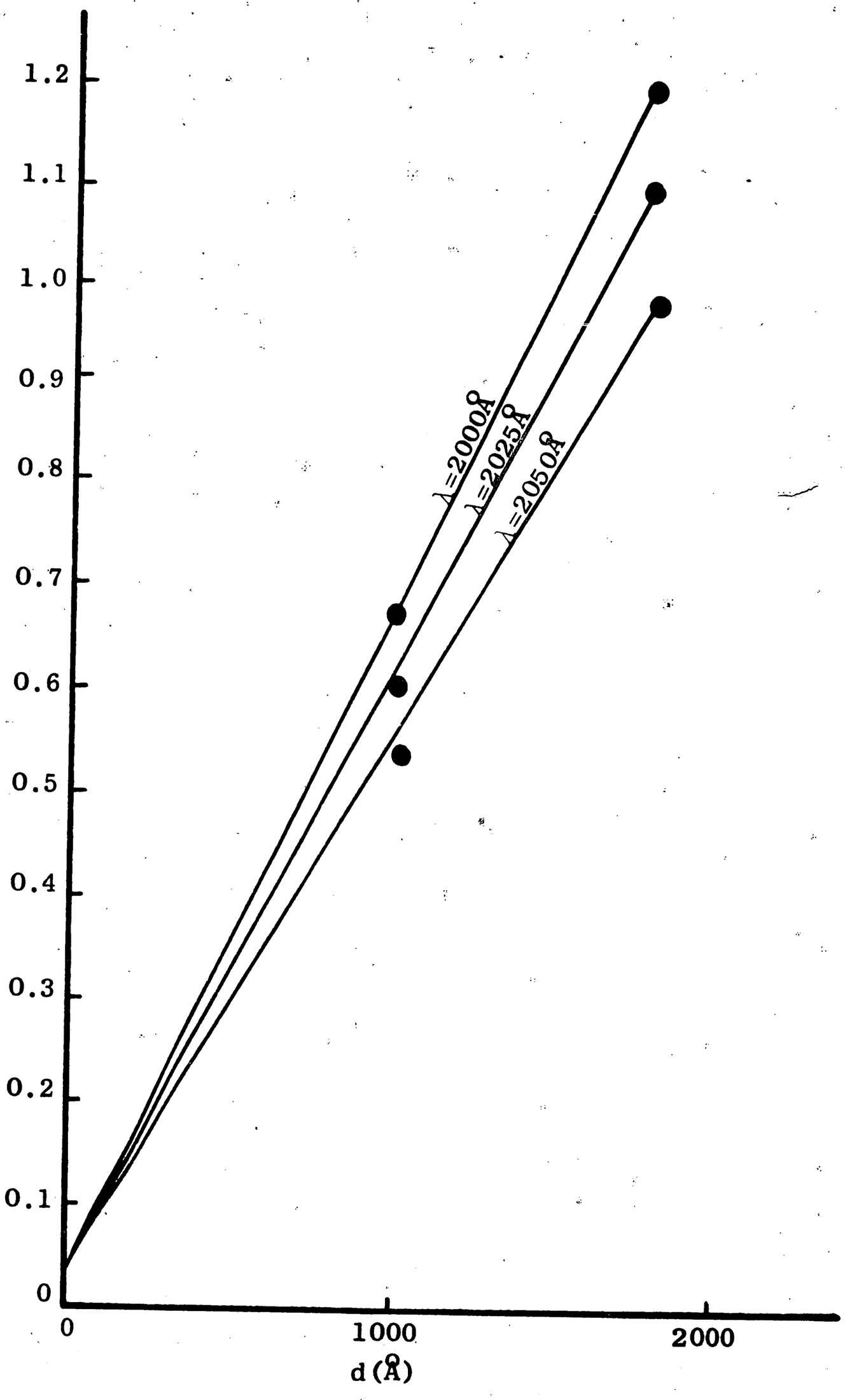

FIGURE 19

Optical Density ($\log \frac{1}{T}$) Versus Film Thickness for Films Deposited at a Rate of 636Å/min. The Reflectivity, R, was Determined to be 0.04.

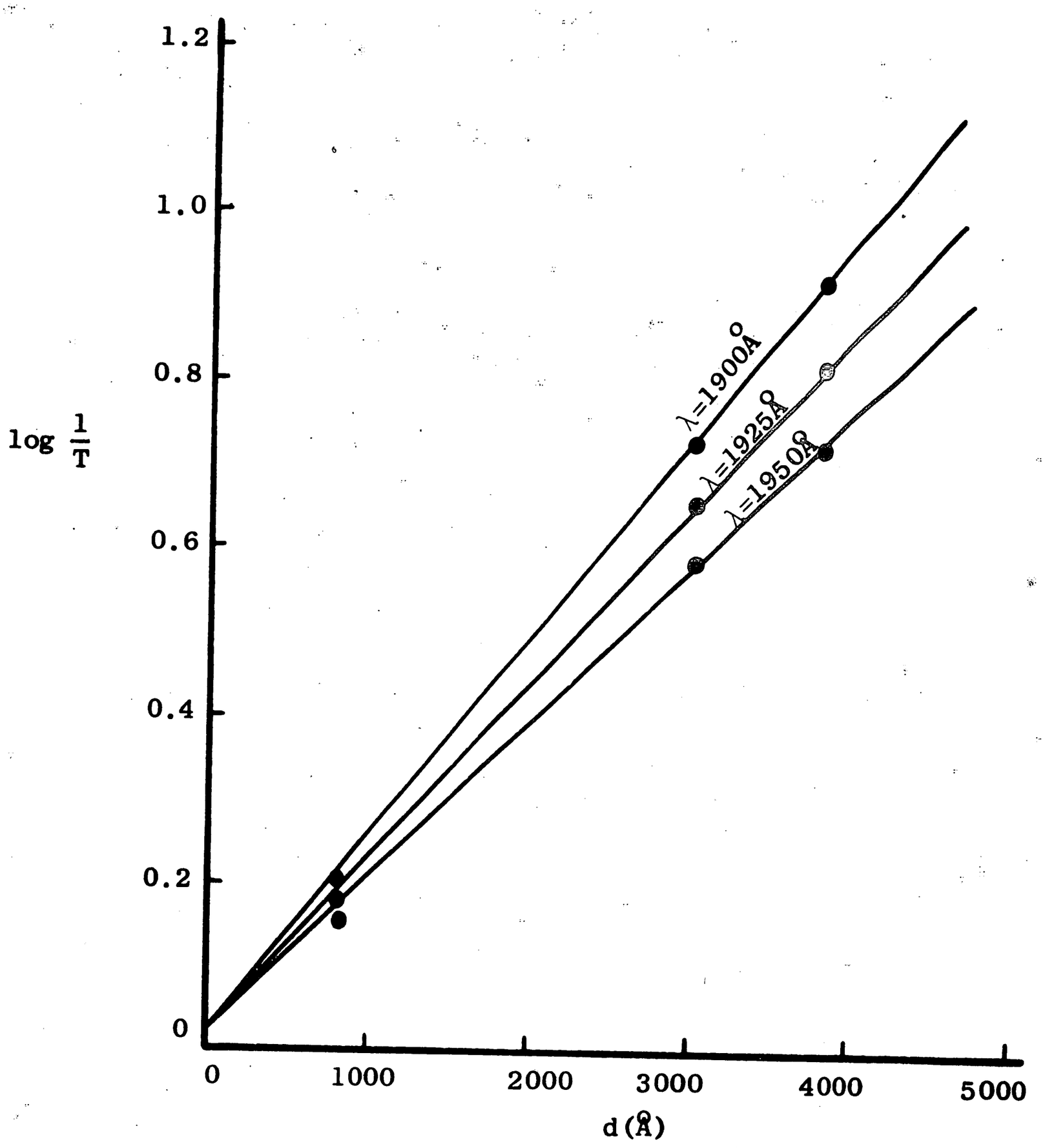

FIGURE 20

Optical Density ($\log \frac{1}{T}$) Versus Film Thickness for Films Deposited at a Rate of 1600 Å/min. The Reflectivity, R, was Determined to be 0.01.

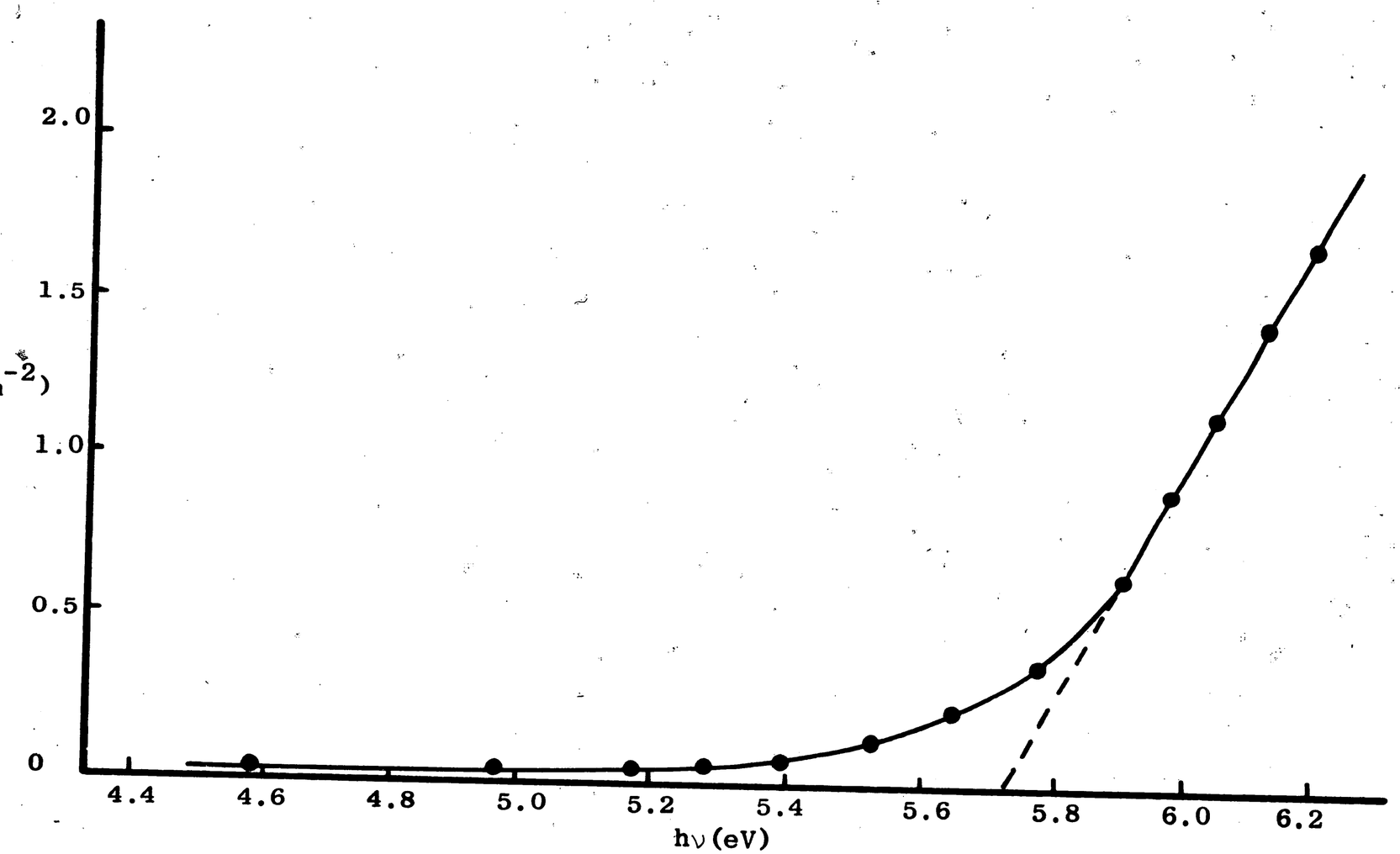

FIGURE 21

Absorption Coefficient Versus Photon Energy of Silicon Nitride Films Grown at a Rate of 200 Å/min. The Energy Gap is 5.72 eV.

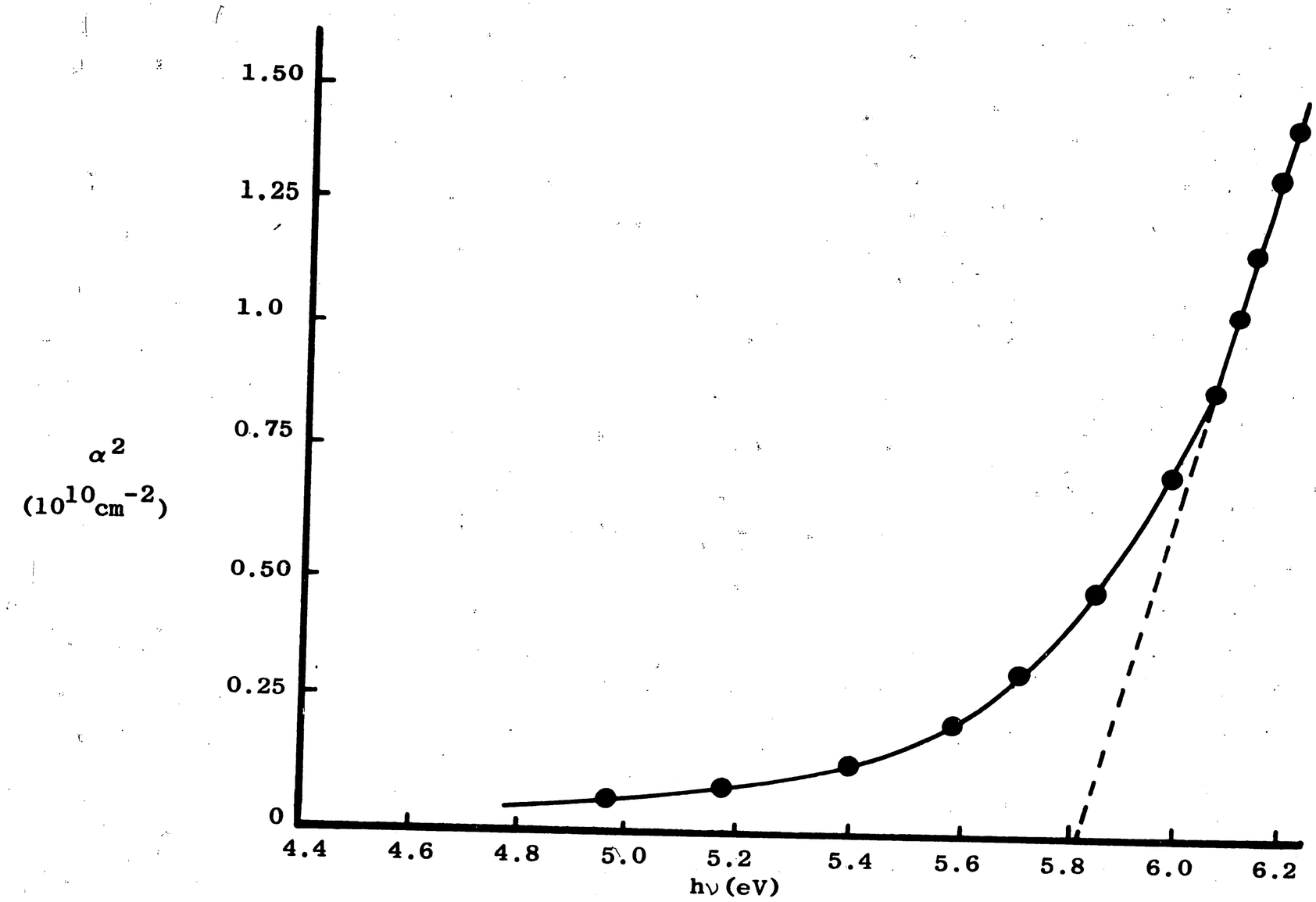

FIGURE 22

Absorption Coefficient Versus Photon Energy of Silicon Nitride Films Grown at a Rate of 636 Å/min. The Energy Gap is 5.81 eV.

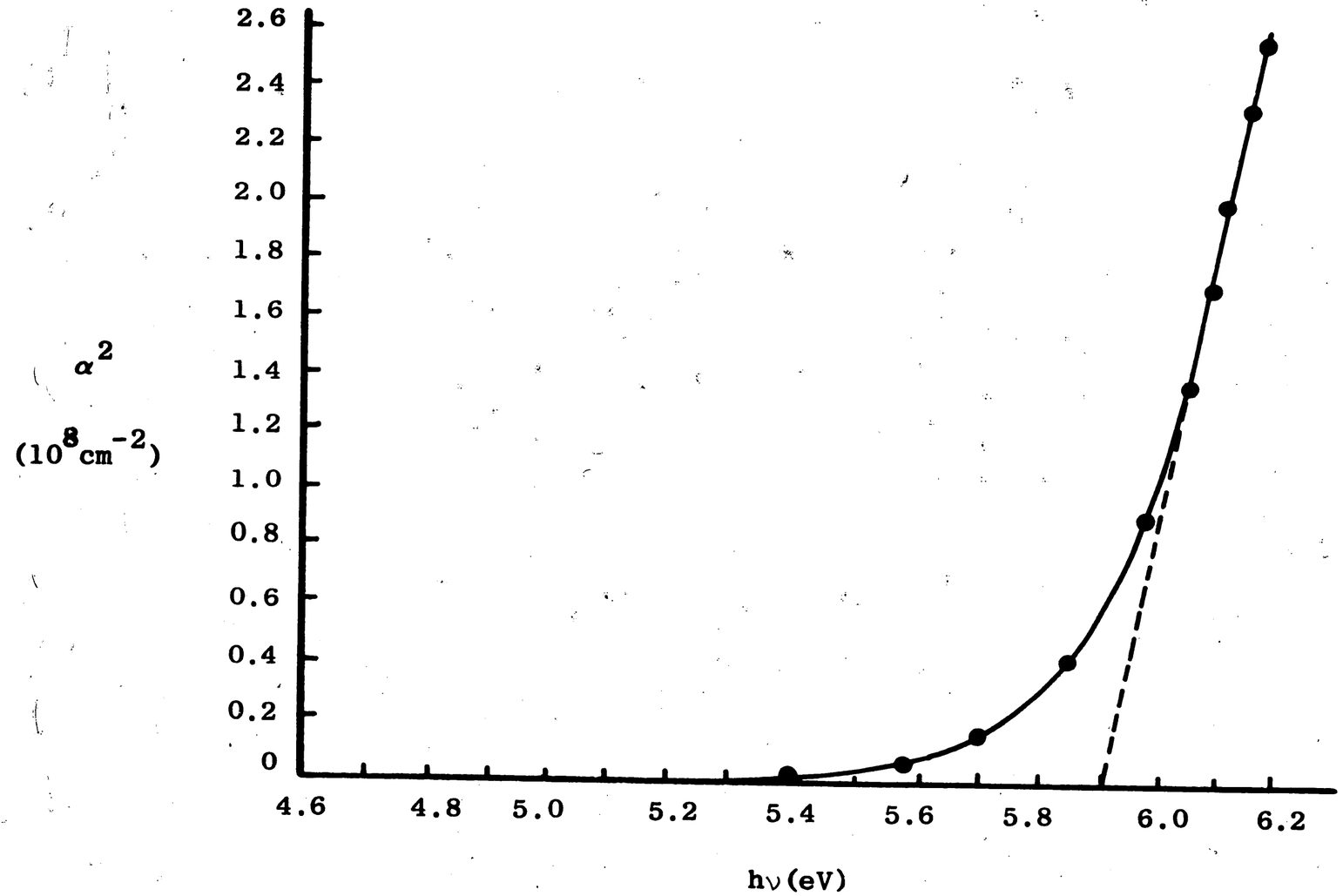

FIGURE 23

Absorption Coefficient Versus Photon Energy of Silicon Nitride Films Grown at a Rate of 1600 Å/min. The Energy Gap is 5.9 eV.

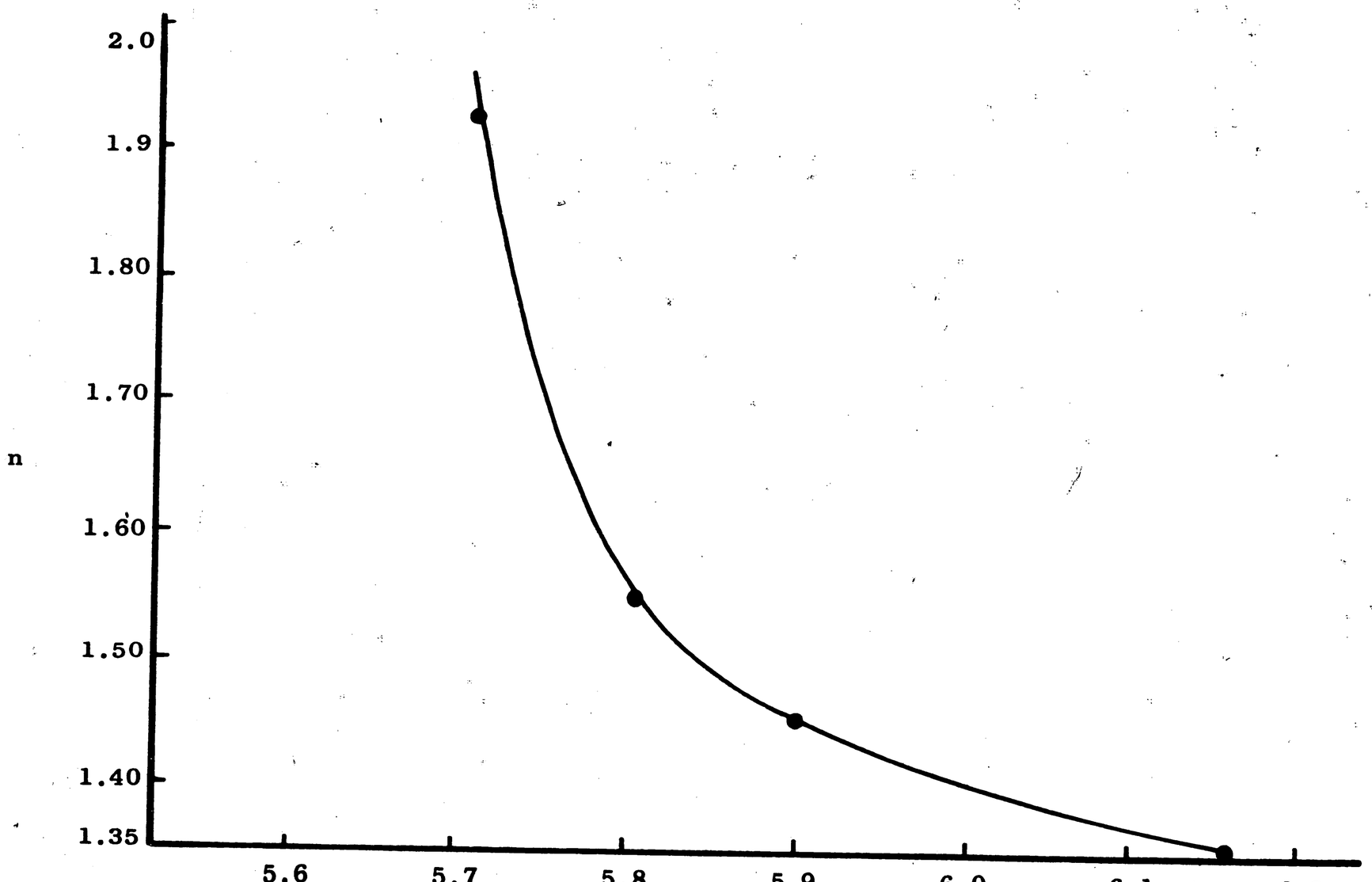

FIGURE 24

Index of Refraction Versus Energy Gap of Silicon Nitride Films

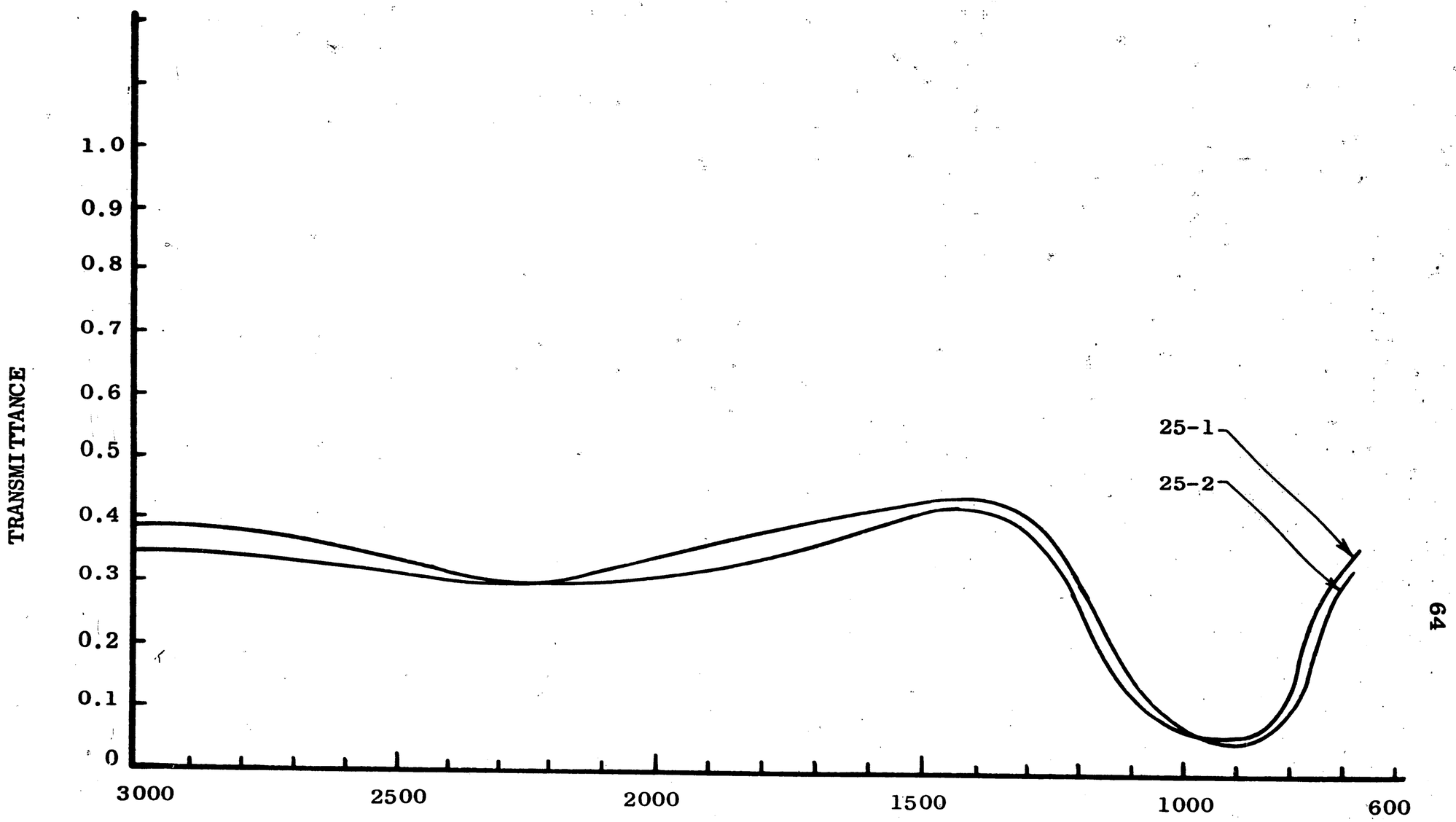

FIGURE 25

Infrared Absorption Spectra of Silicon Nitride Films Grown at a Rate of 230 Å/min. Sample 25-1 was Prepared at 600 ^{o}C and 5.0 Ampere Plasma Current. Sample 25-2 was Prepared at 400 ^{o}C and 1.0 Ampere Plasma Current.

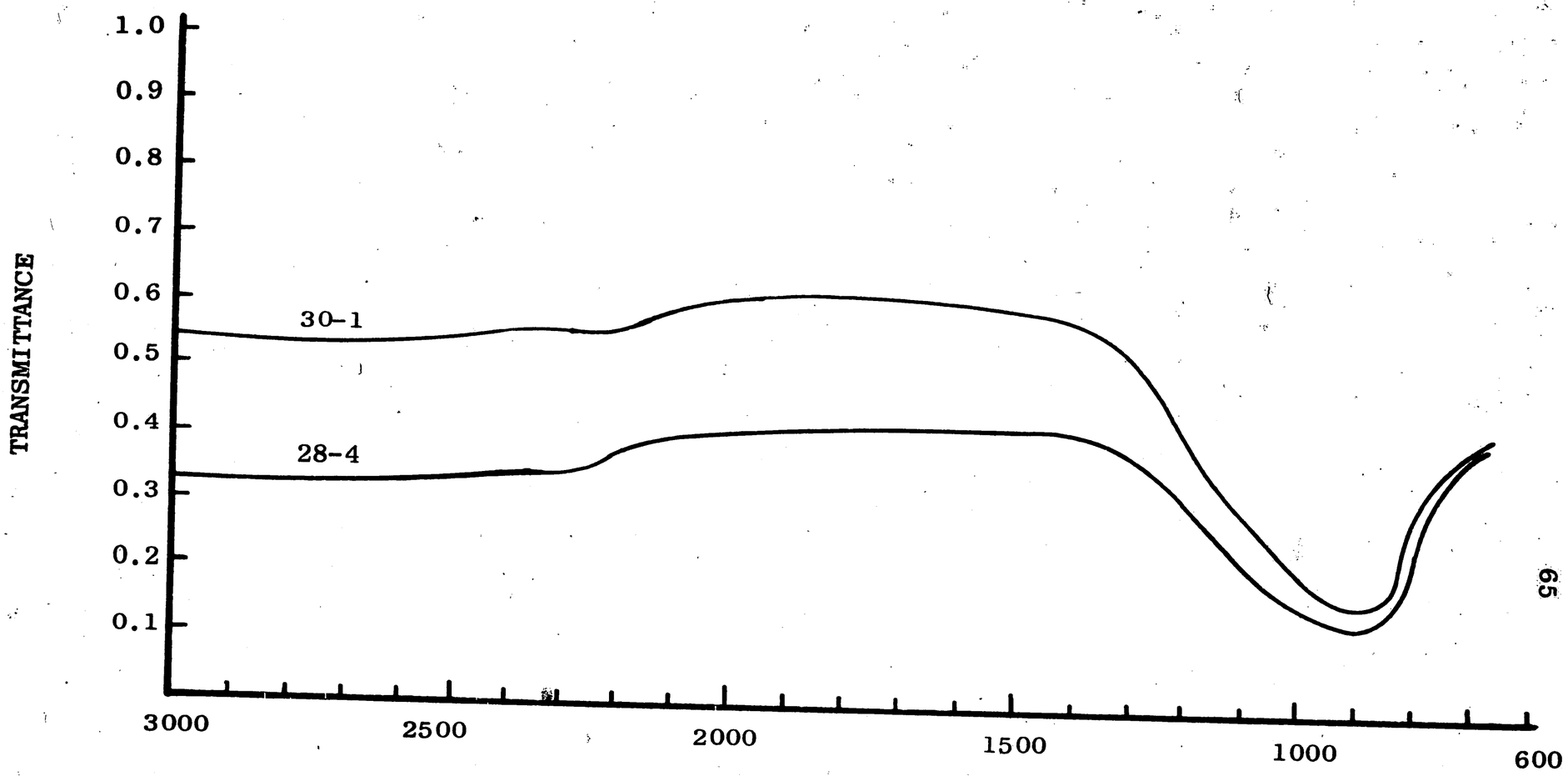

FIGURE 26

Infrared Absorption of Silicon Nitride Films Prepared at 400 ^{o}C and 5.0 Ampere Plasma Current. Samples 30-1 and 28-4 were Grown at a Rate of 500 and 1000 Å/min. Respectively.

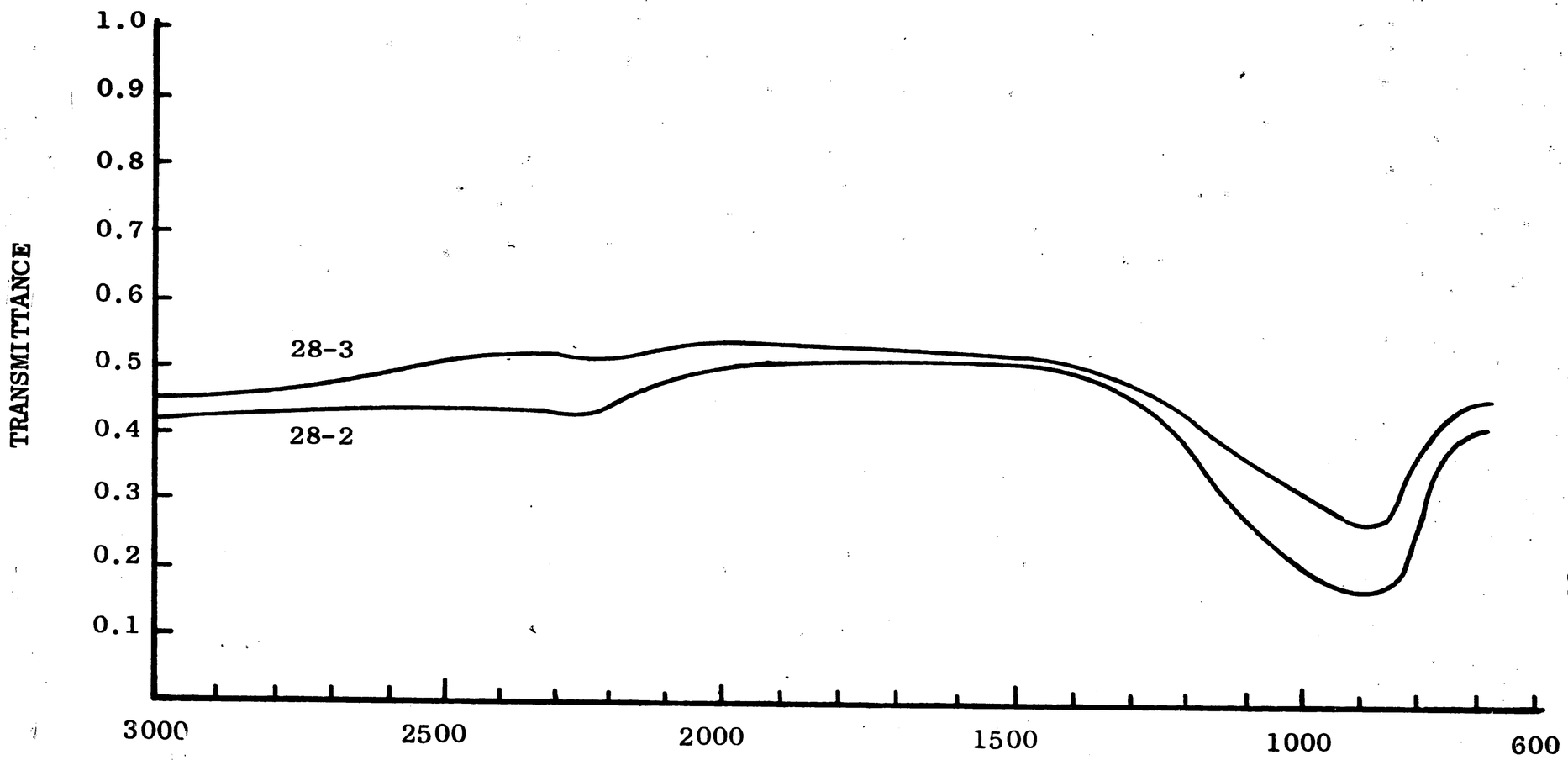

FIGURE 27

Infrared Absorption Spectra of Silicon Nitride Films Prepared at 400 ^{o}C and 5.0 Amperes Plasma Current. Samples 28-2 and 28-3 were Grown at a Rate of 630 and 1600 Å/min. Respectively.

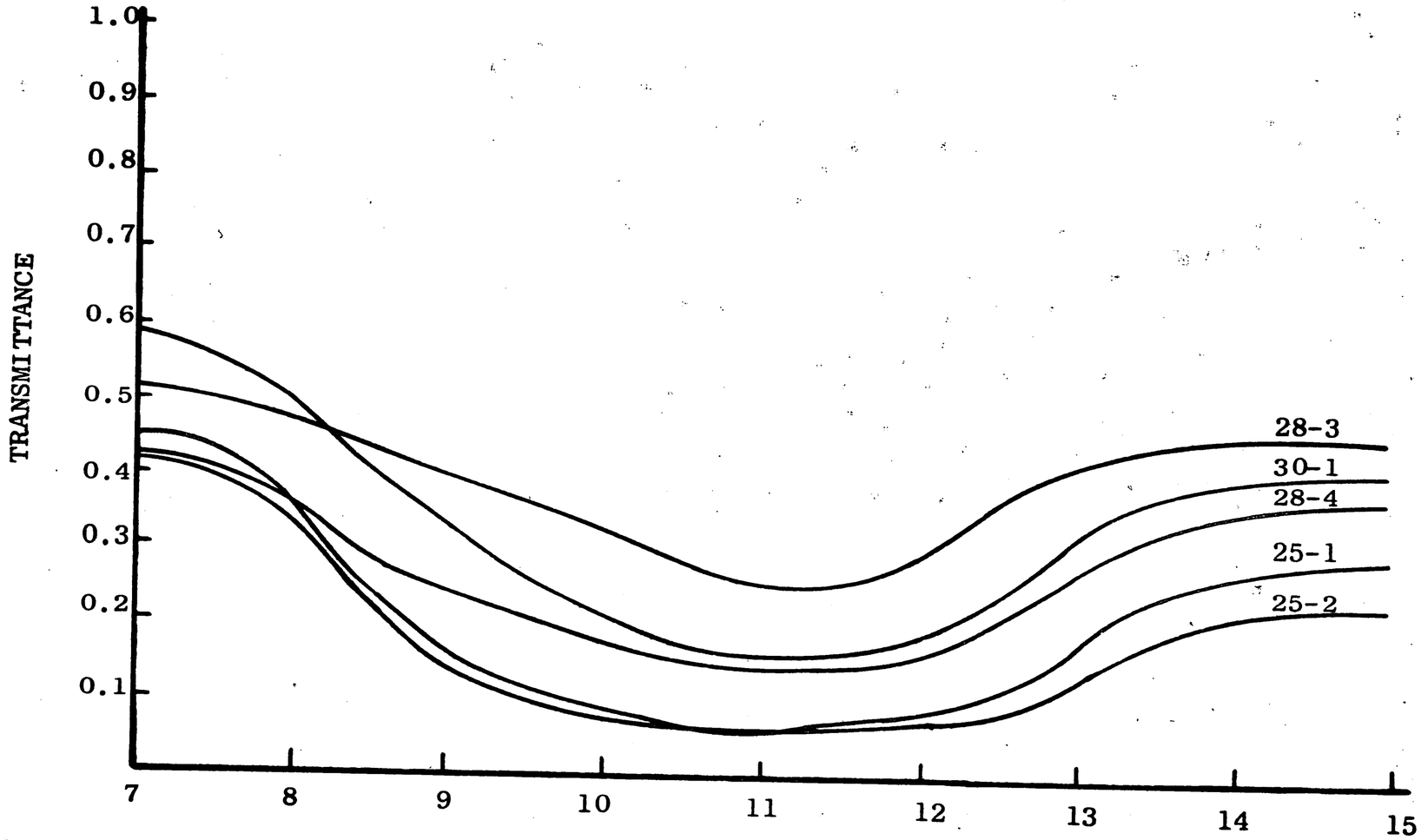

FIGURE 28

Expanded Plot of Transmittance Versus Wavelength in the Region of the Absorption Peak for Samples Shown in Figures 25, 26, and 27.

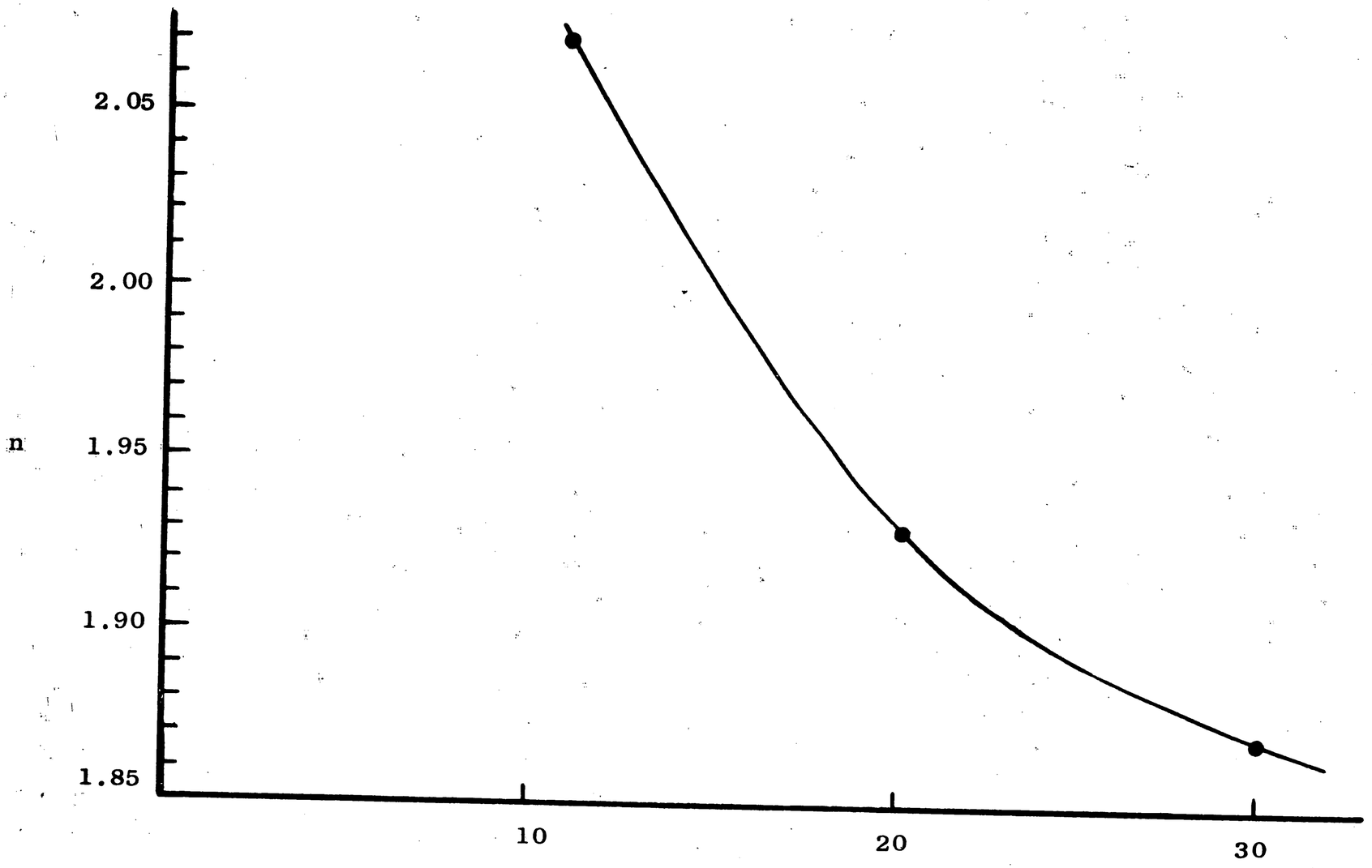

FIGURE 2.9

Index of Refraction Versus Etch Rate of Silicon Nitride Films

TABLE II

COMPARISON OF THE PHYSICAL PROPERTIES OF SILICON NITRIDE FILMS PREPARED BY THE VARIOUS TECHNIQUES WITH THAT OBTAINED IN THIS INVESTIGATION

	T_s (°C)	R_d Å/min.	$\frac{SiH_4}{NH_3}$	Vac [KV (P-P)]	Vdc (KV)	P (μ)	IR (μ)	R (Ω·cm)	n	ρ g/cm³	E V/cm	Ko	Eg (eV)	Ref.
PYROLYTIC:	600						11.5	10^{15}	1.94		$.8/2.3\cdot10^7$	5.6-6.8	4.5-5.5	51,74
	900						12.0		1.98		$\sim10^7$	6.2		71
	800-1000	5000	1/40-1/20						2.1/1.98					43
1. SiH_4+NH_3	700-1150	1500							2.0		10^6-10^7	8-4	4.3	44
	750-1100	850	1/40-1/20				(10-12)12		2.0/2.06	3.02/3.21		6.34		72
	800-1200	400							1.975/2.02	2.78/2.92				41
2. $SiCl_4+NH_3$	550-1250	600							1.99/2.01		$\sim10^7$	7	5.6	45
PLASMA ACTIVATED CHEMICAL VAPOR DEPOSITION														
1. RF DISCHARGE (SiH_4+NH_3)	<500	200	.03-.50				12.1	$8\cdot10^{16}$			$6\text{-}1\cdot10^6$	7-11		42
2. DC PLASMA a. (SiH_4)	<500	400	.1%SiH_4			1000			2.0					48
b. ($SiBr_4$)		400	.1%$SiBr_4$			1000			1.93	3.1/3.2				48
SPUTTERING														
1. RF, Si_3N_4 Cathode in Ar		100					12					8.6		46,50
2. DC, Si Cathode in N_2	200-400	3			2-5	10								47,71
50% N_2+50%Ar		60			1.5	150						10-12		50
3. RF(13.6MH_z), Si Cathode in N_2	25-500	200		3	1.5	5-25	11.3	$>10^{15}$	2.05	2.8/3.0		6-8.3	4-6	47,71
4. DC, Si Cathode in N_2 Supported Discharge	50-230	110			.8	1.5	12.0	$3.4\cdot10^{13}$	2.1	2.82/3.02	1.2-6.0 x10^5	6.2-6.8		46,50
5. AF, Si Cathode in N_2 Hollow Cathode Supported Plasma	200-600	300		1.5-3.6	.8-1.5	200	11.1 (10.1-11.9)		1.97	2.9/3.14	$6\text{x}10^6$		5.72	This Exp.

T_s = Substrate temperature
R_d = Deposition rate
Vac= AC Sputtering potential
P = Gas pressure
IR = Infrared absorption peak
ρ = Film density
E = Dielectric strength
K = Dielectric constant
Eg = Energy gap
R = Film resistivity
Ref = Reference

DISCUSSION

Silicon nitride films deposited on polished silicon substrates by audio frequency reactive sputtering were found to be amorphous at substrate temperatures up to 600°C and plasma currents up to 5.0 amperes. This is also the case for films deposited by the pyrolytic, plasma activated chemical vapor deposition, and sputtering methods[71,48]. The pyrolytic films are amorphous at temperatures up to 900°C where some crystallites begin to form[43].

The properties of the silicon nitride films prepared by audio frequency sputtering are comparable to the properties of films prepared by the above techniques and in some cases superior for particular applications. The mean index of refraction of 1.97 and the range of 1.93 to 2.08 is in agreement with that of 1.93 to 2.10 measured on films prepared by the other techniques shown in Table II. The deviation of the index of refraction from the crystalline value of 2.1 is attributed to varying film density which is a result of the amorphous nature of the films. It was shown in Figure 16 that the index of refraction is nearly a linear function of the film density. The silicon nitride film density varies from 2.95 to 3.14 g/cm^3 over the range of n from 1.93 to 2.08. Doo[72] reported a variation of density from 3.02 to 3.21 g/cm^3 for an index of refraction ranging from 2.0 to 2.06. These films were prepared by the pyrolytic method. The density range predicted by Figure 16 for the above change in index of refraction is 3.05 to 3.16 g/cm^3. The agreement is good.

Lee, Chu, and Gruber[41] reported densities of pyrolytically deposited films of 2.78 and 2.82 g/cm^3 for an index of refraction of 1.975 and 1.980 respectively. These films were prepared at 900°C and 950°C respectively. Chemical analysis of the film composition indicated an increase from 39.9% to 40.0% in the nitrogen content of the film with increasing index of refraction from 1.975 to 1.980 respectively. The theoretical composition is 39.92%N and 60.08%Si. A density range of 2.8 to 3.0 g/cm^3 for films prepared by RF sputtering and a range of 2.82 to 3.02 g/cm^3 for films prepared by DC sputtering in a supported discharge was reported by Hu[47] and Janus[46] respectively. The corresponding range of n for these density values is not known, but the typical values of n reported for the above RF and DC sputtered films are 2.05 and 2.1 respectively.

It is believed that the atoms sputtered from the cathode at low voltages will have many inelastic collisions with the excited nitrogen atoms of the plasma in diffusing to the substrate and transform their large kinetic energy to the potential energy or excited states of the plasma. Hence the surface mobility is maintained at low sputtering voltages and low substrate temperatures. The relatively high density of the films prepared by audio frequency (AF) sputtering in a nitrogen plasma at low substrate temperatures compared to that of other sputtering techniques can be attributed to the increased mobility imparted to the sputtered atoms by the intense nitrogen plasma. With this additional mobility, the atoms can move to preferred locations which results in films that are

more perfect structurally.

The dielectric strength of the silicon nitride films has a mean value of $6x10^6$ V/cm and a range of .2 to $2.2x10^7$ V/cm. This is in agreement with reported values from about 10^6 to 10^7 V/cm as shown in Table II. Dielectric strength measurements are dependent on the type of contact made to the film. Scott[51] determined a value of $8x10^6$ V/cm for pyrolytically grown films using a 1 mm^2 contact area and a value of $2.3x10^7$ V/cm using a point contact to the film. Excessive pressure applied to the film when making contact with the probe will cause structural damage to the film at the contact point. This damage will result in low dielectric strength values for the film. Janus[50] reported a dielectric strength from 1.2 to $6x10^5$ V/cm for films prepared by DC sputtering in a supported discharge using direct current measurements, and a dielectric strength an order of magnitude larger when using rectified AC current measurements. This low dielectric strength was attributed to low film density evidenced by high etch rates, infrared spectral data, and leakage current measurements.

The energy gap of the silicon nitride films was determined to be about 5.72 eV. The range of energy gap measured on films prepared by the pyrolytic method varies from 4.3 to 5.6 eV. Grieco, Worthing, and Schwartz[45] reported an energy gap at 5.6 $\pm$ .2 eV for films prepared by the pyrolytic reaction of silicontetrachloride and ammonia. This value of energy gap is in close agreement with that obtained in this investigation. Murray[51] reported that for films

prepared pyrolytically at 600°C the energy gap ranged from 4.5 to 5.5 eV. The energy gap increased with subsequent heat treatment by about .35 eV as the temperature increased from 600°C to 1300°C. This was accompanied by a decrease in the index of refraction from 1.96 to 1.58. At temperatures greater than 1200°C the films become visibly dull indicating a decrease in the index of refraction. Hu[47] reported a similar phenomena for films prepared by RF sputtering. The energy gap increased from about 4 to 6 eV as the sputtering power increased from about 1 to 5 watts/cm^2. This phenomena has also been observed for films prepared in this experiment. As the deposition rate, and hence sputtering power density, increased above 300 Å/min., the index of refraction and film density decreased and the energy gap increased. The energy gap increased from 5.72 to 5.90 eV as the deposition rate increased from 230 Å/min. to 1600 Å/min.

At high deposition rates, the rate of arrival of sputtered atoms is large compared to the diffusion times of the atoms, causing insufficient reaction of the excited nitrogen with the sputtered atoms. This is thought to result in formation of silicon atoms with three nitrogen bonds instead of the four nitrogen bonds normally present. The number of triply bonded Si≡N atoms increases with increasing deposition rate as evidenced by the decreasing density and index of refraction.

Moss[75] developed a relation between the index of refraction and the energy gap of photoconductors. It is suggested that the

photo - effect and hence optical absorption takes place only at preferred sites in the lattice, such as vacant lattice sites, interstitial ions, or at atoms on the surface or any discontinuity in the lattice. These imperfections will create potential holes in the lattice capable of trapping electrons in a manner similar to an electron in an isolated atom, except that it is immersed in a medium of dielectric constant equal to that of the bulk material. Hence all the energy levels of the electron will be scaled down by a factor $1/(K_{eff})^2$, where K_{eff} is an effective dielectric constant which can be approximated by the square of the refractive index. Thus the optical energy required to raise an electron at one of these irregularities into an excited state should be proportional to $1/K_o^2$. It is to be expected that the threshold of the photoconductive effect, which is determined by the minimum energy required to raise an electron into an excited state, will vary inversely as the fourth power of the refractive index. Thus

$$n^4 E_g = C \tag{33}$$

where C is a constant. It has been found that many of the Group III/Group V inter-metallic semiconductors obey this law satisfactorily[76] For the more refractive compounds, i.e., $n^4 > 35$, the average value of C is 77. The range for C is from 59 to 88. The index of refraction of 1.93 was determined for a film of silicon nitride having an energy gap of 5.7 eV. Hence

$$n^4 E_g = 79 \tag{34}$$

which is in close agreement with the average value of C. This

relation becomes progressively worse as n decreases, but it serves to qualitatively illustrate that the energy gap can be expected to increase as the index of refraction decreases.

Infrared spectra were taken for samples prepared over a large range of deposition rates. Figure 25 compares the spectra of two films of silicon nitride prepared at the same deposition rate of 230 Å/min., but at different plasma currents and substrate temperatures. Sample 25-1 was prepared at a substrate temperature of 600°C and a plasma current of 5.0 amperes. Sample 25-2 was prepared at a substrate temperature of 400°C and a plasma current of 1.0 ampere. The absorption peak of the Si-N stretching band for β - Si_3N_4 occurs at a wavelength of 10.7 [71]. The position of the Si-N stretching band of the amorphous films of samples 25-1 and 25-2 show a considerable shift toward longer wavelengths. This is due to the weaker bonded structure of the amorphous films as opposed to crystalline silicon nitride. The Si-N stretching band of sample 25-1 and 25-2 occurs over a broad range from 10.8 to 11.3 μ and 10.1 to 11.9 μ respectively. This band broadening is attributed to the greater distribution of interatomic distances of the amorphous films. The median of the absorption peak occurs at about 11.1μ. The broader absorption peak of the film prepared at low energy conditions, sample 25-2, can be attributed to less order in the film structure, i.e., a more amorphous film.

Doo[72] reported a broad absorption peak (from 10 to 12μ) for pyrolytically prepared films with the minimum occuring at 12μ. The

shape of the infrared spectra is similar to that obtained in this experiment. Heat treatment of the above pyrolytic films at 1100°C in a N_2 atmosphere for 3 hours decreased the transmittance of the films about 20% on the short wavelength side of the infrared spectrum; there was no change in the shape of the curve. Hu[71] reported an absorption peak at 12 μ for pyrolytically prepared films and a peak at 11.3 μ for RF sputtered films. Both methods showed considerable broadening compared to the absorption peak of β - Si_3N_4. The absorption peak at 12 μ was also obtained for films prepared by RF sputtering from a Si_3N_4 cathode and by DC sputtering in a supported discharge[46,50]. The absorption peak shift to longer wavelengths and broadening observed for all amorphous silicon nitride films is consistent with the decrease in index of refraction and density from that of the crystalline silicon nitride.

The infrared absorption spectra of films prepared at high deposition rates also show a broad absorption peak between 10.5 and 11.8μ. The absorption peak of the films prepared at 500 Å/min. and 1000 Å/min. occurs from 10.5 to 11.8μ, and that for films grown at a rate of 1600 Å/min. occurs from 10.7 to 11.5μ.

Films grown at rates of 1600 Å/min. exhibit colors that are much lighter in appearance than the colors of films deposited at lower rates. This is attributed to decreasing order in the film structure as the deposition rate increases and is accompanied by a decreasing film density and index of refraction.

Hu[71] observed that the infrared spectra of DC reactively

sputtered films showed an absorption peak at a wavelength of 4.7μ. This peak increased in magnitude as the DC sputtering voltage increased and becomes very pronounced when the DC voltage is 3 to 4 KV. It was suggested that this peak is probably due to triply bonded Si≡N molecules, since it occurs at high deposition rates when the diffusion time is short for the sputtered atoms, causing insufficient chemical reaction with the excited nitrogen.

The infrared absorption spectra of the films prepared at high sputtering rates (see Figures 26 and 27) have a slight dip at about 4.5μ, but the intensity of the absorption does not increase with increasing deposition rate. It is thought that the highly excited nitrogen present in the plasma reacts more readily with the sputtered silicon atoms, resulting in fewer triply bonded Si≡N molecules. The Si - N stretching band absorption peak is present in the IR spectra of all films, indicating that the normal Si - N bond is present in significant quantities. However, the degree of the absorption at about 11.1μ decreases with increasing growth rate of the films. The absorption band corresponding to Si - O (9.4μ) was not observed. The etch rate of the silicon nitride films in buffered HF increases with decreasing film density and index of refraction as shown in Figure 29. This is expected since the weaker bonded structure indicated by low film density is more vulnerable to chemical attack. The etch rate of the pyrolytically grown films has been reported[43] to decrease with increasing temperature. This is consistent with the observed increase in film density with increasing temperature[41].

Erdman[48] reported an etch rate of about 10 Å/min. and 20 Å/min. for films grown by reacting SiH_4 and $SiBr_4$ in a nitrogen plasma respectively. Dalton[49] reported that the etch rate of silicon nitride is related to the crystallite size of the α- Si_3N_4 or β- Si_3N_4 present in the amorphous matrix of the films. The etch rate was found to increase with increasing crystallite size to a rate of 500 Å/min. for a crystallite size 100 Å. It was found that the effectiveness of the film as a sodium diffusion barrier was related to the crystallite size and hence to the etch rate of the film. Generally, if the etch rate if less than 30 Å/min., the films are considered to be an effective diffusion barrier. The etch rate corresponding to the mean index of refraction of 1.97 found for the films prepared in this investigation is about 17 Å/min.

It is expected that the technique of audio frequency sputtering in a hollow cathode discharge can be extended to reactively sputtering from any metallic cathode to form insulating or non-insulating films. The process could be improved by sputtering at lower pressures by surrounding the hollow cathode with a solenoid to provide a magnetic field in the region of the hollow cathode such that the discharge or plasma can be maintained at pressures less than 25 microns. Film uniformity obtainable in this experiment is about 2% from center to edge. This could be improved by using a larger deposition chamber with a larger silicon cathode and a greater spacing between the chamber walls and the target cathode.

Another improvement on the technique would be to move the plasma

anode to a position adjacent to the deposition chamber so that it could serve as the anode for both the plasma and supttering potentials. The pedestal should in this case be biased slightly negative to eliminate electron and negative ion bombardment damage to the film. The anode should be gas shielded in a manner similar to that described by Erdman[48] to prevent contamination of the film by the anode material.

CONCLUSIONS

Amorphous silicon nitride films can be prepared by audio frequency reactive sputtering in a hollow cathode supported nitrogen plasma at low substrate temperatures and deposition rates up to 300 Å/min. The properties of the films are comparable to or better than that obtained for films prepared by the pyrolytic methods, RF and DC sputtering, or chemical vapor deposition.

Substrate temperature from 200° to 600°C and plasma current up to 5.0 amperes have little effect on the dielectric strength, index of refraction, and density of the silicon nitride films. However, large plasma currents make possible the use of lower sputtering potentials to obtain a given deposition rate.

The film density is an approximate linear function of the index of refraction. As the film density approaches the theoretical value of 3.18 g/cm^3, the index of refraction approaches the single crystal value of 2.1.

At deposition rates greater than 300 Å/min., the film density and index of refraction decrease with increasing growth rate of the film. This is attributed to the high rate of arrival and short diffusion times of the sputtered atoms, causing insufficient chemical reaction of the excited nitrogen with the silicon atoms. The result is triply bonded Si≡N being present in the film and a weaker bonded film structure.

RECOMMENDATIONS FOR FURTHER STUDY

An investigation of preparing other insulating, dielectric, or metallic films by audio frequency sputtering in a hollow cathode supported nitrogen plasma would be an important extension of this investigation.

The interfacial properties of silicon nitride on silicon substrates is of prime significance to semiconductor devices. Therefore, a study to relate the surface charge density to the film preparation conditions would be valuable in evaluating the silicon nitride films prepared by audio frequency sputtering.

APPENDIX I

LITERATURE REVIEW

LITERATURE REVIEW

Production Methods and Properties of Si_3N_4

In 1910, Weiss and Engelhart[1] made the first systematic study on the formation of silicon nitride by the reaction of silicon and nitrogen. They determined the rate at which silicon absorbed nitrogen at temperatures from 1120°C to 1420°C. The resulting material was a grayish-white amorphous powder contaminated with silica. They found that, when the reaction temperature was held in the range from 1240° to 1300°C for half an hour, the reaction between silicon and nitrogen proceeded at a measurable rate. The density of silicon nitride of 3.64 g/cm^3 obtained by these authors is considered doubtful since the x-ray density is 3.18 g/cm^3.

Funk[2] (1924) studied the formation of silicon nitride by the reaction of nitrogen on finely divided silicon, separated with aluminum. A nitride was formed after 10 minutes at 1450°C.

In 1925, Friederick and Sittig[3] prepared silicon nitride in an impure form by heating a mixture of silica, carbon, and iron oxide in nitrogen at 1250° to 1300°C. The iron could then be removed by treating with HCl leaving a white powder. Hinke and Brantley[4] studied the nitrogen pressures for the reaction $Si_3N_4 \longrightarrow 3Si + 2N_2$ in the temperature range from 1333° to 1529°C. They concluded that the dissociation pressure would reach 1 atm at 1977°C. They found that the only nitride present was Si_3N_4.

Pehlke and Elliott[22] (1959) measured the equilibrium pressure of nitrogen over pure silicon and silicon nitride at 1400° to 1700°C

and the free energies and enthalpies of formation calculated as functions of temperature over the above temperature range. Fesenko and Bolgar[39] measured the vapor pressure of nitrogen over silicon and silicon nitride with results comparable to those of Pehlke and Elliott.

More recently, Leslie, Carrol, and Fisher[6] separated Si_3N_4 from nitrided silicon steels. X-ray and electron diffraction patterns of the material led them to the conclusion that the nitride was probably orthorhombic and of the same structure as Ge_3N_4.

Turkdogan and Ignatowicz[10] found that Si_3N_4 exist is two phases: α - Si_3N_4 and β - Si_3N_4, both hexagonal. This has been confirmed by Turkdogan, Bills, and Tippett[14], Hardie and Jack[11], Forgeng and Decker[15] and Narita and Mori[22]. Vassiliou and Wilde[12] regarded these two phases (α & β) as orthorhombic (α) and hexagonal (β) respectively.

α - Si_3N_4 can be prepared in a fairly pure state by nitriding silicon powder within the temperature range of 1200^{o} - $1300^{o}C$[15]. It occurs as a clear, white or yellowish-white, flattened needles. Chemical analysis showed it to have the composition of Si_3N_4; i.e., 60% silicon and 40% nitrogen. They measured a mean refractive index of 2.1.

β - Si_3N_4 can be prepared by nitriding silicon powder at about $1450^{o}C$ and has been formed from α - Si_3N_4 by heating at $1550^{o}C$[15]. Attempts to reverse the reaction by heating β - Si_3N_4 at temperatures below $1500^{o}C$ have failed. The refractive index of β - Si_3N_4 is

about 2.1. The measured density of β- Si_3N_4 is 3.15 g/cm^3 and the measured density of α- Si_3N_4 is 3.16 g/cm^3 as compared to the theoretical density of 3.187 g/cm^3 and 3.184 g/cm^3 respectively. The above density values are probably for single crystals and do not represent that obtainable by nitriding silicon powder to form bulk Si_3N_4. The values usually reported are from 2.0 to 2.6 g/cm^3. The lattice parameters of α- Si_3N_4 and β- Si_3N_4 are listed in Table III along with other structure properties[11,14,15,29]. The chemical and physical properties are listed in Table IV and Table V respectively.

TABLE III

Crystal Structure of Si_3N_4

Phase	Space Group	Crystal System	Lattice Parameter a	c	c/a	Atoms per Unit Cell	X-Ray Density
α-Si_3N_4	D^2_{3d}-P3/c	hex	7.758	5.623	.725	$Si_{12}N_{16}$	3.184
β-Si_3N_4	C^2_{6h}-$P6_{3/m}$	hex	7.603	2.909	.383	Si_6N_8	3.187

TABLE IV

Chemical Properties of Si_3N_4

Corrodents to which Silicon Nitride is Resistant(16)

HCl (20%), boiling
NNO_3(65%), boiling
H_2SO_4 (10%, 77%, 85%)
HPO_3
$H_4P_2O_7$
NaOH (25%)
Cl (gas), wet
Cl (gas), 900°C
H_2S (gas), 900°C
H_2SO_4, boiling, conc. + $CuSO_4$ + $KHSO_4$
$NaNO_3$ + $NaNO_2$ salt bath at 350°C
NaCl + KCl salt bath at 790°C

Corrodents that Attack Silicon Nitride(16)

	Time of test to first observed corrosion (hrs)
NaOH (50%) boiling	115
NaOH at 450°C, molten	5
HF (48%) at 70°C	3
HF (3%) + HNO_3 (10%) at 70°C	116
NaCl + KCl salt bath at 900°C	144
NaB $(SiO_3)_2$ + V_2O_5 at 1100°C	4
NaF + ZrF_4 at 800°C	100

Resistance of Silicon Nitride to Attack Of Molten Metals(16)

Metal	°C	Time (hrs)	Remarks
Aluminum	800	950	No Attack
Aluminum	1000	100	No Attack
Lead	400	144	No Attack
Tin	300	144	No Attack
Zinc	550	500	No Attack
Magnesium	750	20	Slightly Attacked
Copper	1150	7	Attacked

TABLE V

Physical Properties of Si_3N_4

Color: pale to dark grey[34]

Appearance: dull surface with a matt texture[34]

Density: 3.18 g/cm^3 (x-ray density)
2.0 to 2.5 g/cm^3 (bulk density)[20]
3.16 α-Si_3N_4 (single crystal)[15]
3.15 β-Si_3N_4 (single crystal)[15]

Hardness: 9 (Moh's scale)[32]
1000 to 1100 D.P.H.[34]
55 Rockwell "A"[34]

Strength: (bend) 12,000 to 25,000 psi[34] (25°-1000°C)
(compressive) 70,000 to 90,000[34] psi (25°-1000°C)

Youngs Modulus: 9 x 10^6 psi average[34] (25°-1000°C)

Coefficient of Thermal Expansion:
1.7x10^{-6}/°C at 100°C[34]
3.0x10^{-6}/°C at 1000°C[34]
2.5x10^{-6}/°C average over range[34]
3.0x10^{-6}/°C α-Si_3N_4 20°-1420°C[21]
3.5x10^{-6}/°C β-Si_3N_4 20°-1420°C[21]

Thermal Conductivity: .067 cal./cm°C/sec[32]

Thermodynamic Properties:

Specific Heat, Cp: 16.83 + 23.6 x 10^{-3}T cal/g/°C, (300°-900°C)
0.2145 cgs (0°-585°C)[31]

Entropy: S_{298} = 22.8 cal/mole/°K[7]

Heat Formation: ΔH_{298} = 179.25 Kcal/mole[7]

Free Energy of Formation: ΔG°_{298} = 154.740 Kcal/mole[7] at 700°K

Heat of Formation: ΔH_{1700} = -176.300 K cal/mole[4]

Melting Point: 1900°C (under pressure)

Electrical Resistivity: 10^{13} to 10^{14} ohm-cm (25°C)[30][26]
10^7 to 10^{13} ohm-cm (1000°-25°C)[27]

Energy Gap: 3.9 - 4.0 ev[30]

Dielectric Constant: 5 at 5 mc/s[34]
7.2 to 8.5 (20°-400°C) at 1 to 30 mc/s[39]

Infrared Absorption Band: 10.6[17]

Solubility in Silicon: 10^{12} atoms/cm^3 (25°C)[17]
10^{19} atoms/cm^3 (in melt at m.p.)[17]

Index of Refraction: 2.1[15]

Methods of Preparation of Si_3N_4 Thin Films

More recently, the emphasis has been on developing methods of producing thin continuous films of Si_3N_4 with bulk properties for use as an insulating layer, passivator, and diffusion mask in the production of semiconductor devices, integrated circuits, and capacitors.

The methods of producing thin films of silicon nitride will be discussed under three different categories: (1) pyrolytic decomposition methods; (2) DC and RF plasma activated chemical vapor deposition; (3) sputtering.

1. Pyrolytic Decomposition

Gleemser[36] prepared Si_3N_4 by reacting $SiCl_4$ with NH_3 at 1200°C. Jenkner and Schmidt[37] produced high purity Si_3N_4 by reacting silane or methysilane with dry, oxygen-free NH_3. Silane (3 vol.) and NH_3 (5 vols.) are treated in a quartz furnace at 800°C. A finely divided light brown silicon nitride is formed.

The decomposition of $SiBr_4$ or $SiCl_4$ with N_2 and H_2 at temperatures below 1000°C to form Si_3N_4 thin films has been investigated by Barnes and Geesner[24]. Schumb and Lefeuer[8] formed Si_3N_4 by the reaction of hexachlorodisilane with NH_3 at 1600°C.

Many investigators have recently utilized the following reaction to form thin films of Si_3N_4 on various substrates.

$$3SiH_4 + 4NH_3 \longrightarrow Si_3N_4 + 12H_2$$

Doo and Nichols[43] prepared films of Si_3N_4 at silane: ammonia ratios of 1:20 to 1:40 on silicon substrates at 800° to 1000°C. The films prepared at 800°C were amorphous with some crystallites appearing above 900°C. The index of refraction of these films varied from 2.10 to 1.98 for temperatures from 800°C to 1000°C when the silane: ammonia ratio was greater than 1:2. However, at lower ratios, the films prepared at 800°C and 900°C had indices of refraction greater than 2.1 indicating an excess of silicon in the films.

Bean, Gleim and Runyan[44] deposited Si_3N_4 on silicon substrates over the temperature range from 700° to 1150°C. As the temperature is increased the film growth increases rapidly up to 900°C where leveling off occurs. Deposition rates up to 900 Å/min. were reported. The behavior of the index of refraction vs. silane: ammonia ratio was about the same as observed by Doo and Nichols. Films deposited below 800°C were amorphous. Between 900° and 1100°C some crystallites are observed; above 1100°C many hexagonal rods grow over the surface. The optical absorption edge was determined to be 0.29μ. The dielectric strength is in the range from 10^6 to 10^7 V/cm, and the dielectric constant from 4 at optical frequencies to 8 at low frequencies. Conduction was determined to be by Schottky emission with carrier concentration of $10^{15}/cm^3$ and an activation energy of 0.5 ev.

Scott and Olmstead[51] and Lee, Chu, and Gruber[41] also have reported investigations using the silane-ammonia reaction. Scott and Olmsted reported values for index of refraction from 1.84 to 1.81 at a wavelength of 3μ. The energy gap was determined to be

4.5 $\pm$ 0.3 eV. Lee, Chu, and Gruber deposited Si_3N_4 on silicon substrates over a wide temperature range, 800°-1200°C. The density, index of refraction, and composition was determined as a function of substrate temperature.

T(°C)	% Si	%N	Density (g/cm^3)	n
800				1.975
850			2.78	
900	60.5	39.9		1.975
950	59.1	40.0	2.82	1.980
1100			2.92	
1200				2.020
α-Si_3N_4	60.08	39.92	3.18	

They also concluded that a 500 Å film of Si_3N_4 on silicon serves as an effective diffusion mask against boron and 1300 Å is a mask against phosphorous.

Grieco, Worthing, and Schwartz[45] have deposited Si_3N_4 on silicon substrates over the temperature range from 550°-1250°C by reacting $SiCl_4$ with NH_3. They found the dielectric strength to be independent of contact area and film thickness. The index of refraction of the films was from 1.99 to 2.01, energy gap of 5.6 $\pm$ .2 eV, dielectric strength of 10^7 V/cm and dielectric constant of 7. A low fast state density of $4.4 \times 10^{11}/cm^2/eV$ and a normal range from $7\text{-}15 \times 10^{11}$ was reported. The usual value is about $1\text{-}5 \times 10^{12}/cm^2/eV$. Deposition rates obtained were comparable with those using the silane-ammonia reaction.

2. DC and RF Plasma Activated Chemical Vapor Deposition

Swann, Mehta, and Cauge[42] prepared silicon nitride films at substrate temperatures less than 500°C by reacting silane and ammonia

in a radio frequency glow discharge. The deposition rate of 200 Å/min. is lower than that of the higher temperature pyrolytic method, but may not represent the upper limit. The dielectric constant ranged from 7 to 11 as the percent silane ranged from 3% to 50%. The dielectric strength decreased from $6x10^6$ V/cm at 3% to $1x10^6$ V/cm at 50% silane. The resistivity varied from $8x10^{16}$ to $5x10^{12}$ ohm-cm.

Erdman[48] prepared silicon nitride films by reducing silane or silicontetrabromide in a nitrogen plasma at temperatures between 300° to 400°C and obtained deposition rates as high as 400 Å/min. Most films were prepared using 0.1% $SiBr_4$ or 0.1% SiH_4 and a nitrogen flow rate of 200 cm^3/min. at 1 mm pressure. Some typical properties are as follows:

	$SiBr_4$	SiH_4
Etch Rate in buffered HF(Å/min.)	20	10
Density (g/cm^3)	3.15	
Refractive index	1.93	2.0
Surface Charge Density ($/cm^2eV$)	1 to $4x10^{12}$	1 to $4x10^{12}$

3. Sputtering

Hu and Gregor[47] formed silicon nitride thin films by reactive sputtering using a silicon cathode in a nitrogen atmosphere. This method required high sputtering voltages (2-5 KV) and the deposition rates were from 2 to 3 Å/min. The films were generally of lower quality than those obtained by other methods and showed evidence of electron and negative ion bombardment damage. Difficulty has been reported with glow instability in the form of arcing at the cathode

surface caused by back diffusion of silicon nitride to the cathode surface[50].

Hu and Gregor[47] also prepared films of Si_3N_4 by RF reactive sputtering from a silicon cathode in a nitrogen atmosphere. At RF sputtering voltages of about 3 KV at 13.6 mc/s and a self generated DC voltage of about 1.5 KV, the deposition rate was about 200 Å/min. The nitrogen pressure ranged from 5 to 25 microns. No dependence of deposition rate on substrate temperature was observed between 25°C and 500°C. The physical and chemical properties of the films were reported to be comparable to that obtained for the pyrolytically deposited films when the sputtering is done at low nitrogen pressures. At higher nitrogen pressures, the film properties are significantly affected.

Janus and Shirn[46,50] have prepared Si_3N_4 films by RF sputtering from a silicon cathode in a supported nitrogen glow discharge. Deposition rates of about 70 Å/min. were reported. The film density ranged from 2.82 to 3.02 g/cm^3, the dielectric constant was between 6.4 and 7, and the refractive index was about 2.1. These values are comparable to that obtained by the pyrolytic methods. The etch rate was found to decrease as the sputtering voltage increased. All films were shown to be amorphous by electron diffraction. Silicon nitride films were also obtained by RF sputtering in an Argon atmosphere[46,50] using a Si_3N_4 cathode. This method yielded films of approximately the same properties as above, but the deposition rate was 30 Å/min.

Dalton and Drobek[49] determined that the depth of sodium penetration by diffusion in silicon nitride was a function of the crystallite size. Amorphous films were the best diffusion barriers with depth of penetration increasing with increasing crystallite size as determined by low angle electron diffraction. Amorphous films were found to be slower and more uniform in etching in buffered HF acid. The etch rate increased to 500 Å/sec at a crystallite size of about 100 Å.

BIBLIOGRAPHY

1. Weiss, L. and T. Engelhart, "Herstellung von Siliciumnitrides," Zeitschrift fur anorganische und allgemeine Chemie, Vol. 65, 1910, pp. 38-52.

2. Funk, H., "Uber das Verhalten des aus abgeschreckten Aluminunischmelzen gewonnenen Silicium gegen Stickstoff," Zeitschrift fur anorganische Chemie, Vol. 133, 1924, pp. 67-72.

3. Friedrich, E. and L. Sittig, "Herstellung und Eigenschaften von Nitriden," Zeitschrift fur anorganische Chemie, Vol. 143, 1925, pp. 293-320.

4. Hincke, W. B. and L. R. Brantley, "The High-Temperature Equilibrium Between Silicon Nitride, Silicon, and Nitrogen," Journal of the American Chemical Society, Vol. 52, 1930, pp. 48-52.

5. Juza, R. and H. Hahn, "Uber die Kristallstrukfuren von Zn_3N_2, Cd_3N_2 and Ge_3N_4," Zeitschrift fur anorganische Chemie, Vol. 244, 1940, pp. 125-132.

6. Leslie, W. C., K. G. Carrol, and R. M. Fisher, "Diffraction Patterns and Crystal Structure of Si_3N_4 and Ge_3N_4," Journal of Metals, Vol. 4, 1952, pp. 204-206.

7. Rossini, F. D., "Selected Values of Chemical and Thermodynamic Properties," Circular of the Bureau of Standards, No. 500, 1952.

8. Schumb, W. C. and R. A. Lefeuer, "The Ammonolysis of Hexachlorodisiloxane," Journal of the American Chemical Society, Vol. 76, 1954, pp. 5882-5884.

9. Collins, J. E. and R. W. Gerby, "New Refractory Uses for Silicon Nitride Reported," Journal of Metals, Vol. 7, 1955, pp. 612-615.

10. Turkdogan, E. T. and S. Ignatowicz, "The Solubility of Nitrogen and Formation of Silicon Nitride in Iron-Silicon Alloys," Journal of the Iron and Steel Institute, Vol. 185, 1947 pp. 200-206.

11. Hardie, D. and K. H. Jack, "Crystal Structure of Silicon Nitride," Nature, Vol. 180, 1957, pp. 332-333.

12. Vassiliou, B. and F. G. Wilde, "Hexagonal Form of Silicon Nitride," Nature, Vol. 179, 1957, pp. 435-436.

13. Popper, P. and S. N. Ruddlesden, "Structure of the Nitrides of Silicon and Germanium," Nature, Vol. 179, 1957, pp. 1129-1135.

14. Turkdogan, E. T., P. M. Bills, and V. A. Tippett, "Silicon Nitrides: Some Physico-Chemical Properties," Journal of Applied Chemistry, Vol. 8, 1958, pp. 295-302.

15. Forgeng, W. D. and B. F. Decker, "Nitrides of Silicon," Transactions of the Metallurgical Society of AIME, Vol. 47, 1958, pp. 343-348.

16. Evans, J. W. and S. K. Chatterji, "Kinetics of the Oxidation and Nitridation of Silicon at High Temperatures," Journal of Physical Chemistry, Vol. 62, 1958, pp. 1064-1067.

17. Kaiser, W. and C. D. Thurmond, "Nitrogen in Silicon," Journal of Applied Physics, Vol. 30, 1959, pp. 427-431.

18. Pehlke, R. D. and J. F. Elliott, "High Temperature Thermodynamics of the Silicon, Nitrogen, Silicon Nitride System," Transactions of the Metallurgical Society of AIME, Vol. 215, 1959, pp. 781-785.

19. Kelley, K. K., U. S. Bureau of Mines Bulletin, No. 407, 1937.

20. Parr, N. L., G. F. Martin and E. R. W. May, "Preparation, Microstructure, and Mechanical Properties of Silicon Nitride," Special Ceramics, ed. P. Popper, (London: Academic Press, 1959) pp. 102-135.

21. Iwai, S. and A. Yasunaga, "Thermal Expansion of Si_3N_4, "Naturwissenschaften, Vol. 46, 1959, pp. 473-474.

22. Karita, K. and K. Mori, "Crystal Structure of Silicon Nitride," Bulletin of the Chemical Society of Japan, Vol. 32, 1959, pp. 417-419.

23. Pratt, P. L., "Microstructure and Mechanical Properties of Silicon Nitride," Mechanical Properties Engineering Ceramics Conference, (Raleigh, N. C., 1960), pp. 507-519.

24. Barnes, C. R. and C. R. Geesner, "Silicon Nitride Dielectric," Journal of the Electrochemical Society, Vol. 107, 1960, pp. 98-100.

25. Cook, W. H., "Corrosion Resistance of Various Ceramics and Cermets to Liquid Metals," U. S. Atomic Energy Commission, ORNL-2391, 1960, p. 26.

26. Samsonov, G. B. and G. G. Tsebulya, "Effect of Carbon and Titanium Additions on the Electrical Conductivity of Silicon Nitride," Ukrains Ku Fizichnu Zhurnal, Vol. 5, 1960, pp. 615-619.

27. Sage, A. M. and J. H. Histed, "Applications of Silicon Nitride," Powder Metallurgy, Vol. 8, 1961, pp. 196-212.

28. Deeley, G. G., J. M. Herbert, and N. C. Moore, "Dense Silicon Nitride," Powder Metallurgy, Vol. 8, 1961, pp. 145-151.

29. Borgen, O. and H. M. Seip, "Crystal Structure of β- Si_3N_4, Acta Chemica Scandinauica, Vol. 15, 1961, p. 1789.

30. Samsonov, G. B., "Thermophysical Properties of Alloys in Systems of Boron-Nitrogen, Boron-Carbon, Silicon-Nitrogen, and Boron-Silicon-Carbon," Poroschkovaya Met. Akad. Nauk. Ukr. SSR, Vol. 1.

31. Sage, A. M. and J. H. Histed, "Applications of Silicon Nitride," Powder Metallurgy, Vol. 8, 1961, pp. 196-212.

32. Popper, P. and R. N. Ruddlesden, "The Preparation, Properties, and Structure of Silicon Nitride," Transactions of the British Ceramic Society, Vol. 60, 1961, pp. 603-626.

33. Feldman, C. and M. Hacskaylo, "Temperature Characteristics of Vacuum Deposited Dielectric Films," Reviews of Scientific Instruments, Vol. 33, 1962, pp. 1459-1460.

34. Gill, R. M. and G. Spense, "Self-Bonded Silicon Nitride," Refractories Journal, Vol. 38, 1962, pp. 92-96.

35. Popper, P., "Formation of Nonoxide Coatings by Pyrolysis," Special Ceramic Processes Symposium, British Ceramic Research Association, 1962, pp. 137-148.

36. Glemser, O. and H. G. Horn, "Uber die Bildung Spiralformiger Kristalle von α-Si_3N_4," Naturwissenschaften, Vol. 49, 1962, pp. 538-539.

37. Jenkner, H. and H. W. Schmidt, Ger. 1, 136, 315, September 13, 1962.

38. Suzuki, H., "Synthesis and Properties of Silicon Nitride," Bulletin of the Tokyo Institute of Technology, Vol. 54, 1963, pp. 163-177.

39. Frenko, V. V. and A. S. Bolgar, "Rate of Evaporization and Vapor Pressure of Carbides, Silicides, Nitrides, Borides," Poroshkovaya Met. Akad. Nauk. Ukr. SSR, Vol. 3, 1963, pp. 17-25.

40. Lindop, T. W., "Silicon Nitride - New Engineering Ceramic," Spechsaal Keram, Glas Email, Silikate, Vol. 99, 1966, pp. 6-9.

41. Lee, C. H., T. L. Chu, and G. A. Gruber, "Properties of Silicon Nitride Films," Presented at the meeting of the Electrochemical Society, Philadelphia, Pa., October 11, 1966.

42. Swann, R. C. G., R. R. Mehta, and T. P. Cauge, "Properties of Silicon Nitride Deposited from a Gaseous Source by Radio Frequency Discharge," Presented at the meeting of the Electrochemical Society, Philadelphia, Pa., October 11, 1966.

43. Doo, V. Y. and D. R. Nichols, "Effect of Various Composition Reactants on Pyrolytic Silicon Nitride Films," Presented at the meeting of the Electrochemical Society, Philadelphia, Pa., October 11, 1966.

44. Beam, K. E., P. S. Gleim, and W. R. Runyan, "Some Properties of Vapor Deposited Silicon Nitride Films Using the SiH_4-NH_3-H_2 System," Presented at the meeting of the Electrochemical Society, Philadelphia, Pa., October 11, 1966.

45. Grieco, M. J., F. L. Worthing, and B. Schwartz, "Silicon Nitride Thin Films from $SiCl_4$ and NH_3: Preparation and Properties," Presented at the meeting of the Electrochemical Society, Philadelphia, Pa., October 11, 1966.

46. Janus, A. R. and G. A. Shirn, "Some Properties of Thin Films of Silicon Nitride Prepared by Sputtering," Presented at the meeting of the Electrochemical Society, Philadelphia, Pa., October 11, 1966.

47. Hu, S. M. and L. V. Gregor, "Silicon Nitride Films by Reactive Sputtering," Presented at the meeting of the Electrochemical Society, Philadelphia, Pa., October 11, 1966.

48. Erdman, W. C. and A. Androshuk, "The Preparation of Insulating Films by Vapor Deposition in Direct Current Plasma," Presented at the meeting of the Electrochemical Society, Philadelphia, Pa., October 12, 1966.

49. Dalton, J. V. and J. Drobek, "Dependence of Etch Rate and Sodium Diffusion upon Structure of Silicon Nitride Films," Presented at the meeting of the Electrochemical Society, Philadelphia, Pa., October 12, 1966.

50. Janus, A. R. and G. A. Shirn, "Preparation and Properties of Reactively Sputtered Silicon Nitride," Symposium on the Deposition of Thin Films by Sputtering, University of Rochester, June 9, 1966.

51. Scott, J. H. and John Olmsted, "Low Temperature Deposition of Si_3N_4," Presented at the meeting of the Electrochemical Society, Philadelphia, Pa., October 12, 1966.

52. Davidse, P. D., "Theory and Practice of RF Sputtering," Symposium on the Deposition of Thin Films by Sputtering, University of Rochester, June 9, 1966.

53. Musha, T., "Cathode Sputtering in Hollow Cathode Discharges," Journal of the Physical Society of Japan, Vol. 8, 1962, pp. 1440-1446.

54. Musha, T., "Theory of Negative Resistance in Hollow Cathode Discharges," Journal of the Physical Society of Japan, Vol. 8, 1962, pp. 1447-1453.

55. Gerry, E. T. and D. J. Rose, "Combined Anode - Cathode Feed of a Hollow - Cathode Arc," Journal of Applied Physics, Vol. 37, 1966, pp. 2725-2726.

56. Little, P. F. and A. Von Engel, "The Hollow - Cathode Effect and the Theory of Glow Discharges," Proceedings of the Royal Society (London), 1954, pp. 209-227.

57. Ciobofaru, D., "On the Hollow Cathode Effect," Journal of Electronics and Control, Vol. 17, 1964, pp. 529-540.

58. Struges, D. J. and H. J. Oskam, "Hollow - Cathode Glow Discharge in Hydrogen and the Noble Gases," Journal of Applied Physics, Vol. 37, 1966, pp. 2405-2412.

59. Johnson, E. O. and L. Malter, "A Floating Double Probe Method for Measurements in Gas Discharges," Physical Review, Vol. 80, 1950, pp. 58-68.

60. Vasicek, A., Optics of Thin Films, p. 115, North-Holland Publishing Company, Amsterdam (1960).

61. Archer, R. J., "Determination of the Properties of Films on Silicon by the Method of Ellipsometry," Journal of the Optical Society of America, Vol. 52, 1962, pp. 970-977.

62. Aza'roff, L. V., Introduction to Solids, p. 398, McGraw-Hill, New York (1960).

63. Bube, R. H., Photoconductivity of Solids, p. 211, John Wiley & Sons, New York (1960).

64. Dexter, D. L., Paper in "Photoconductivity Conference," p. 155, John Wiley & Sons, New York (1956).

65. Dexter, D. L., op. cit., p. 165.

66. Bube, R. H., op. cit., p. 212.

67. Fan, Shepard, and Spitzer, Paper in "Photoconductivity Conference," p. 184, John Wiley & Sons, New York (1956).

68. Bardeen, Blatt, and Hall, Paper in "Photoconductivity Conference," p. 146, John Wiley & Sons, New York (1956).

69. Moss, T. S., Optical Properties of Semiconductors, p. 14, Academic Press, New York (1959).

70. Hannay, N. B., Semiconductors, p. 437, Reinhold Publishing Corporation, New York (1959).

71. Hu, S. M., "Properties of Amorphous Silicon Nitride Films," Journal of the Electrochemical Society, Vol. 113, 1966, pp. 693-698.

72. Doo, V. Y., D. R. Nichols, and G. A. Silvey, "Preparation and Properties of Pyrolytic Silicon Nitride," Journal of the Electrochemical Society, Vol. 113, 1966, pp. 1279-1281.

73. Ligenza, J. R., Bell Telephone Laboratories, U. S. Patent 3,287,243.

74. Murray, L. A. and J. H. Scott, "Optical Properties of Deposited Silicon Nitride," Presented at the meeting of the Electrochemical Society, Philadelphia, Pa., October 12, 1966.

75. Moss, T. S., "A Relationship between the Refractive Index and the Infrared Threshold of Sensitivity for Photoconductors," Proceedings of the Physical Society, Vol. 63B, 1950, pp. 167-176.

76. Moss, T. S., Optical Properties of Semiconductors, p. 48, Academic Press, New York (1959).

VITA

Hugh M. McKnight was born at Winston-Salem, North Carolina, on July 9, 1935. He attended public schools in Winston-Salem, North Carolina, and was graduated from James A. Gray High School.

In September 1954, the author entered High Point College, High Point, North Carolina, as a pre-engineering student. In September 1956, he entered North Carolina State University as a student in the Department of Electrical Engineering. While a student at North Carolina State University, he was elected to membership in Tau Beta Pi and Eta Kappa Nu. In June 1959, the author graduated with the degree of Bachelor of Electrical Engineering.

After graduation the author was employed by the Western Electric Company and worked on various manufacturing and development projects. From this position, he was transferred to the Defense Projects Division and assigned to the Bell Telephone Laboratories where he worked on the development of Weapon direction equipment.

In September 1965, Mr. McKnight entered the Graduate School of Lehigh University as a student of the Lehigh-Western Electric solid-state Master's Program at Princeton, New Jersey. He was assigned to the area of thin film research at the Princeton Western Electric Engineering Research Center.